DESULPHURIZATION OF DIESEL FUEL USING CARBON-BASED METAL OXIDE NANOCOMPOSITES

This dissertation is submitted in fulfilment of the requirements for Master of Technology (Chemical)

CHERUBALA Rusumba Bienvenu

210058846

Presented to

Faculty of Engineering and Technology

Department of Chemical Engineering

Vaal University of Technology

Supervisor/Promoter: Dr J K TSHILENGE

Co-supervisor/Promoter: Prof. L RUTHO

April 2021

AUTHOR'S DECLARATION

I hereby declare that I am the sole author of this thesis. This is a true copy of the thesis, including all required final revisions, as accepted by my supervisors. Therefore, the thesis has not been submitted to any other institution. Also, the present work has been referenced accordingly and there is no plagiarism included.

I fully understand that my thesis may be made available to the public electronically for the research references.

ABSTRACT

This thesis presents a slight on desulphurization process of the commercial diesel fuel using the carbon-based metal oxide nanocomposites such as graphene oxide, ZnO, rGO as a nano-adsorbent, activated carbon (PAC and AC) and charcoal Granular active carbon (GAC) to produce a fuel of less than 10 ppm sulphur content. Due to the high percentage of sulphur compounds in the fuel causing air pollution, acid rain and other problems related to combustion process. The synthesised of sorbents were achieved using incipient impregnation, microwaved-assisted and chemical exfoliation methods. The materials were characterized using Thermogrametric Analyzer (TGA), Fourier transform infrared spectroscopy (FTIR) and X-ray diffractometer (XRD), Brunauer, Emmett and Teller (BET). The examination effect of operating conditions on the adsorption capacity with DBT and Sulphur compounds adsorption, the isotherms and the adsorption kinetic models were evaluated.

The experimental data for PAC and AC were well suited to Freundlich isotherm and pseudo second-order kinetic models. The results shown that the sulphur feed concentration, the space velocity and the functional groups of the adsorbents have a considerable effect on the adsorption. In addition, it was observed that the temperature in the range of 30 to 80^{o}C has a significant effect on the adsorption of Sulphur compounds from diesel fuel using 20 wt.% of sorbents. The rGO substrate which contained abundant oxygen functional groups was confirmed to promote the dispersion metal oxide and increased the adsorption efficiency of sulphur compounds (H_2S and SO_2) by providing oxygen ions weakly bound to the sulphur molecules. For the desulfurization process by adsorption, PAC and AC exhibited a better affinity for 80% removal of sulphur compared to the GAC and GO. The effects of metal species such as zinc oxide (ZnO) and reduced graphite oxide (rGO) composite on the adsorption capacity of hydrogen sulphide (H_2S) were investigated. It was found that depending on the copper load, the adsorption capacity of H_2S increased up to 20 times compared to pure ZnO. To study the oxidation changes on copper and zinc oxides, crystallite analysis by XRD and chemical state analysis by XPS were performed.

PUBLICATION

A manuscript AJSE-D-21-01924 “Desulphurization of diesel fuel using carbon-base metal oxide nanocomposites” was submitted and is under review from the Arabian Journal of for Science and Engineering.

Authors: Bienvenu cherubala*, John Kabuba, Limo Rutto

ACKNOWLEDGEMENTS

First of all, I thank the Almighty, my supervisors, Doctor J K Tshilenge for his guidance and help throughout this study. His wise direction and broad knowledge are instrumental to this research work, and his persistent research style always gives me great encouragement and Prof. L Rutho who showed great confidence in me and provided great support for the work. Without forgetting my family for providing me with their endless love and support, my colleague Miss Makhele who gave me valuable support and guidance for this thesis.

I would also like to thank the Department of Chemical Engineering at the Vaal University of Technology for providing support to my study.

CONTENTS

LIST OF FIGURES

LIST OF TABLES

LIST OF ABBREVIATIONS AND ACRONYMS

- **4, 6 – DMDBT**: 4, 6 dimethyl dibenzothiophene.
- **AC**: activated carbon.
- **AC_{30}, AC_{60}, AC_{120}**: activated carbon samples treated and given temperature and specific time.
- **ACS – 1**: coconut-shell activated carbon.
- **Ag**: silver.
- **Al_2O_3**: aluminium oxide.
- **AMIM**: 1 – alkyl 3 – methylimidazolium.
- **BDS**: bio-desulphurization.
- **BET**: Brunauer, Emmett and Teller analyser.
- **BMIM**: butyl 3 – methylimidazolium.
- **BT**: benzothiophene.
- **C_0**: initial concentration.
- **C_2 – DBT**: compounds.
- **CAC**: commercial activated carbon.
- **CeO_2**: cerium dioxide earth metal oxides.
- **CMK – 3**: mesoporous templated carbon.
- **CN**: cetane number.
- **C_o, C_e, Ct**: concentrations.
- **CO**: carbon oxide.
- **Co**: cobalt.
- **CO_2**: carbon dioxide.
- **COS**: carbonyl sulphide.
- **Cu**: copper.
- **CuGr** copper graphene.
- **CuO**: copper oxide.
- **DBT**: dibenzothiophene.
- **DMSO**: dimethyl sulfoxide.
- **ED-XRF**: Energy dispersive x-ray fluorescence spectrophotometer.

- **EMIM**: ethyl 3 – methylimidazolium.
- **Fe**: iron.
- **FT – IR**: Fourier transform infrared spectroscopy analyser.
- **FTIR** The Fourier Transformer Infrared Spectroscopy.
- **GAC** granular activated charcoal.
- **GAC:** granular activated carbon.
- **GO**: graphene Oxide.
- **Gr**: graphene.
- **H_2O_2**: hydrogen peroxide.
- **H_2S**: Hydrogen sulphide.
- **HDS**: Hydrodesulphurization.
- **HNO_3**: nitric acid.
- **ILs**: Ionic liquids.
- **k_1**: the equilibrium rate constant of the pseudo-first-order adsorption.
- **k_2**: as the equilibrium rate constant.
- **K_F**: and n are the Freundlich constants.
- **k_L**: the Langmuir constant.
- **KOH**: potassium hydroxide.
- **La_2O_3**: lanthanum oxide.
- **MeO**: metal oxide.
- **mg/g**: milligram per gram.
- **mg/L**: milligram per litre.
- **MIM**: 3 – methylimidazolium.
- **mL/min**: millilitre per minute.
- **Mo**: molybdenum.
- **Mo^{3+}** and **Mo^{5+}** molybdenum ions.
- **MoS_2**: molybdenum sulphide.
- **N_2**: nitrogen gas.
- **Ni**: nickel.
- **NO_x**: nitrogen oxides.

- **O^{2-}**: oxygen ion.
- **O_2**: oxygen gas.
- **ODS**: oxidative desulphurization'
- **PAC** powdered activated carbon.
- **PACS**: polystyrene-based activated carbon spheres.
- **PFPD**: selective pulsed flame photometric detector.
- **PM**: particulate matter.
- **ppmv**: parts per million by volume.
- **ppmw**: part per million by weight.
- **q_e** and **q_t**: the amounts of sulphur adsorbed at equilibrium.
- **q_m**: maximum adsorption capacity of the adsorbent.
- **rGO**: reduction of graphene oxide.
- **S^{2-}**: sulphur ion.
- **SEM**: scanning electron microscope.
- **SO_2**: sulphur dioxide.
- **SO_3**: sulphur trioxide.
- **SOFCs**: synthetic liquid fuel, solid oxide.
- **SO_x**: sulphur oxides.
- **SRGO**: desulphurization of the straight run gas oil.
- **t**: experimental time breakthrough.
- **TC**: technetium.
- **TGA**: thermo-gravimetric analysis.
- **ULSD**: ultra-low sulphur diesel.
- **WS_2**: tungsten disulphide.
- **wt.%**: wet percentage.
- **XPS:** x-ray photoelectron spectroscopy.
- **XRD**: X-ray diffractometer.
- **$ZnCl_2$**: zinc chloride.
- **ZnO**: zinc oxide.

CHAPTER 1: INTRODUCTION

1.1. BACKGROUND

The Sulphur compound has been presented as a contaminant in different forms in the environment. The compound causes environmental damages especially as acid rain, corrosion of equipment and deactivation of catalysts in the industries (Song, 2014). Refineries convert crude oil to higher products (for examples: liquid fuel, liquid petroleum gas, gasolines, jet fuel and diesel) by employing various technologies such as distillation extraction, reforming, cracking and others (Katzer, Ramage and Sapre, 2000). Therefore, increasing attention on the chemistry of diesel fuel processes with regard to challenges that refineries and auto-motives have been looking on the reduction of the released sulphur and sulphur oxides into the air from the combustion (Song and Ma, 2003).

According to Chevron (2007), diesel is one of the most widely used forms of energy for: road transportation such as trucks and buses which are used to transport or move goods from manufacturers to consumers and long-distance public transportation, farming, rail transportation, electrical power generation, marine shipping and military transportation. Environmental restrictions regarding the quality of fuels produced and emissions from the refineries and automotive combustions have been made from different countries to decrease the sulphur content for past decades (Lam et al., 2012).

Sulphur is the third most abundant element in diesel and a global concern due to the combustion of the sulphur compounds present in diesel from the engines used in the major applications mentioned above. The compounds such as thiophene, mercaptan and sulphides burn to form sulphur dioxide (SO_2) during the combustion process (complete or incomplete combustion) which in turn reacts with oxygen and moisture in the atmosphere to produce sulphur trioxide (SO_3) and acid rain pollutants that are both harmful (dangerous and toxic) to the environment (see Figure 1.1). Sulphur compounds in petroleum fractions also cause poisoning of catalytic converters used in automotive engines and corrosion in engines combustion (Zaheer and Syed, 2010). In this regard, the implementation of global industrial regulation requires that the sulphur content of

refinery diesel be reduced from 15 to 10 ppm (Gatan, 2004) with a sulphur content of 10 ppm in South Africa diesel is being used.

In addition to the sulphur content in liquid fuels, the sulphur compounds present in the gases are also a source of environmental concern. Hydrogen sulphide is the most common sulphur component in process gases that are toxic, corrosive and burn to form SO_2. The main sources of H_2S emissions are: oil refineries, natural gas processing, coal mines, and coke ovens. The main concerns regarding H_2S emissions come from the refining of crude oil, coal and acid natural gas processing, where gas flows as raw waste with an H_2S content of up to 65% by volume (You, 2002).

Figure 1.1: The effects of Sulphur on the atmosphere from combustion systems. Source: Shairanada (2013).

1.2. PROBLEM STATEMENT

It should be borne in mind that several desulphurization processes have been proposed and used in the industry where diesel is produced from various material resources such as: coal, natural gas, crude oil and as an under-product. Hydrodesulphurization (HDS) is the conventional industrial process and is used to treat diesel for the removal of sulphur compounds. In the process, HDS diesel reacts with hydrogen in the presence of a metal catalyst and converts organic sulphur compounds to H_2S. The disadvantage of the HDS

process is that the process is carried out at both elevated temperature and pressure using hydrogen resulting in high investment and operating costs. Shockingly due to stereo clutter (delay), hydrodesulphurization is inefficient at removing complex thiophene derivatives (Zaheer and Syed, 2010; Campos-Matin, 2010).

The environmental challenges in sulphur contamination poses conditions on fuel production with specific to air, terrestrial and aquatic impacts as points of reference for contamination. Those conditions are driven by legislators to change the fuel specifications and in what quantities the contaminants and properties should be in fuel. Consequently, fuel properties need to be less harmful to the environment. Petrol, diesel and jet fuel are among the main energy sources for transportation in South Africa (Randal Marius Colin Albertus, 2012). A significant environmental pollution in South Africa is due to road vehicle transportation which causes drought air pollution and land dryness. However, the small changes in the fuel quality can result in a good control of the environmental impact on the pollution from the end-users. The refinery investigation results in the technologies and processes that are more energy intensive than current practices or uses substances that are more hazardous than those currently in use (De Klerk, 2007).

In addition, a mixture of crude synthesis gas is mainly composed of hydrogen and carbon monoxide, that is used for commercially interesting applications such as Fischer-Tropsch in the production of synthetic liquid fuel, solid oxide (SOFCs) requiring a synthesis gas enriched with hydrogen, as well as the synthesis of bulk chemicals for example: ammonia, methane and methanol. The processes mentioned above use transition metal/metal oxide catalysts which have little or no tolerance to gaseous sulphur contaminants, for example: H_2S, COS that act as catalyst poisons. In addition, H_2S in synthesis gas is the main cause of corrosion of pipelines, instruments and equipment used to transport gas. Therefore, the concentration of H_2S in the raw synthesis gas must be reduced to less than 1 ppm for most commercial applications (Behl, 2014).

Although conventional H_2S removal technologies like Rectisol and Claus have been found to be effective, they are energy intensive, require substantial investment and operational costs. According to Chevron (2007), when sulphur is emitted into the atmosphere from engine combustion via exhausts this may have a negative impact on both health and

environmental conditions. If sulphur is emitted to the atmosphere, it may lead to longer term exposure of high levels of SO_2 in conjunction with high levels of particulate matter (PM), respiratory sickness, alteration in the lungs, defences and aggravation of existing cardiovascular diseases, effect on aqua-lives, dryness of lands and sulphur dioxide together with NO_x are the major precursors to acidic rain.

1.3. JUSTIFICATION OF STUDY

Activated carbon has attracted special attention because of its high adsorption capacity, its large surface area which can be chemically modified using different methods. Chemical and thermal stability, low cost of production which makes them profitable for large-scale production, and a wide structural variety. All of these make the active carbon ideal for the adsorption of gaseous and aromatic sulphur compounds (Noora Naïf Darwish, 2015).

Recently, many adsorbents having various physical and chemical properties have been developed for the purpose of studying their adsorption capacity for the removal of sulphur compounds. The increasing attention on these absorbents has been directed to carbon-based materials such as activated carbon (Bamufleh, 2009), carbon nanotubes (Zaheer and Syed, 2010) and graphene (Wang and Yang, 2013).

Carbon materials at the nanoscale level, named nano-carbon materials, because of not only exhibiting better properties compare to those of conventional or microscale materials, but also possess new characteristics that conventional materials lack. Both nanomaterials and carbon materials are attracting quite a bit of attention within the scope of material science and technology. Recent studies proved that nano-carbon materials could be use as medical materials, electronic materials and environmental protection materials, all of which are revolutionary materials in the twenty-first century (Wang et al., 2014).

Graphene has also received increased global attention due to its large surface area, electronic conductivity capacity, high mechanical strength, and thermal properties. It is a two-dimensional carbon material and it can be produced from graphite using a number of different techniques with the simplest being the Hummer’s method. One of the best ways

to harness the unique properties of graphene is to incorporate it as a composite (Dubey et al., 2015). Previous studies (Lonkar et al., 2016) investigated adsorption using metal oxide/reduced graphene composites for the removal of H_2S in syngas and organic sulphur compounds in diesel (Song, 2014).

Despite the fact that the physicochemical characteristics of the functionalized metal oxide and carbon nanocomposites and their desulphurization potential have been studied individually, little work has been done to determine the difference between MeO/AC and MeO/GO in terms of equilibrium adsorption capacity, kinetics, and rendering. In addition, current South African legislation requires a concentration of 10 ppmw of sulphur in diesel. This study aims to synthesize adsorbents capable of reducing sulphur concentrations to less than 10 ppmw than the actual from the market, according to Euro 5 (Nazal, 2015).

The oxygen functional groups present on the surface for both graphene oxide and the activated carbon surface significantly improve the adsorption process; this is due to their redox properties that allow them to act as active centres that anchor catalyst precursors and metal ions. When used for the synthesis of metal oxide composites, graphene oxide and activated carbon not only support the metal oxide, but also act as an active catalyst. Deposition of metal oxides on the carbon surface effectively captures chemisorption-containing sulphur compounds where π-electron interactions occur, thereby increasing the adsorption capacity and selectivity of adsorbents (Bagheri, 2016), (Fallah, 2012).

1.4. RESEARCH QUESTIONS

- Can carbon-based metal oxide nanocomposite be effective to reduce sulphur in the diesel fuel?
- Can the sulphur adsorption capacity on the Activated Carbon (AC) and Graphene Oxide (GO) be improved by depositing metal oxides onto their surfaces?
- How can sulphur adsorption performance be effective on activated carbon-based adsorbents, compared to that of graphene-based adsorbents?

- In what way can the sorbent synthesis method be used to influence desulphurization capability?
- Can the carbon metal oxide nanocomposite be a good choice to reduce sulphur in diesel, and if so, to what extent?
- At which temperature and pressure can sulphur be reduced as far as possible from diesel by using carbon-based metal oxide nanocomposites with very low wear for the engine at very low temperature operability?

1.5. RESEARCH-AIM

The main aim of this study is:

Desulphurization of diesel fuel using carbon-based metal oxide nanocomposites.

1.5.1. SPECIFIC OBJECTIVES

1. To evaluate the desulphurization and re-generable performance of activated carbon-based adsorbents and graphene-based adsorbents.
2. To synthesize MeO/GAC and MeO/GO nanocomposites using chemical and thermal methods.
3. To characterize the adsorbents before and after sulphidation using the X-ray diffractometer (XRD), Fourier transform infrared spectroscopy (FT-IR), Brunauer, Emmett and Teller analyser (BET), scanning electron microscope (SEM), and thermo-gravimetric analysis (TGA).
4. To investigate the effects of operational conditions on desulphurization efficiency by using different sorbents.
5. To study the adsorption isotherms and the kinetic models of the sorbents.

1.6. REPORT STRUCTURES

This thesis has the following structures and are given as chapters:

- Chapter 1: Introduction.

The chapter is providing the introduction of the thesis, research topic, and the statement of the problem in the regard of sulphur content in diesel fuel, the justification and objectives of the research.

- Chapter 2: Literature review.

This chapter provides a clear understanding and extensive literature review on the desulphurisation methods used previously and currently being used for diesel fuel.

- Chapter 3: Experimental methodology.

The chapter provides details on the experimental methods, setups, adsorption and adsorbent synthesis methods, operational parameters and procedures, regeneration of adsorbents and lastly adsorbent characterization methods.

- Chapter 4: Results, discussion and findings.

The chapter gives a clear understanding on the results obtained from the sample collections and the discussion of each depending on the specific methodology of the experiment.

More continuous explanation of the research data collections is discussed to give more details and understanding of the research findings.

- Chapter 5: Conclusion and recommendations.

The results and finding of the research work presented in the thesis were summarized and recommendations were given for proposed future studies.

CHAPTER 2: LITERATURE REVIEW

Sulphur content in diesel fuel affects particulate matter (PM) emission because some of it in the fuel is converted to sulphate particulates in the exhaust. The fraction converted to PM varies from one engine to another but reducing sulphur decreases PM linearly (up to a point that sulphur is not the only source of PM) in almost all engines. Limited sulphur content of on-road diesel from 10 – 15 ppm was achieved from the year 2006 to 2009 and was called ultra-low sulphur diesel fuel in Europe-Asia. With Health and Environmental effects by sulphur contaminant once long-term exposure of high levels of SO_2. In conjunction with high level of PM, health issues including respiratory illness, alterations in the lungs, defences and aggravation of existing cardiovascular disease occur. Together SO_2 with NO_x are the major precursors to acidic deposition (acid rain), whilst sulphur dioxide is also a major precursor to 2.5 PM (De Klerk et al., 2007; Chevron et al., 2007).

According to Meckinly (2003), gasoline is characterized by its lowest boiling point range due to the existence of impurities with lower boiling points, including thiophene and its alkyl derivatives. Both diesel and gasoline fuels are favoured due to several reasons; for example, high energy associated with them, their availability, and simple storage and safety issues that are easy to handle. As mentioned earlier, petroleum products or petroleum distillates, including gasoline, diesel fuel, and jet fuel, are defined as complex mixtures of organic molecules or compounds. Such complex mixtures are classified according to their boiling point ranges. Variations in the boiling point ranges are controlled by the type of sulphur compounds or impurities mainly contained in the petroleum product. Diesel fuel is characterized by its highest boiling point range. This is due to the existence of the heaviest sulphur compounds or impurities, such as dibenzothiophene (DBT) and its alkyl derivatives.

The main emissions of SO_x, NO_x, CO_2 and CO are associated with the combustion of diesel fuels. Generally, these emissions can be reduced through the reduction/elimination of the amount of sulphur compounds contained in the diesel fuel. This can be achieved either by utilizing different desulphurization processes for the fuel products, which is commonly carried out using the catalytic hydrogen processing approaches, or by removing sulphur compounds contained in stack gases. BT and DBT compounds

contained in diesel feeds compose around fifty percent of the total sulphur compounds available in most diesel fuels. However, the C_2-DBT compounds, including 4, 6dimethyldibenzothiophene (4, 6-DMDBT), compose most of the sulphur compounds in low sulphur diesel fuels which is the diesel oil produced after the HDS process. The preferred limit of sulphur content in diesel fuels is around 0.1 ppm by weight provided that the main sulphur compounds existing in most hydro-Desulphurized diesel include the alkyl DBTs with alkyl groups at 4- or/and 6-positions (Jawad, 2008; Ma et al., 2006). Moreover, converting normal diesel oil to clean or ultra-deep Desulphurized diesel oil is a complicated process that is controlled by several factors that have considerable effects on the desulphurization process. These factors include the type of the catalysts used, the selected operating conditions, feedstock source, reactivity of sulphur compounds, and other impurities contained in the diesel oil (Marafi and Rana, 2010).

The adsorption of desulphurization of diesel fuel uses three types of carbon-based adsorbents. High percentages of the crude oil, including the diesel oil and gasoline, are used widely in different transportation applications. Such fuels contain high contents of sulphur compounds or sulphur impurities, mainly in the form of organic sulphur compounds. Reducing and/or eliminating such compounds is essential; this is because the quality of fuel is significantly affected by the present impurities, such as the sulphur and nitrogen compounds. Moreover, sulphur emissions are the most critical environmental issue that needs to be controlled through specifying and allowable sulphur content limits in the different types of fuels. The control limit is required due to the negative effects of sulphur emissions on air quality. Diesel oil is composed mainly of complex mixtures of hydrocarbon compounds that have different boiling points and molecular weights (Darwish, 2015).

In recent years, various environmental/climate change issues, in particular global warming, have been gaining major importance among researchers. Greenhouse gases that are emitted directly to the atmosphere because of combusting the different petroleum products are the major causes of global warming. Currently, direct-injection diesel oil engines are utilized extensively. This is due to their high thermal efficiency and low emission rates compared to other types of diesel engines. However, reducing the emissions produced from these engines is still of critical necessity due to their harmful

impacts on the environment. Furthermore, one of the main reasons for reducing such emissions is the stringent emission regulations initiated and imposed by several countries in order to protect the environment (Al-Hamad and Bamufleh, 2009). Reducing the exhaust emissions can be achieved through either improving the process of oil combustion or improving the properties of fuel that are directly related to its quality. Improving the quality of any fuel can be achieved by enhancing the ignition quality associated with that fuel, such as Cetane Number (CN), aromatic content, distillation temperature and viscosity (Sertic-Bionda et al, 2010).

According to Cooper (2002) and Perry and Harrison (1986), the combustion process generates sulphur emissions in the form of sulphur dioxide (SO_2), responsible for damaging the plants by chlorosis, and sulphur trioxide (SO_3). However, the concentration of SO_2 in the atmosphere is very low, as its concentration in urban areas does not exceed 0.5 ppm; thus, its effects on human health are not clear. Moreover, SO_2 is of little concern due to the fact that once it exists in the atmosphere, it is oxidized in gaseous and aqueous phases to form sulphate and sulphite. Most of the sulphur compounds in the gaseous phase react with the hydroxyl radicals through the reaction (1), where around 15% of the sulphur was oxidized:

$$SO_2 + 2OH^- \rightarrow H_2SO_4 \quad (1)$$

In the aqueous phase, the oxidation process takes place in the water droplets and follows the set of reactions:

$$SO_2 + H_2O \rightarrow SO_2.H_2O \quad (2)$$

$$SO_2.H_2O \rightarrow H^+ + SO_3^- \quad (3)$$

$$SO_2 + 2OH^- \rightarrow H_2SO_4 \quad (4)$$

$$HSO_3^- + O_3 + H^+ \rightarrow H_2SO_4 + O_2 \quad (5)$$

2.1. TYPES OF DESULPHURIZATION PROCESSES

In recent years, various techniques and technologies have been employed to focus on the reduction of sulphur content due to its environmental impact from fuel and oil, especially diesel during combustion processes. Some of those processes are hydrogen consuming processes (hydrodesulphurization), oxidative desulphurization, biological sulphur removal, extractive desulphurization, photochemical desulphurization and adsorptive desulphurization.

2.1.1. HYDRODESULPHURIZATION

The catalytic process consuming hydrogen or hydrodesulphurization (HDS) is the catalytic process, which is commonly used to reduce and/or remove organic sulphur compounds contained in hydrocarbons. However, this process is associated with the use of extremely harsh conditions at high temperature (up to 400 °C) and pressure (up to 100 bar) and extensive catalysts (Rang, Kann and Oja, 2006). In addition, one of the main inefficient aspects of this process is its low efficiency in removing certain sulphur compounds, including thiophenes and multi-ring aromatics. This is due to the fact that such compounds require a high consumption of hydrogen as well as difficult operating conditions at temperature and pressure. Thus, due to the high cost and the various limitations which are associated with the HDS process, alternative or complementary technologies are increasingly selected in the petroleum industry. These include desulphurization by adsorption, desulphurization by extraction, biological sulphur removal and desulphurization by oxidation. The main objective of these technologies is to find an efficient alternative for the desulphurization of weakly reactive sterically hindered alkyl DBTs. Desulphurization by adsorption processes are among the best techniques that are economically attractive and respectful of the environment. This is due to their simple operating conditions, the availability of economical and re-generable absorbent materials (Stanislaus, Marafi and Rana, 2010).

Likewise, known HDS is the conventional process used for the removal of sulphur compounds contained in diesel oil. However, the process has a number of limitations which have forced the petroleum refineries to seek other alternative processes. The

adsorption desulphurization process is one of the alternative methods suggested for the HDS. Various adsorbents, such as reduced metals, metal oxides, activated charcoal, alumina, metal sulphides, zeolites and silica are being used in this regard (Malki, 2004, Van Veen and Ito, 2006). Desulphurization by adsorption is simply accomplish by placing an active adsorbent on a porous, unreactive substrate that tolerates a high surface area for the adsorption of sulphur compounds (Bharvani and Henderson, 2014). This process mainly used for the removal of certain impurities contained in fuels such as aromatics from aliphatic and refractory sulphur compounds. The removal of such molecules can be achieved by different suggested methods, such as replacing the catalysts used with other highly active catalysts, or using higher temperatures and pressures, or adjusting the end point of the feed, or using purer hydrogen, or by increasing the partial pressure of the hydrogen, or by increasing the volume of the reactor by adding one or more reactors, or by removing H_2S from the recycled gas and finally improving the distribution of the charge to the trickle-bed reactor (Noora Naïf Darwish, 2015).

2.1.2. OXIDATIVE DESULPHURIZATION

The work done by Dasgupta et al., (2009) and Noora Naïf Darwish (2015) found that hydrogen peroxide-formic acid has been used as an oxidizing reagent for the sulphur compounds present in diesel oil with a total sulphur content of 500 ppm. Their results showed that after oxidizing the sulphur contained in the oil with the aforementioned reagent, a complete conversion of the DBT into DBT-sulphones suggested that either extraction or adsorption can be attained in the removal of sulphur. The effect of applying the ultrasound during the oxidation process, was examined. The results showed a good enhancement on the efficiency of oxidizing sulphur compounds into their sulphones. Successful implementation of ODS can be achieved in refinery applications by integrating the ODS unit with the diesel hydro-treating unit. When the oxidative desulphurization method is utilized as a second step after the HDS unit, it can produce low sulphur diesel (approximately 500 ppm) down to ultra-low sulphur diesel (ULSD) (less than 10ppm). Nevertheless, even when applying this technology, the cost on reduction is still limited

because the deep desulphurization through HDS process requires elevated temperature and pressure (Stanislaus, Marafi and Rana, 2010).

Moreover, the combination of the ODS process in the presence of molecular oxygen and a catalytic component such as iron (III) salts with an adsorptive desulphurization using activated carbon (AC). Results showed that the use of Iron (III) salts are effective in converting the benzothiophenic compounds contained in the fuel to sulphones or sulphoxides (Zhou, Song and Ma, 2007). The catalytic oxidation of the sulphur compounds contained in the liquid hydrocarbon fuels to form sulphones and sulphoxides increased the adsorption of sulphur compounds significantly because the ACs showed higher adsorption affinity for both sulphones and sulphoxides compared to thiophenic compounds. It was shown that the advantages of the ODS process include the low temperature and pressure requirements for the reaction, as well as the absence of hydrogen. Moreover, the ability of converting the refractory-S-containing compounds by oxidation is another important feature of the ODS (Nair, 2010).

2.1.3. EXTRACTIVE DESULPHURIZATION

Extractive desulphurization is another alternative in the production of ultra-low sulphur diesel oil. Nowadays, researchers consider the extractive desulphurization as a promising technology due to the significant cost reduction as no hydrogen is used, the mild conditions that are required (ambient temperature and pressure) and the wide range of fuels that can deal with including all kinds of middle distillates. In this process, the sulphur compounds removal was obtained using selective solvents (Noora Naïf Darwish, 2015 and Alexander Samokhvalov, 2012).

2.1.3.1. CONVENTIONAL EXTRACTIVE DESULPHURIZATION

The conventional solvent extraction technique has been in practice for the removal of sulphur compounds from petroleum feeds. This process is based on the solvent's polarity. For this process to be efficient, solvents should show higher solubility of the organo-sulphur compounds contained in the fuel when compared with their solubilities in the

hydrocarbons. Thus, increasing the efficiency of this process is related to the optimization of the operating conditions to maximize the sulphur extraction and the careful selection of the required extractants (Dastgheib, Elham and Moosavi, 2012) (Aida and Funakoshi, 1998). Several solvents have been examined for the removal of sulphur compounds, for example acetone, carbon disulphide, ethanol, dimethyl sulfoxide (DMSO), n-butyl alcohol, methanol, lactones, n-containing solvents and water. Solvent polarity is not the only parameter that governs the process of selecting the appropriate solvent; other factors need to be considered carefully as they may affect the separation and recovery of the solvent. These factors include melting point, boiling point and surface tension. However, this process is characterised by a poor sulphur removal capacity that resulted from the slight difference of the polarity between the contained sulphur compounds and the aromatic hydrocarbons (Dastgheib, Elham, and Moosavi, 2012).

Different studies have investigated the use of extractive desulphurization for the removal of sulphur compounds. The light oil was mixed with different organic solvents like DMSO, acetonitrile and tetramethylenesulphone at ambient conditions in order to examine the sulphur compounds and aromatics extractability (Topalova and Toteva, 2007). This study showed that the extraction equilibrium between the oil and the solvents was attained in about five minutes whereas the phase separation was attained in ten minutes or less. The main conclusion was drawn from this study is that the most suitable solvent for light oils or distillates is the acetonitrile. Another study utilized a two-stage extraction process with dimethylformamide as a solvent. Results showed that the sulphur content in diesel oil was reduced from 2.0 wt.% to around 0.33 wt.% (Topalova and Toteva, 2007). In spite of the fact that ultra-low sulphur content cannot be attained using the aforementioned solvents, the polarity and the solubility of the sulphur compounds in the solvent can be improved by oxidizing the sulphur compounds before employing the extraction step.

2.1.3.2. EXTRACTION USING IONIC LIQUIDS

Ionic liquids (ILs) are defined as salt in the liquid state: salt whose melting points are below some arbitrary temperature like 100 °C. Currently, ILs are applied widely in the liquid-liquid extraction processes due to their flexibility in modulating their hydrophobic or hydrophilic nature by modifying the cations and anions (Edward, Maginn, and Brennecke, 2004). ILs have been used in chemical industries, pharmaceuticals, algae processing, gas separation, nuclear fuel reprocessing, solar thermal energy, waste recycling and fuel desulphurization. Some types of ILs, such as tetrafluoroborate, chloroaluminate and hexafluorophosphate are efficient in the extraction of DBT derivatives contained in diesel oil. The first study that was published related to the deep desulphurization of industrial diesel oil by extractive desulphurization using ionic liquids was conducted by Bösmann (2001). In this study, chloroaluminate ionic liquids were used, and results showed that by using a five-stage-extraction process operated at a temperature of 60 °C, around 80% of the available sulphur compounds can be removed successfully. However, hydrolytic instability was created, which made it difficult to be used.

Afterwards, a number of studies considered the extractive desulphurization of sulphur compounds from diesel oil using stable ILs. The main challenge that researchers faced was to find an efficient way to regenerate the ILs. This is because regenerating the ILs using distillation or stripping was inefficient (Zhu et al., 2009). This is mainly because of the significantly low vapour pressure of the sulphur compounds extracted and contained in the IL. A suggested solution was to apply the re-extraction procedures; however, significant amounts of solvents were required for the process. In Lopez-Martin (2008), experienced the use of different ionic liquids with different cation classes, such as pyridinium and pyrrolidinium, and a set of anion classes for liquid-liquid extraction of DBT and dodecane. Results indicated that the partition ratio of DBT to the IL showed a clear variation with cation class when compared to the variation with anion class. It was found that the highest extraction potential is attained using a poly-aromatic quinolinium-based ionic liquid.

Another study Noora et al. (2015) indicated that there is a direct proportionality between the absorption capacity of ILs and the number of alkyl groups. Results showed that using

different ILs based on 3-methylimidazolium (MIM) such as 1-alkyl 3-methylimid-azolium (AMIM), butyl 3-methylimidazolium (BMIM) and ethyl 3-methylimidazolium (EMIM), increased the absorption capacity of thiophene to higher than 2-methylthiophene. Advances in liquid-liquid extraction technologies involve combining oxidative desulphurization and ILs. This approach is capable of removing sulphur species from DBT model diesel oil by around 96.1%, which is much better than that of either using the conventional solvent extraction approach or the oxidative desulphurization (Zhu et al., 2009)

2.1.4. PHOTOCHEMICAL DESULPHURIZATION

In this process, organosulphur compounds were removed from fuel oil by liquid extraction as a first step and a polar solvent such as water or acetonitrile is used. A process called photochemical oxidation, and is carried out in the solvent phase, followed this. This leads to the accumulation of sulphoxides and sulphones in the polar phase (Thomas, 2008).

2.1.5. BIOLOGICAL SULPHUR REMOVAL

Another process for the sulphur removal from fossil fuel is through bio-desulphurization (BDS). BDS has been used significantly where organosulphur compounds are bio-transformed to the corresponding sulphones or sulphoxides by bio-catalytic activity. The basis for this process is the removal of organosulphur compounds present in the fuels while keeping the carbon structure unchanged (Samokhvalov, 2012). Micro-organisms need sulphur to achieve both growth and biological activity as it forms around 1% of the dry weight of the bacterial cell. Some micro-organisms have the ability to supply their needed sulphur from various sources because sulphur exists in the structure of some enzyme's cofactors, amino acids and proteins. Some micro-organisms have the ability to consume sulphur in the thiophenic compounds and thus reduce the sulphur content in the fuel. This method is considered as an advantageous process as it can be conducted under mild conditions (room temperature and pressure) and requires biocatalysts or

enzymes that make this process highly selective. However, it is also characterised by a low bio-catalytic activity and low stability of the biocatalysts afterward (Nair et al., 2010).

Note that both aerobic and anaerobic micro-organisms are effective in the desulphurization process while protecting the aliphatic and aromatic contents of the fuel. The bio-desulphurization process has been conducted using R-sphaericus, Rhodococcuserythropolis, Arthrobactersp and R-rhodochrous under mesophilic conditions (temperature range of 25 to 40^{o}C) and using Paenibacillus sp. under thermophilic conditions (under a temperature higher than 50^{o}C) (Lee et al., 1999). However, the main challenge in the use of bio-desulphurization as an alternative industrial method for producing ultra-low sulphur content is the isolation or design of a microbial strain that is characterised by a higher efficiency. Different studies are considering the use of BDS for the removal of sulphur compounds especially the least reactive ones in the HDS, such as the sterically hindered alkyl-DBTs (Ball and Mohebali, 2018).

In Ball and Mohebali (2018), it was found that Rhodococcus sp. has the ability to use DBT as a source of sulphur and the results proved that it has the ability to transform DBT into sulphite and 2-hydroxybiphenyl that builds up in the medium. Although some researchers are focusing on implementing the BDS processes on a large scale, the BDS rates are still low when compared to the HDS. This is due to the limitations that the process was facing. Main limitations include the need to enhance the thermal stability of desulphurization, the limited transport of the sulphur compounds from the oil to the membrane of the bacterial cell and the limited ability to recover the biocatalyst (Darwish, 2015).

Most BDS processes are used currently as complementary steps for deep desulphurization, where the BDS is integrated with the existing HDS units. BDS have been used either before or after the HDS unit. Some researchers have suggested that the BDS should follow the HDS in order to achieve the removal of the remaining sulphur compounds that have the lowest reactivity with the HDS. Other researchers believe that employing the BDS before HDS is more efficient as a major part of the hydro-treating resistant compounds with result in less hydrogen consumption in the HDS unit (Darwish, 2015).

2.2. ADSORPTION

Adsorption is a process used to remove undesirable compounds in the fluid stream by passing the current through a bed of solid material (Maldonaldo 2004). Surface adsorption mechanisms on a solid can be classified into two categories that are either physical sorption or chemical sorption. In physical sorption, the adsorbate molecules adhere to the solid adsorbent via weak Van der Waal or electrostatic forces. The adsorption process is multi-layered and not limited by the availability of the solid surface. Physical sorption is generally exothermic, and it can be reversed by increasing the process temperature or decreasing the pressure of the gaseous adsorbate (Song, 2002; Maldonaldo et al., 2004). In chemisorption a chemical reaction between the solid adsorbent and the adsorbate occurs. The process is much slower than that of physical sorption and limited by the formation of a single layer of monomolecular adsorbate. Chemisorption is irreversible and usually involves breaking a π – bond and requires activation energy (Darwish, 2015).

From an economic point of view, a good adsorbent should allow deep desulphurization below 100 ppmv (parts per million by volume) (Karayilan, 2004) while maintaining its desulphurization properties over a large number of sulphurization regeneration cycles. The required sorbent properties can be summarized as follows:

- It should have high sulphur removal selectivity, without any undesirable side-reaction.
- Its sulphur loading capacity should be high in order to reduce the size of the reactor and minimize operational cost.
- It must retain its structural integrity and mechanical stability and chemical properties over extended periods of use.
- It must provide good, simple re-generability.

The adsorption of desulphurization of diesel fuel uses three types of carbon-based adsorbents (Zhou, Ma and Song, 2009). High percentages of the crude oil, including the diesel oil and gasoline are used widely in different transportation applications. Such fuels contain high contents of sulphur compounds or sulphur impurities, mainly in the form of organic sulphur compounds. Reducing and/or eliminating such compounds is essential; this is because the quality of fuel with it is significantly affected by the present

impurities, such as the sulphur and nitrogen compounds (Doung, 1998; Reed, 2008). Moreover, sulphur emissions are the most critical environmental issue that need control through specifying and allowable sulphur content limits in the different types of fuels. The control limit is required due to the negative effects of sulphur emissions on air quality. Diesel oil is composed mainly of complex mixtures of hydrocarbon compounds that have different boiling points and molecular weights (Darwish, 2015).

2.2.1. ADSORPTIVE DESULPHURIZATION

Regarding Selective Adsorption of sulphur compounds found in diesel oil is an economically acceptable and alternative for the attainment of diesel oil with low sulphur content (EAP diesel RIA 2000, Flora et al., 2005). Adsorptive desulphurization processes are among the most economically attractive techniques due to their simple operating conditions, the availability of inexpensive and re-generable adsorbents such as reduced metals, metal oxides, alumina, metal sulphides, zeolites, silica and activated carbon (Darwish, 2015). This process occurs as the sulphur molecules attach to the adsorbent and stay there separate from the fuel. The main part of any adsorption process is a porous solid medium as it offers high surface area or high micropore volume and convert into high adsorption capacity (Srivastava and Srivastav, 2009).

There are three different mechanisms for adsorption separation in a form of steric, equilibrium and kinetic mechanisms (Darwish, 2015). An adsorption separation is said to be a steric mechanism if the dimensions of the pores of the porous solid medium allow the small molecules to enter while prohibiting the large molecules. However, it can also be called an equilibrium mechanism if the solid medium has different abilities to accommodate different species according to the strength of the adsorbing species. Moreover, kinetic separation mechanism is based on the rate of diffusion of different species into the pores. Adsorption process is classified into two categories: physical adsorption (physisorption) or chemical adsorption (chemisorptions) according to the nature of the adsorbent-sorbate interaction (Ma et al., 2016).

The most important challenge in adsorptive desulphurization is in producing an easily remunerable adsorbent that is characterised by high adsorption capacity and high

selectivity incoming for the removal of refractory aromatic sulphur compounds, which are not removed through the HDS process (Ng and Jiang, 2006). Most adsorbents are modified through different treatment techniques, such as metal impregnation and oxidation, in order to improve their affinities for the TC removal from liquid fuels. For example, activated carbon, alumina, silica and zeolites are impregnated with different transition metals, including copper, nickel, zinc, iron and lead in order to produce an adsorbent with higher TC removal capacities for both model and commercial fuels (Jiang and Ng, 2006).

The TC adsorption is controlled by different factors such as the chemical interactions between the metals impregnated with the adsorbents and the thiophenic molecules, as well as the adsorbent pore geometry. Moreover, according to the fact that the diesel fuel contains sulphur compounds, nitrogen compounds, as well as a large number of aromatic compounds that have an aromatic skeleton structure similar to the coexisting sulphur compounds. There is a great challenge in developing an effective adsorptive desulphurization process that is able to select the adsorption of the sulphur compounds (Ng and Jiang et al., 2006 and Ma, Sprague and Song, 2005).

2.2.1.1. MERITS OF ADSORPTIVE DESULPHURIZATION

Currently, adsorptive desulphurization appears as a promising alternative for HDS for several reasons. Adsorptive desulphurization is considered as an effective process for the separation processes that involve low sorbate concentrations; thus, it is a good candidate for the removal of the contained refractory sulphur compounds in the feed streams (Reed, 2008; Velu et al., 2005). The adsorptive desulphurization process requires mild conditions (i.e. low temperature and pressure) when compared with several other sulphur removal techniques, especially the HDS- which decrease the operating cost of the process. Most of the adsorbents used can be regenerated easily either by thermal processes, or by washing with a solvent. Most sorbent properties such as the adsorption capacity, surface area and selectively are directly affected by their structure and composition. These properties may be enhanced by modifying their preparation methods and conditions (Darwish, 2015).

2.2.1.2. ADSORBENTS AND THEIR PROPERTIES

The porous solid medium for a certain adsorption process is usually considered as a critical variable. Performing a successful adsorption process depends on the performance of the solid medium in equilibria and kinetics (Darwish, 2015). A solid medium that is characterized by acceptable adsorption capacity and slow kinetics is not efficient, as it requires a long time for the adsorbate molecules to reach the particle interior. In addition, a solid medium is characterised by fast kinetics and low capacity is not efficient either as a large amount of adsorbent is required. Therefore, the solid medium should have high adsorption capacity and good kinetics which can be attained if the solid medium has a reasonably high surface area or micropore volume and relatively large pore network for the transport of the molecules to the interior (Doung, 1998).

Adsorbents can be classified according to their physical, chemical and dynamic properties. The physical properties include surface area, particle size, pore volume as well as some mechanical properties. The dynamic properties include the selectivity, capacity and re-generability of the adsorbents taken into account in selecting the adsorbent in order to achieve the required goals. Chemical properties also related to the composition and structure of the adsorbents, acid and base properties, and electrostatic properties (Darwish, 2015).

2.2.1.3. ADSORPTION AT SOLID SURFACES

Generally, physical adsorption takes place due to Van der Waals forces and electrostatic forces in molecules with a permanent dipole moment. Sulphur molecules are adsorbed onto the solid surface through physical adsorption (physisorption) or chemical adsorption (chemisorption). In physical adsorption, the forces that attract a molecule to the surface do not change the adsorbate molecule and are usually weak (Darwish, 2015). However, in the chemical adsorption chemical bonds are formed between the adsorbate molecule and the surface. This is a result of one or more free valences on the surface of an adsorbent material resulted from the broken covalent bonds between atoms at the surface. This causes an imbalance of forces at the surface as well as a net surface energy at the free valences (Velu et al., 2005). Chemical adsorption involves molecular

interactions with these free valences, which leads to a monolayer coverage on the surface of the adsorbent. Chemical adsorption that involves dissociation of the adsorbed molecules is referred to as dissociative adsorption. However, molecules that are adsorbed chemically through pi-electrons and lone pair electrons do not necessarily go through dissociation, yet they participate in free valences via non-dissociative adsorption (Bond, 2007).

2.2.2. MATERIALS USED FOR ADSORPTIVE DESULPHURIZATION

Adsorptive desulphurization is based on removing the organo-sulphur compounds from the liquid hydrocarbon fuels while keeping the other compounds present in the fuel unchanged (Zubaidy, 2013). Several materials have been developed and tested to improve the adsorptive desulphurization process. Generally, the performance of the sorbent material used is estimated by its dynamic properties, such as selectivity for sulphur compounds and the ease of re-generability (Darwish, 2015).

2.2.2.1. ADSORPTION ON CARBON MATERIALS AND ACTIVATED CARBON

Several studies have explored the adsorption of different sulphur compounds, including BT, DBT and 4,6 –DMDBT, from both model and commercial fuels using various types of activated carbon (Darwish, 2015). Song and his colleagues have performed a set of experiments on adsorptive desulphurization for various types of fuels using different adsorbents, such as transition metals supported on different porous materials, activated carbon, zeolites and metal oxides. Such studies helped researchers to propose a new process that consists of three main stages, which are the selective adsorption for sulphur removal, the recovery of the concentrated sulphur compounds and finally hydrodesulphurization of the concentrated sulphur compounds (Reinoso and Marsh 2006; Li et al., 2013).

AC has been used and studied widely for the removal of TC from different fuels. Moreover, the slit shape geometry of the pores of the activated carbon is suitable for the aromatic compound’s adsorption in comparison with the cylindrical zeolite pores that are suitable

for non-planer molecules adsorption (Rodríguez-Reinoso, 1998, Ma, Song and Zhou, 2006). Activated carbons (AC) are characterized by their low cost, both thermal and chemical stability under anoxic conditions, high and tuneable surface area that is widely affected by the precursors of carbonaceous materials and the preparation methods, modification receptivity, and high affinity to adsorption of both aromatic and refractory sulphur compounds (Zhou, Ma and Song, 2009).

In general, AC is mainly a micro-porous solid, however, besides micro-pores, it may contain meso and macropores (Darwish, 2015). The gas-adsorbing carbons typically have more micropores whereas the liquid-adsorbing carbons have significant mesopores that are important because of the larger size of liquid molecules (Li et al., 2013). Mostly, activated carbons were utilized for the adsorption of compounds that have weaker polarity from gas phase or polar fluid-phase, such as the adsorption of organics in wastewater. Consequently, the major challenge of using adsorptive desulphurization for liquid hydrocarbon fuels is to selectively separate the sulphur compounds with low polarity from a non-polar fluid phase (Zhou et al., 2006).

Lu (2007) investigated the effects of certain modification approaches, such as the use of steam and concentrated H_2SO_4, on the adsorption capacity. The adsorption experiments of DBT removal on the modified ACs were conducted using a fixed-bed flow reactor under ambient temperature and pressure. A model diesel fuel used contained DBT in heptane with a total sulphur content of 220 mg/dm^3 (Darwish et al., 2015).

According to Al-Hamad and Bamufleh (2009), granular activated carbon (GAC) was produced from dates' stones through chemical activation using $ZnCl_2$ as an activator was used as a sorbent for sulphur compounds' removal. Moreover, model diesel oil that is composed of n-$C_{10}H_{34}$ and dibenzothiophene (DBT) as sulphur-containing compound was prepared. Results showed that approximately 86% of the DBT was adsorbed during the first three hours. Sulphur adsorption increased gradually to reach a value of around 92.6% in 48 hours and no more sulphur was removed after that (Darwish et al., 2015).

In the area of adsorptive desulphurization, the study found that activated carbons are capable of removing both nitrogen compounds and refractory sulphur compounds simultaneously (Choi et al., 2004). These studies showed that at a temperature of 30 ^oC,

the adsorption capacity for sulphur compounds was around 0.098-gram sulphur; whereas, it was around 0.039-gram nitrogen per 1 gram of activated carbon (Choi and Sano, 2004). The same group of researchers proposed a two-step adsorption process for achieving ultra-low sulphur diesel (ULSD). In the first stage, both nitrogen and refractory sulphur compounds contained in the feed stream were removed via adsorptive desulphurization using activated carbon fibre; then, the treated stream was hydro-Desulphurized under mild conditions (Sugahara et al., 2005, Stanislaus, Marafi and Rana, 2010).

Moreover, Loh (2011) used different types of commercial activated carbon from different sources (pitch, apricot, coconut and wood) with surface areas that vary between 713 to 1403 m^2 /g were used, the particle size chosen for the activated carbon used varied between 400-800 µm. The adsorption process was carried out using both real diesel oil with a sulphur content of 398 ppmw (Singapore Refinery Co. Ltd.) and model diesel oil with a sulphur content of 400 ppmw (prepared by adding sulphur compounds, such as 4,6 – dimethyl dibenzothiophene, and various mono-aromatic, di-aromatic and tri-aromatic compounds to hexadecane) diesel oil in batch and fixed-bed adsorption systems. This study proved that various factors play an important role for an effective adsorption process. First, the pore size should be at least larger than the critical diameter of the adsorbate (Darwish, 2015). Second, it should also be sufficiently large in order to reduce diffusional resistance during adsorption. The sulphur removal percent reaches a maximum value of around 96%.

This study also concluded that the adsorption selectivity increases as follows: naphthalene < dibenzothiophene < 4,6-dimethyl dibenzothiophene anthracene < phenanthrene (Loh at al., 2011). The examined adsorptive desulphurization process for the removal of the refractory sulphur compounds conducted by Chidambarama (2009) with a diesel oil containing mainly dibenzothiophene (DBT), 4-methylbenzothiophene (4MDBT) and 4,6-dimethyldibenzothiophene (4,6-DMDBT) with the total sulphur compounds of 290 ppm. In this study, two commercial activated carbons A and B, modified forms of the aforementioned activated carbon, nickel loaded on modified activated carbons, alumina, silica and Y- zeolite samples were utilized for the adsorption

process (Ma et al., 2003). Results showed that the maximum value of sulphur removal was around 90.7%.

Qin and his colleagues (2009) studied the performance of Polystyrene-based activated carbon spheres (PACS) in the adsorption of sulphur-containing dibenzothiophene (DBT). The production of activated carbon was from polystyrene ion exchange resin spheres by carbonization and steam activation, which had a surface area of 1672 m^2/g and total pore volume of 1.63 cm^3/g. The fuel oil used was prepared by dissolving DBT in n-heptane with initial concentration of DBT solution varying from 0.882 g/L to 0.0882 g/L. the results showed a maximum DBT adsorption capacity of 109.36 mg/g of the PACS (Darwish, 2015).

In addition, the use of oxygen plasma to enhance the ACs greatly increased the carbon surface oxygen-containing groups (Darwish, 2015). This enhanced the adsorption capacities of DBT significantly. Moreover, this technology helped in minimizing the mass loss of the ACs as it keeps it within a narrow range of ± 2%, unlike the conventional thermal oxidation treatment that resulted in 31.7 – 91.4% mass loss. AC particles with a modified surface area of 1187 m^2/g by oxygen plasma for 30, 60 and 120 min. The working results adsorption capacities of AC_{30}, AC_{60} and AC_{120} show an increase by 35.1%, 44.7% and 49.1% respectively compared to the original AC (Zhang and Liu, 2012).

Mykola (2012) used polymer-derived carbons with incorporated heteroatom of oxygen, sulphur and phosphorus as adsorbents for sulphur compounds from diesel oil. Model fuel contained the same molar concentrations of dibenzothiophene, 4,6 DMDBT, naphthalene and 1– methylnaphthalene in mixture of decane and hexadecane (Darwish 2015). Results showed that incorporating the phosphorous to the carbon matrix has a positive effect on the adsorption process according to the fact that phosphorus species have a strong acidity. This enhanced the attraction of slightly basic dibenzothiophenes. The adsorption isotherms of low sulphur diesel oil (72 ppmw) using four different types of commercial activated carbons having a surface area of more than 1000 m^2/g (Kumar and Chandra, 2012). A Dutch company produced these activated carbons from bituminous coal to lignite. The results after the adsorption process showed the sulphur content in the diesel

oil was around 15 ppmw. This experiment was carried out in a batch system at 30^{o}C and atmospheric pressure over 18 hrs (Luis et al., 2010).

Al Zubaidy et al. (2013) studied the adsorptive desulphurization process using commercial activated carbon and carbonized date palm kernel powder at room temperature. Diesel oil used had a total sulphur content of 410 ppmw. The use of used activated carbon reduced the sulphur content by more than 54% as results, whereas, the carbonized date palm kernel powder showed lower sulphur removal efficiency.

Choi et al. (2004) used the activated carbon for the desulphurization of the straight run gas oil (SRGO) as a pre-treatment step for the HDS in order to achieve ultra-deep desulphurization under normal operating conditions. A high adsorption saturation capacity of around 0.098 g of sulphur/g of activated carbon was produced. Again, the study of Chandra and Kumar (2012) in which response surface methodology was employed for sulphur removal from model oil (dibenzothiophene; DBT dissolved in isooctane) using commercial activated carbon (CAC) as a sorbent material. Experiments perform with four input parameters with initial concentration (C_o: 100 – 900 mg/L), adsorbent dosage (m: 2 – 22 g/L), time of adsorption (t: 15 – 735 min) and temperature (T: 10 – 508 ^{o}C). The results showed highest removal of sulphur by CAC with m = 20 g/L, t = 6hr and T= 308 ^{o}C (Darwish, 2015).

The study done by Pengpanich, Hunsom, and Nunthaprechachan (2013) investigated the adsorptive desulphurization process for the removal of DBT from n-octane using sewage sludge-derived activated carbon under ambient conditions. The effect of different operating conditions, such as the type of activating agents $ZnCl_2$, HNO_3 and KOH, activating agent: char weight ratio, carbonization temperature and time on the adsorption capacity and physicochemical properties were studied and their results showed that varying all parameters has a direct effect on both surface chemistry and physicochemical properties. Varying the type of the activating agent has a clear effect on the textural properties, surface chemistry and the iodine number of the produced activated carbon. Moreover, char weight ratio, the activating agent, did not show any effect on both physicochemical properties and surface chemistry of the produced activated carbon with the exception of the activation of KOH, char weight ratio of 6 (Darwish, 2015).

Furthermore, they found that the adsorption capacity of DBT increased as the oxygen containing-groups increased. AC activated using KOH showed the highest adsorption capacity as it removes about 70.6 % of the DBT contained in the diesel oil, which is higher than that attained by the commercial activated carbon, by 1,28-fold (Pengpanich, Hunsom and Nunthaprechachan, 2013; Darwish, 2015).

2.2.2.2. OTHER ADSORBENTS

Different adsorbents are used in the adsorptive desulphurization processes. A study showed that Cu^{+} and Ag^{+} zeolite Y are efficient in adsorbing sulphur compounds contained in industrial diesel fuel. Results indicated that the sulphur compounds contained in diesel oil were reduced from 430 ppmw to 0.2 ppmw (Choi et al., 2004). Another study conducted by Yang, Hernández-Maldonado and Yang (2003) utilized nickel (II) exchanged zeolites as an adsorbent for the desulphurization of diesel oil containing initially around 297 ppmw sulphur content. This conducted experiment was at ambient temperature and pressure in a fixed-bed adsorber. The best adsorbent used was (alumina)/Ni (II) – Y which is 25 wt.% activated alumni followed by nickel (II) exchanged Zeolite – Y, which produced diesel oil with 0.22 ppmw sulphur content. Another study proved that Sodium – Y type zeolite is efficient in removing thiophenic sulphur compounds from model oils (Yang, Hernández-Maldonado and Yang et al., 2004). Moreover, metal sulphides were also used for the adsorptive desulphurization of refractory sulphur compounds from different fuels. These adsorbents are useful under ambient temperature and pressure (Ma et al., 2014).

2.2.3. APPLICATIONS USING ACTIVATED CARBON ADSORBENTS

Recently, numerous studies have been conducted on desulphurization by adsorption of H_2S in synthesis gas, as well as on sulphur compounds present in commercial fuels and models. Velu and colleagues (2003) studied the removal of 4,6-DMDBT from the refractory sulphurous compound of diesel, using ‘sense and grab’ and ’sense and ‘shoot’ approaches. In the first approach, adsorption was found to be physical when adsorbents

supported by activated carbon simply grabbed the 4,6 - DMDBT present in the diesel model, without a chemical reaction occurring. The diesel used was modelled using 220 ppmw (part per million by weight) of 4,6 - DMDBT in a mixture of decane and hexadecane solvents (Ma, Song and Velu, 2003).

The adsorption performance of transition metal oxide supported on either activated carbon or MCM – 41 (mobile composition of matter 41) mesoporous material will be compared. The spent adsorbent will be regenerated by using solvent washing with a methanol: toluene mixture at 70°C, followed by oxidation with air at 300°C, and finally reduction with H_2 at 700°C (Velu et al., 2003).

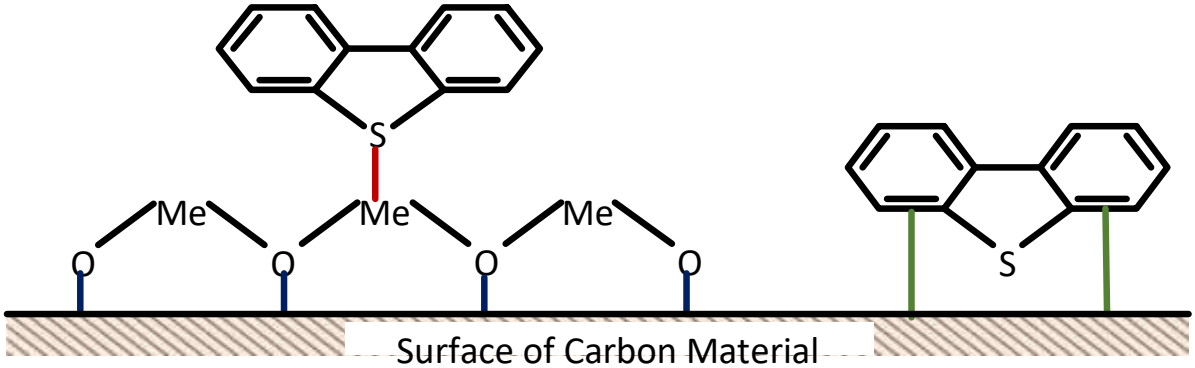

Figure 2.1: Possible mechanisms of surface reactions between the DBT molecule, metal oxide and carbon material (Velu et al., 2003)

Shi et al., (2015) used a coconut-shell activated carbon (ACS – 1) adsorbent to simultaneously remove H_2S and SO_2 from modelled Claus tail gas. Adsorption tests were carried out at atmospheric pressure and 30°C temperature, using a feed gas containing 20 000 ppmv H_2S, and 10 000 ppmv SO_2, balanced with N_2. Results showed that the breakthrough sulphur capacity of ACS – 1 is 64.27 mg of S/g of adsorbent, and the concentrations of H_2S and SO_2 in the Claus tail gas were reduced to less than 10 mg/m^3 (Ma et al., 2006; Velu et al., 2005). The micropores of ACS – 1 with sizes of about 0.5 nm were the main active sites of adsorption, whereas the mesopores showed minimal activity. Although the adsorption mechanism of the desulphurization process was both physical and chemical, the majority of H_2S and SO_2 was removed through physisorption. Furthermore, it was found that the ACS – 1 adsorbent could be completely regenerated using water vapor at 450°C, for a duration of five adsorption−regeneration cycles (Shi et al., 2015).

The H_2S product is then in sufficient quantity to keep the catalyst sulphide and prevent reduction of the catalyst to the inactive metal. Some authors have proposed a monolayer of S^{2-} ions superimposed over a second layer containing O^{2-}, Mo^{3+} and Mo^{5+}, and stabilized by Co promoter ions contained in sublayers of the underlying support. Eight other authors have suggested that intercalation of cobalt or nickel occurs at the edges of partially reduced structures of MoS_2 or WS_2 (Leliveld and Eijsbouts, 2008).

Lison (2010) used activated carbon derived from polymer deposited with metal species (Fe, Cu, Co, Ag, Ni) in its study of the selective adsorption of DBT (dibenzothiophene) and 4,6-DMDBT (dimethyl dibenzothiophene 97%) in the diesel model. Two types of fuels were used – one with diesel containing only n-decane and n-hexadecane solvents, and the other containing additional aromatics naphthalene and 1-methylnaphthalene (Darwish 2015). The results showed that deposition of metal species on the adsorbents decreased their porosity but increased the number of active adsorption sites with cobalt, copper and iron being the most active. Adsorbents with high acidity at their surface showed higher selectivity for 4,6-DMDBT than for DBT, probably because it is more basic (Leliveld and Eijsbouts et al., 2008; Lison et al., 2010).

The synthesized adsorbents outperformed two commercial carbons which were also studied in all aspect of desulphurization (Lison et al., 2010). According to Li (2008), the adsorptive desulphurization of H_2S from modelled syngas was carried out using materials including carbon black, graphite and activated carbon fibres. They used rare earth metal oxides La_2O_3 and CeO_2 to modify the activated carbon fibres due to their potential to effectively remove H_2S and promote multi-cycle regenerability. The effects of water vapour and temperature on H_2S removal were also investigated (Song et al., 2014).

Li (2008) proposed that the presence of basic functional groups on the carbonaceous surface lead to the adsorption of H_2S. In determining the activation energy required to desorb sulphur compounds from sulphur adsorbents, he concluded that chemisorption is the dominant mechanism at high desulphurization temperatures, while physisorption is the control mechanism at lower temperatures (Ma et al., 2014). The results also showed that during the sulphidation-regeneration cycles of the sorbent, N_2 could only remove physically adsorbed H_2S and the hydroxide could prevent the formation of by-products to

a certain extent. Activated carbon fibres modified with metal oxides have the highest breaking capacities (up to 35 mg H_2S per gram of adsorbent) (Kim et al., 2006; Noora, 2015).

2.3. APPLICATIONS USING GRAPHENE AND GRAPHENE OXIDE

With Nazal et al. (2015) the desulphurization of DBT in model diesel was carried out with the adsorbents such as commercial coconut activated carbon, multiwall carbon nanotubes, and graphene oxide which was synthesized using the Hummer's method. To improve the chemical properties of adsorbent surfaces, the wetness impregnation technique was used to load 5% and 10,9% aluminium in the form of an aluminium oxide precursor (Song 2015). Studies on adsorption isotherms of DBT, and desulphurization kinetics were carried out and results showed that the desulphurization capacity of adsorbents could be doubled by introducing a Lewis acid (Al_2O_3) onto their surfaces, instead of increasing pore volume or surface area. The activated carbon loaded with 5% aluminium had the highest adsorption capacity for DBT (85 ± 1 mg/g). The selectivity factors of the adsorbent were 25 and 225, for DBT/naphthalene and DBT/thiophene, respectively (Alexander Samokhvalov, 2012).

Lonkar and his colleagues (2016) on their work in the field of adsorptive desulphurization of H_2S, developed a simple and scalable approach for one-step synthesis of CuO/reduced graphene nanocomposites. They used graphite oxide and copper hydroxide precursors to simultaneously reduce graphite oxide and uniformly deposit in situ formed CuO nanoparticles onto the graphene surface. Results showed that CuO/reduced graphene nanocomposite had a H_2S adsorption capacity of 1.5 mmol H_2S/g adsorbent or 3 g S/100 g adsorbent, which was significantly higher than of pristine graphene and CuO adsorbents studied under the same experimental conditions (Lonkar et al., 2016). Furthermore, no toxic reducing agents or organic modifiers were used in the synthesis of the nanocomposite, which makes the method of a greener and more efficient approach, that shows tremendous potential for environmental and energy applications (Lonkar et al., 2016).

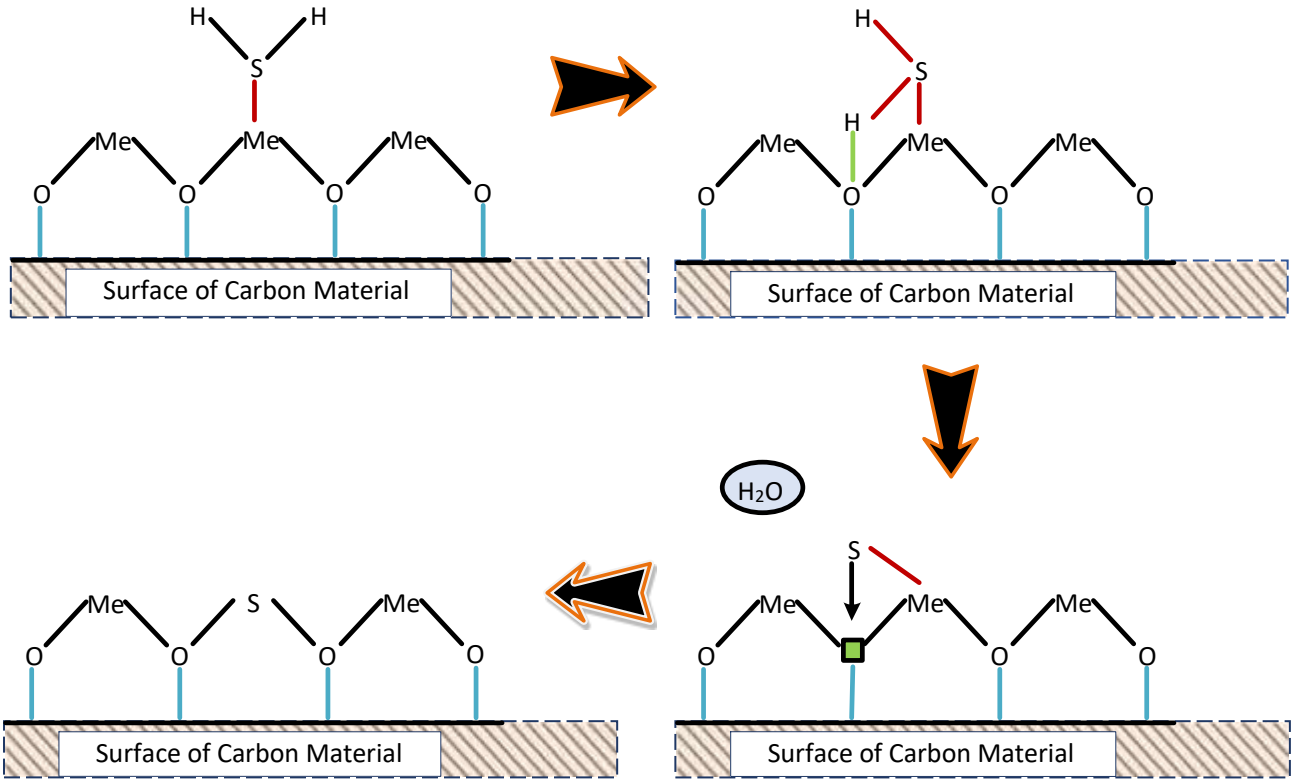

Figure 2.2: Possible mechanisms of surface reactions between the H_2S molecule and metal oxide (Lonkar et al., 2016).

Wang and Yang (2013) investigated the adsorption of thiophene from an n-octane solution using graphene, activated carbon (AC), mesoporous templated carbon (CMK-3), and Maxsorb super-activated carbon. Their results showed graphene had highest sulphur adsorption capacity of 0.06 mmol S/g adsorbent, followed by 0.027, 0.017 and 0.007 mmol-S/g for CKM-3, AC, and Maxsorb, respectively (Wang and Yang 2013). The obtained sulphur capacities corresponded well with the relative heats of adsorption. Moreover, although the thiophene adsorption capacities of adsorbents followed the order of graphene > CMK-3 > Maxsorb > AC, the results from the BET surface area were in the order of Maxsorb > CMK-3 > AC > graphene which indicated that surface area is not the critical factor that influences the sulphur removal capacity of carbon adsorbents (Braz 2019; Srinivas et al., 2015). The authors concluded that in all four sorbents graphene has the superior thiophene adsorption capacity and proposed that the carbine-type armchair

edge sites and carbene-type zigzag edge sites present on graphene (Wang & Yang, 2013; Srinivas et al., 2015) attribute the strong interaction of graphene and thiophene.

In another study, the adsorptive desulphurization of H_2S at ambient temperature, using synthesized nanocomposites of copper hydroxyl-chlorides with graphene (Gr) or graphite oxide (GO), was examined (Song, 2014). Their results indicated that the H_2S sulphur adsorption capacity of the Cu/graphene composite was higher than that of the Cu/graphite oxide. Another observation was that reduced copper species were highly dispersed on the surface of the CuGr, this enhanced O_2 activation, and led to the formation of sulphites and sulphates (Mabayoje et al., 2012).

2.4. ADVANTAGES OF ACTIVATED CARBON

Activated carbon (AC) is a nano-carbon possessing a structure of sponge, an AC made up of small chemically bonded heteroatoms, chiefly oxygen and hydrogen. The manufacture of AC magnification had tailored pore widths and other pores having an adjustable width. In general, there are many physical forms of ACs; which include granular AC, powdered AC, AC fibres, and AC cloths as indicated in Table 1. In synthesizing AC, nearly any carbon-based materials are applicable as precursors (Hameed, Din Ahmad, 2007). In practice, this includes nutshells and fruit stones, charcoal, wood, peat, soft coal, lignite, petroleum coke, and bituminous coal, among others. Taking into consideration that these materials are of high carbon content, low in inorganic content, composed of a high proportion of carbon and low number of inorganic components, it makes them suitable for the synthesis of ACs (Fig. 2.3).

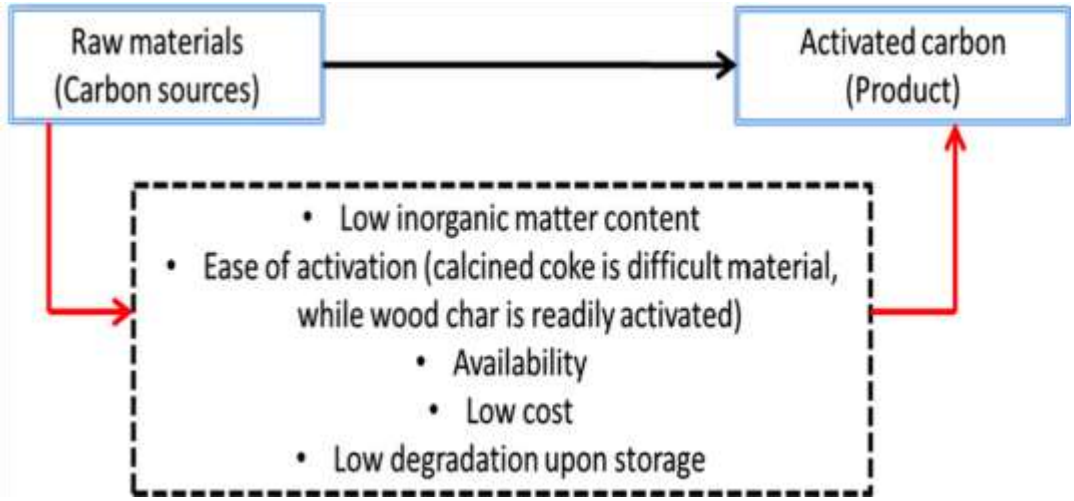

Figure 2.3: The selection criteria of raw material for AC production (Samira et al., 2016).

Table 2.1: Preparation of different physical forms of AC (Samira et al., 2016).

AC categories	Preparation methods	Characteristics
Granular AC	Prepared from hard material such as coconut shells and includes particles retained in a 0.177 mm mesh sieve	• Column filler for liquid and gas treatments • Can be regenerated after utilizing
Powdered AC	• Obtained in particles less than 0.1777 mm • Usually mixed with the liquid to be treated and disposed of afterwards	• Because of its small particles, the adsorption is normally very effective. • settling and removal tend to be slower
AC fibres	Prepared from the homogenous polymeric raw material	• Indicates a monodispersed pore size distribution. • Its thin fibre shape enhances intraparticle adsorption and

		contact efficiencies between the aqueous media.
AC cloth	Developed by using a precursor phenolic or viscose rayon	Well thought of to be good adsorbents because of its low-pressure drop during the process, flexibility and high contact efficiency.

With Chena et al. (2003), the heterogeneous surface property of AC came from two foundations as chemical and geometrical. Geometrical heterogeneity is mainly due to the variation of shape and size of pores, cracks, steps, and pits. Chemical heterogeneity is not only related to different functional groups, chiefly oxygen groups often positioned at the turbostratic crystallites' edges, but also relevant to several surface impurities (Zhaohong et al., 2007; Aimin et al., 2005). Both kinds of heterogeneity result in exceptional absorption properties of ACs. The control of the porous structure of ACs was done by the precursor used in the manufacturing process, the activation technique utilized, and the activation amounts (Erol and Numan, 2005).

Therefore, AC characterization techniques greatly influence the adsorption rate and capacity. Subsequently, AC was characterised for high carbon proportion, great surface areas, abundant micro-pores, and narrow or small aperture having the advantage of fast adsorption rate, large adsorption capacity, and simpler regeneration in the gas–liquid adsorption fields (Fronczak et al., 2019; Samira et al., 2016). Other leading benefits of AC are its high purity, which prevents poisoning/side reaction, the chemical stability in basic/acidic media, and excellent mechanical performance (Aimin et al., 2005). Moreover, AC tends to agglomerate with high specific surface areas and pore volumes, even when lacking micro-porosity. Pores in the mesoporous range and low tortuosity were formed due to the network-like assembly of AC aggregation, encouraging mass transfer. This is mainly favourable for quick reactions and limited diffusion applications such as liquid phase uses (Erol et al., 2005).

CHAPTER 3: EXPERIMENTAL METHODOLOGY

All reagents and gases were supplied by Labchem, Minema chemicals, Afrox and Air by-product. Other chemicals used in the study were of analytical grade.

3.1. MATERIALS

3.1.1. PREPARATION OF MODEL DIESEL

The raw diesel fuel material “commercial ultra-low Sulphur 50 ppm Diesel” used in this accomplishment of study was purchased from Total Bonjour garage local petrol station. Using a gas chromatographer, the diesel composition properties listed in Table 3.1 were pre-determined.

Table 3.1: Physical Properties of Diesel Fuel

Property	**ASTM Number**	**Diesel fuel**
Aniline point, ^{o}C	D 611	9.403
Ash content, wt.%	D482	0.012
Calorific value, J/g	D 240	5766.579
Cetane index	D613	7.484
Copper strip corrosion rating 3hrs at 50^{o}C	D130	-
Diesel index	D611	8.662
Flash point, CCPM, ^{o}C	D 93	10.154
Kinematic viscosity at 40^{o}C, cSt	D445	1.320
Lubricity, 60^{o}C	D6079	312
Specific gravity at 15^{o}C	D98	0.103
Sulphur content, ppm	D5453	49.931
Water and sediment vol. %	D1796	-
Water content, vol. %	D96	-

3.1.2. PREPARATION OF GRAPHITE OXIDE USING A CHEMICAL EXFOLIATION METHOD

Graphite oxide (GO) was synthesized using the modified Hummers method (Dubey et al., 2015). Sulphuric acid (Minema chemicals, 95.0 – 98.0%) as a strong oxidizing acid was mixed with sodium nitrate (Labchem, ≥ 85% by weight). Once the sodium nitrate dissolved, the mixture of graphite powder (Control laboratories, ≥ 99.99%) was added and the mixture ultrasonicated to exfoliate the GO sheets. This mixture was then placed in an ice bath and continuously stirred as potassium permanganate (Labchem, > 99.0%) was added dropwise for about 30 min. The mixture was then transferred to a heated magnetic stirrer where the oxidation process took place for 20 additional hours. Once the mixture has cooled down to room temperature, the oxidation reaction was completed by progressively adding a solution of hydrogen peroxide (Labchem, 30% by weight in H_2O) and de-ionized water. The colour of the mixture changed from dark brown to bright yellow. Finally, the GO solids were centrifuged and washed twice using a solution of hydrogen chloride (Labchem, 37%) and de-ionized water. The filtrate was then rinsed until the pH of the de-ionized water went neutral. The graphite oxide was then dried in an oven at 80°C for 10h.

3.1.3. SYNTHESIS OF ADSORBENTS USING A MICROWAVE-ASSISTED CHEMICAL REDUCTION METHOD

The metal oxide nanocomposites were synthesized by dissolving a known mass (weight at different mass, 20 to 200g) of either granular activated carbon (monitoring and control laboratories) and graphite oxide, in ethylene glycol (Labchem, Anhydrous, 99.8%), the mixture was then ultra-sonicated for 1h. Sodium hydroxide solution (Labchem, ≥ 97.0%) was added, and the mixture ultra-sonicated for a further 30 min. Aqueous metal acetate solutions (zinc, copper, manganese, cobalt) (Monitoring and control laboratories, ≥ 98.0%) with the desired weight of metal species (5 to 50 mg) were added drop wise into the mixture. The mixture was chemically reduced using a hydrazine solution (Labchem, 35wt %). The mixture as then further reduced using a hydrothermal method, by exposing it to microwave irradiation for periods ranging from 3 to 7 min. Once the mixture had

cooled down to an ambient temperature, it was centrifuged and washed with de-ionized water until the rinsing water pH went to neutral. The metal oxide nanocomposites dried in an oven for approximately 18h.

3.1.4. SYNTHESIS OF ADSORBENTS USING AN INCIPIENT IMPREGNATION/ THERMAL REDUCTION METHOD

Metal species of manganese zinc, cobalt and copper were loaded on granular activated charcoal (GAC) (monitoring and control laboratories) and graphite oxide (GO) using the incipient wetness impregnation method.

First, the amount of de-ionized water that was fully absorbed by (20 to 250 mg) mass of GAC and GO. Metal acetates carefully weighed with the desired weight percent of metal species and dissolved in de-ionized water while keeping in mind the water solubility of the acetates. A slow addition of aqueous solutions of metal acetates was stirred in carbonaceous materials. The resulting mixtures was then ultra-sonicated for 2h, by ensuring a uniform deposition. The mixture was then dried in an oven for approximately 18 to 24h at 120°C. The solids result was torched at temperatures ranging from 200°C to 500°C.

3.1.5. CARBON MATERIALS

The range of three activated carbons were used as adsorbents in this study and where purchased from Monitoring & Control Laboratories company. The first adsorbent was powdered activated carbon (labelled as PAC), second was activated carbon (AC) and the last one was granular activated charcoal (GAC).

3.2. CHARACTERIZATIONS

3.2.1. SEM ANALYSIS

The morphology of the MeO/GO and MeO/GAC sorbents was determined using a Scanning Electron Microscope (SEM), whereby the cross-sectional area of adsorbents was observed before and after each sulphidation regeneration cycle. The observation provided information such as pores, size, shape, distribution, element determination and density. The images were obtained using a Zeiss Supra 55 VP with an acceleration voltage of 5KV. The sweep was performed on powder sample dried at 120^{o}C.

3.2.2. XRD ANALYSIS

An X-Ray Diffractometer (XRD) was used to identify and characterize the crystal phases present on the sorbents, their atomic structure and size. An X-ray beam scattered when it hits the atoms in a crystal. XRD patterns are generated using a stationary X-ray source (typically Cu Kα, l = 0.154nm operating at 30mA and 35kV with a scan rate of 1^{o}/min), and the scattered X-rays are detected by a mobile detector. Since crystals are made up of regular and repeated lattices of atoms, the x-ray beam diffracted by atoms has a regular lattice of waves. Diffractograms were analysed using MDI JADE 8.0 software and standard JCPDS files.

3.2.3. FTIR ANALYSIS

The Fourier Transformer Infrared Spectroscopy (FTIR) was used to identify the types of functional groups present on the surface of the MeO/GO and MeO/GAC sorbents before and after each sulphidation regeneration cycle. Analysis was performed using a Nicolet Magna-IR 830 spectrometer using the Attenuated Total Reflectance (ATR) method. The assay is widely known for its uniqueness in identifying the vibrational structure of various materials since the spectra are capable of measuring complex molecular vibrational modes. FTIR radiations are electromagnetic waves between 100 cm^{-1} and 14,285 cm^{-1} microns (longer than the red of visible light and shorter than microwaves). When chemical bonds absorb IR radiation, the bonds vibrate and the intermolecular distance of two or

more atoms changes. There are two general types of vibration: stretching and bending. Stretching is a symmetrical or asymmetrical rhythmic movement while bending vibration involves changes in the bond angles of atoms. Therefore, specific information of functional groups can be identified due to the correlation between the wave numbers at which a molecule absorbs IR radiation and its structure. As the beam passes through the sample, the sample adsorbs all of the different characteristic wavelengths of its spectrum.

3.2.4. BET ANALYSIS

The Brunauer, Emmett and Teller (BET) analyser was used to measure the surface area and pore size distribution of MeO/GO and MeO/GAC of sorbents. The BET measurements for pure MeO/GAC and MeO/GO composites were conducted using a Micromeritics Gemini 32375. Nitrogen gas was used as the adsorbate. Around 100 mg of the pelletized catalysts were loaded and pre-treated at 200°C in vacuum overnight to remove any impurities and moisture on the surface. The surface area was measured at the boiling point of nitrogen 77^{o}K within a P/P_0 range between 0.05 to 0.5 Pa.

3.2.5. TGA ANALYSIS

The thermogravimetric analysis (TGA) was used to measure the mass characterization of the desulphurization samples during a given time at a given temperature. The IHFB-TGA was used as an instrument as it has the ability to control the temperature at heating rates up to 100^{o}C/s while maintaining an isothermal bed of the lift tube, as the sample was held below the heated zone as the temperature increased. When the reaction zone reached the set point, the lift tube rises up into the heated zone. The analyser has platinum rods 3 mm in diameter symmetrically placed in a circular configuration inside the reactor. A magnetic field created by a power supply induces an electric current with a high frequency (40 to 500 kHz).

3.3. PERFORMANCE TESTING

3.3.1. DBT ADSORPTION TESTS

For the adsorption of 4,6-dimethyldibenzothipohne (4,6 DMDBT) and 4-dibenzothiophene in model and commercial diesel a variety of experiments was carried out using batch and packed bed reactors, at varying temperatures (30^{o}C – 80^{o}C) and atmospheric pressure (100 bar). In batch experiments, the investigation effects of adsorbent compositions (0.3 g/L – 0.8 g/L), adsorption temperatures (30^{o}C – 50^{o}C), and mixing speeds (120 rpm – 250 rpm) were conducted. While in continuous flow experiments, the effects of diesel flow rate 2 L/min, adsorbent compositions (0.3 g/L – 1.2 g/L), and adsorption temperatures (30^{o}C – 80^{o}C) were also investigated. The Desulphurized diesel products were analysed using liquid gas chromatography. Experimental data used to determine the adsorbents breakthrough capacity, adsorption isotherms and kinetics. The packed bed adsorbents regenerated through solvent washing with a toluene/methanol (50/50, 60/40 and 40/60 concentration ratios) mixture, followed by oxidation using an O_2/N_2 (1:4, 3:4 and 2:3) ratios) gas mixture. Adsorbent characterization was conducted before and after each sulphidation and regeneration experiment.

3.3.2. H_2S ADSORPTION TESTS

The adsorption of 200 ppm H_2S from a H_2S/N_2 gas mixture was conducted using a stainless-steel packed bed tube reactor. The syngas passed through the adsorbent bed at a fixed flow rate and adsorbent temperature. The outlet sulphur gas concentration was determined using a H_2S analyser. Experimental data collected determined the adsorbents breakthrough capacity, adsorption isotherms and kinetics. The adsorbents were regenerated in the same reactor by heating the bed at 110^{o}C and passing through N_2 gas to remove any chemisorbed H_2S. When H_2S was undetectable in the reactor outlet stream, air passed through the bed.

The 200 ppm feed H_2S concentration with a total flow rate of 200 mL/min was sent into the system. The product stream was further diluted with 1600 mL of N_2 before injection to the H_2S analyzer since the limitation of the H_2S analyzer detectable range was only up

to 20 ppm. The experiments (see the experimental setup Figure 3.1) were carried out until the output H_2S concentration reached 5 ppm from the analyzer reading while the actual concentration leaving the bed being 30 ppm.

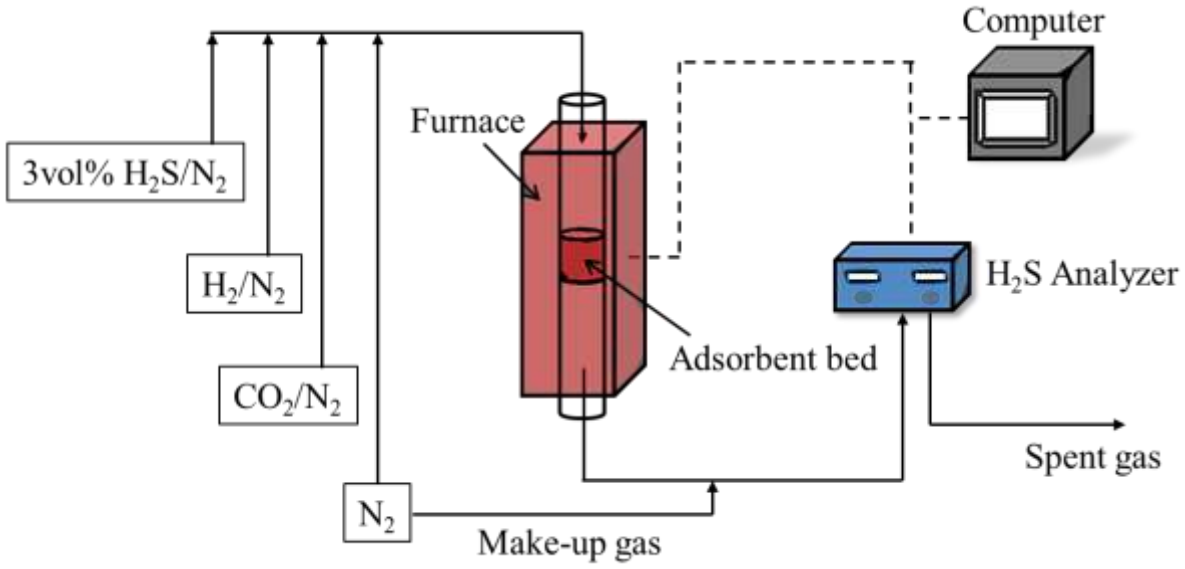

Figure 3.1. H_2S adsorption setup (Song, 2014).

The experimental breakthrough time was determined when the outlet H_2S concentration reaches 1 ppm and regeneration tests, the spent adsorbent was heated to 600°C in N_2 for approximately 1h. After the hydrothermal decomposition, the adsorbent was cooled down to 200°C temperature for another sulphidation reaction.

3.3.3. ADSORPTION ISOTHERM MODELS

Adsorption isotherm models determined the adsorption mechanism behaviour of sulphur compounds on metal oxide nano-composites; as well as the favourability and extent of adsorption. Langmuir and Freundlich isotherms were used to model the equilibrium adsorption data obtained from batch and continuous adsorption experiments. The equilibrium adsorption capacities (q_e) and adsorption capacities at time t (q_t) were determined using the following equations:

$$q_t = \frac{(C_O - C_t)V}{W} \quad (1)$$

$$q_e = \frac{(C_O - C_e)V}{W} \quad (2)$$

Where:

- V was the volume of the model diesel or syngas,
- W was mass of dry adsorbent used, and
- C_o, C_e, C_t (mg/L) represents the concentration sulphur compounds in the diesel or syngas at initial, at equilibrium, and at time (t), respectively.

The Langmuir isotherm was represented as follows:

$$q_e = q_m \frac{k_{eq} C_e}{1 + k_{eq} C_e} \quad (3)$$

With the linear form expressed as:

$$\frac{1}{q_e} = \frac{1}{q_m} + \left(\frac{1}{q_m k_L}\right)\frac{1}{C_e} \quad (4)$$

Where:

- q_e ($mg.g^{-1}$) was the equilibrium amount of sulphur compound adsorbed per mass of adsorbent,
- q_m ($mg.g^{-1}$) was the maximum adsorption capacity of the adsorbent, and
- K_L was the Langmuir constant, which related to the temperature of adsorption.

Freundlich isotherm will be represented as follows:

$$q_e = k_f C_e^{1/n} \quad (5)$$

With the linear form will be expressed as:

$$\log q_e = \log k_f + \frac{1}{n} log C_e \quad (6)$$

Where:

- K_F and n are the Freundlich constants, which related to the adsorption capacity and adsorption intensity of the adsorbent respectively.

3.3.4. ADSORPTION KINETIC MODELS

In order to measure the rate of sulphur adsorption under various experimental conditions, pseudo-first-order and pseudo-second-order kinetic models were used.

The pseudo-first-order model was expressed linearly as follows:

$$ln(q_e - q_t) = ln(q_e) - k_1 t/2.303 \quad (7)$$

Where:

- q_e, q_t (mg/g) were the amounts of sulphur adsorbed at equilibrium and time t (min) respectively.
- k_1 (min^{-1}) as the equilibrium rate constant of the pseudo-first-order adsorption.

The pseudo-second-order model was expressed linearly as follows:

$$\frac{1}{q_m} = \frac{1}{k_2 q_e^2} + \frac{1}{q_e} t \quad (8)$$

Where:

- k_2 (min^{-1}) as the equilibrium rate constant of the pseudo-second-order adsorption.

3.4. EXPERIMENT

3.4.1. DETERMINATION OF DIESEL INDICES AND SULPHUR REMOVAL PERCENTAGE

Diesel indices were calculated for all diesel samples prepared. In general, calculating the diesel index for a particular sample requires determining the density and action of aniline. Regarding the percent Sulphur removal, the calculation was made using equation (9) as the ratio of the concentration of sulphur absorbed by the sorbents to the initial concentration of sulphur present in diesel.

$$Sulphur\ removal\ percentage = \frac{S_{initial} - S_{final}}{S_{initial}} * 100 \quad (9)$$

3.4.2. DESULPHURIZATION PROCESS

The desulphurization process with the three adsorbents was studied at different volume levels of sorbent materials (1 wt. % – 20 wt. %), with the operating temperature (room temperature, 30^{o}C and 80^{o}C) and the contact time (1 – 3h) according to the following procedure:

- Before starting the experiments, the three adsorbents (PAC, AC and GO / GAC) were dried at a temperature of 100 ^{o}C for 2h.
- 10 litre of commercial diesel fuel was mixed with adsorbents and stirred using a glass stirrer oscillating at 310 oscillations /min.
- Filtration of the mixtures was performed to separate the sorbent solids from the filtrate.
- Sulphur and metal contents were analysed in diesel fuel samples using an ED-XRF spectrophotometer.
- During the formation of two layers, the mixture was heated in a water bath at a controlled temperature and at which the rate of sample recovery was recorded.
- 20 wt.% of three adsorbents were mixed in the 20g of dual at controlled room temperature with the interval stated above to achieve equilibrium time for high sulphur removal after one hour.

3.4.3. CHARACTERIZATIONS OF GRAPHENE ADSORBENTS

The interlayer *d*-spacing between the graphite layers should be an indicator of the degree of oxidation of the graphite oxide. Once the graphite oxide layers are exfoliated and reduced, they revert to a sp^2 layer structure. Therefore, the intensity of the graphite oxide peak has completely disappeared in the XRD pattern of graphene, characterized by a broad peak centred around 24° and corresponding to an interlayer spacing of 3.69 Å with a structure (002). This result could indicate the recovery of the graphitic crystal structure. Oxygen-containing functional groups, such as hydroxyl, epoxy, or carboxyl groups, on and between the graphite layers widen the spacing between the graphite layers and transform the graphite oxide into a sp^3 configuration. A larger spacing between the layers should therefore indicate a higher degree of oxidation of the graphite oxide.

Figures 3.2 and 3.3 show the XRD models for graphite oxide and graphene, respectively (Wu et al., 2010). With A and B representing the stacking of the layers in the GO which deduces from the electronic diffraction. A represents the reduction of graphene oxide and B represents the present graphite oxide as the spacing d is increased. These stacking orders are the compound composition of GO prepared using a simplified body method to identify the functional group present in GO by solid state (Jeong, 2008; Wu et al., 2010).

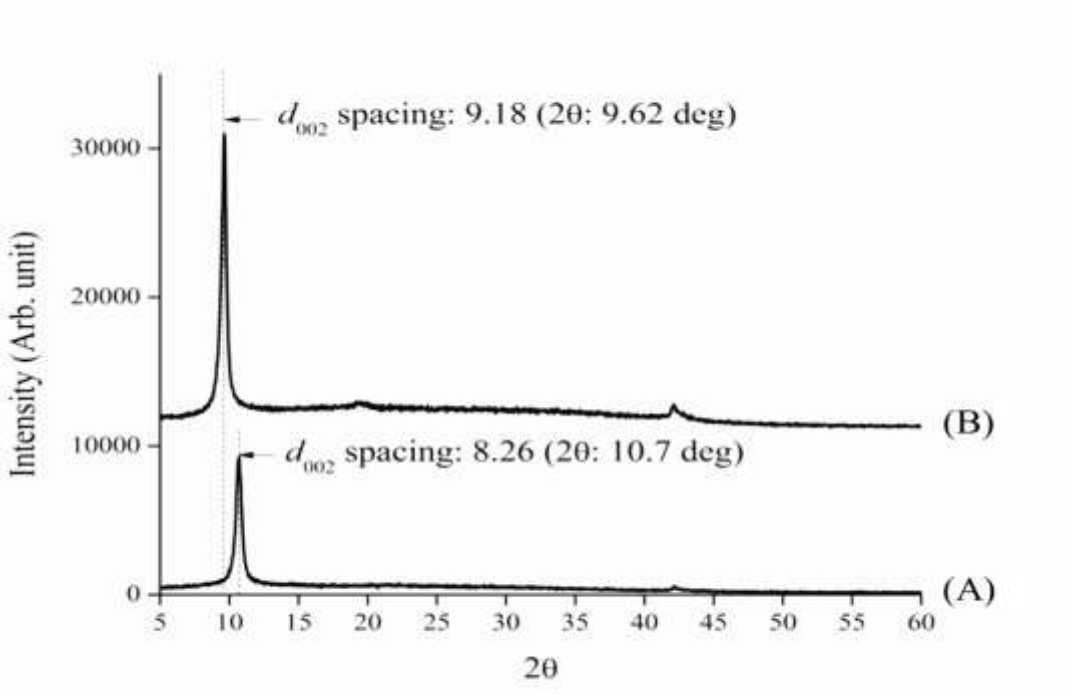

Figure 3.2: XRD for graphite oxide and interlayer *d*-spacing (Wu et al., 2010).

.

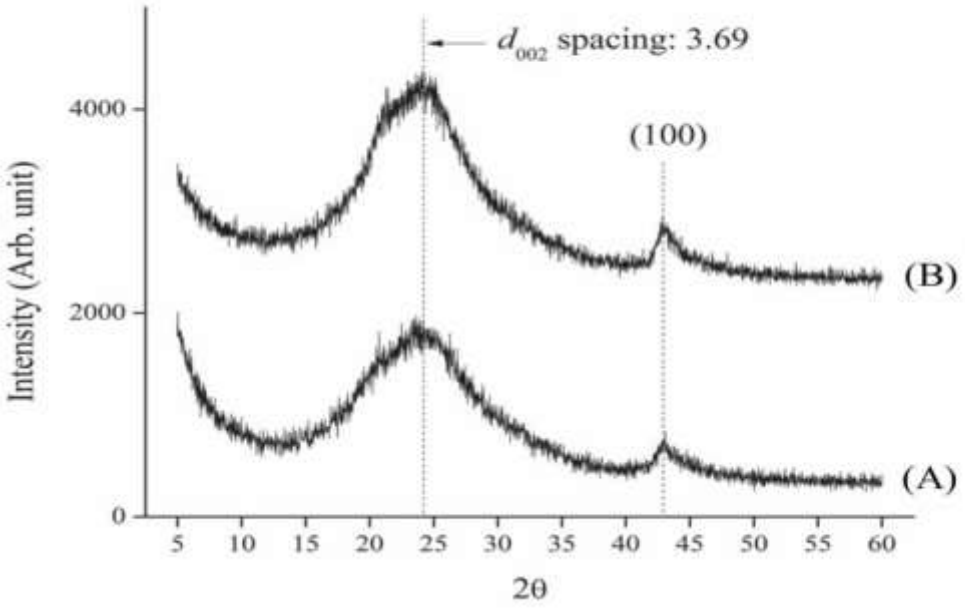

Figure 3.3: XRD of graphene and interlayer *d*-spacing (Wu et al., 2010).

CHAPTER 4: RESULTS, DISCUSSION AND FINDINGS

The main goal of this work was the desulphurization of diesel fuel using carbon-based metal oxide nanocomposites species. A wide variety of materials, including metal ions loaded on mesoporous materials, mixed metal oxides, metal modified activated carbon, supported metals and others were tested as adsorbents. Most of these materials were synthesized the laboratory as described in Chapter 3 to treat the diesel fuel used as a feedstock. The adsorbent was packed in a stainless-steel column with an internal diameter of 36 cm and length of 1200 mm. The adsorbent bed volume was 2.49 mL. The sulphur removal efficiency was done with different carbon-based adsorbents for the adsorptive in diesel fuel while bearing in mind the ignition quality of diesel fuel after the absorption process.

4.1. ADSORPTIONS

4.1.1. KINETICS MODELS

The adsorption capacity of sorbent materials and the adsorption results of sulphur compounds slowly increased after one hour. The rate constants of the adsorption processes were found using the pseudo first order equation or model (Equation 7). The values of k_1 (0.069, 0.127 and 0.019) from the table 4.1 were kept constants throughout while the plots of ln (qe - qt) versus t for each sorbent material (see Figures 4.1 (a), 4.2 (a) and 4.3 (a)). The results obtained showed that the values (2.856, 2.565, 2.036, 1.845, 1.664, 1.442, 1.40, 2.650, 2.566, 2.242, 2.001, 1.897, 1.223, 1.154, 2.716, 2.542, 2.195, 1.861, 1.512, 1.324 and 1.124) of qe obtained experimentally do not agree with the values (0.505, 2.185, 6.895, 9.995, 10.52, 11.13, 11.225, 0, 2.685, 7.385, 9.395, 10.770, 11.670, 12.295, 0.620, 1.585, 3.275, 5.055, 6.665, 8.810 and 10.270) calculated for all the adsorbents. Thus, this proves that the adsorption kinetics of sulphur compounds using the three adsorbents does not follow the first order kinetic model.

Alternatively, a pseudo second order model equation (Equation 8) was used. The calculated values (2.876, 2.668, 2.232, 2.092, 1.701, 1.476, 1.415, 2.674, 2.656, 2.222, 2.054, 1.653, 1.233, 1.151, 2.748, 2.668, 2.293, 1.714, 1.467, 1.315 and 1.154) of qe must correspond to the same values of equilibrium capacity acquired experimentally for this model to be valid. Likewise, the graphs of t/q_t versus *t* were plotted. Line graphs (see Figures 4.1 (b), 4.2 (b) and 4.3 (b)) indicated an agreement between the experimental and calculated values for the adsorbents.

Table 4.1: Comparison of the Pseudo First- and Second-order Adsorption Rate Constants using 20 wt.% of the Different Adsorbents.

PAC							
Ce (mg/L)	$q_e\ exp$ (mg/g)	First-order kinetic model R^2 = 0.9319			Second-order kinetic model R^2 = 0.9715		
		k_1(min^{-1})	q_e Cal. (mg/g)	Time (min)	k_2 [g(mg.min^{-1})]	q_e Cal. (mg/g)	Time (min)
48.99	2.856	0.069	0.505	0	0.513	2.876	0
45.63	2.565	0.069	2.185	10	0.513	2.668	10
36.21	2.036	0.069	6.895	20	0.513	2.232	20
30.01	1.845	0.069	9.995	30	0.513	2.092	30
28.96	1.664	0.069	10.52	40	0.513	1.701	40
27.74	1.442	0.069	11.13	50	0.513	1.476	50
27.55	1.40	0.069	11.225	60	0.513	1.415	60
AC							
		First-order kinetics model			Second-order kinetics model		

Ce (mg/L)	$q_e\ exp$ (mg/g)	R^2 = 0.9402			R^2 = 0.9332		
		k_1 (min^{-1})	$q_e\ cal.$ (mg/g)	Time (min)	k_2 [g.(mg.min^{-1})]	$q_e\ cal.$ (mg/g)	Time (min)
50	2.650	0.127	0	0	1.307	2.674	0
44.63	2.566	0.127	2.685	10	1.307	2.656	10
35.23	2.242	0.127	7.385	20	1.307	2.222	20
31.21	2.001	0.127	9.395	30	1.307	2.054	30
28.46	1.897	0.127	10.770	40	1.307	1.653	40
26.66	1.223	0.127	11.670	50	1.307	1.233	50
25.41	1.154	0.127	12.295	60	1.307	1.151	60
GAC							
C_o (mg/L)	q_e,exp (mg/g)	First-order kinetic model R^2 = 0.877			Second-order kinetic model R^2 = 0.9617		
		k_1 (min^{-1})	q_e,$cal.$ (mg/g)	Time (min)	k_2 [g (mg.min^{-1})]	q_e,$cal.$ (mg/g)	Time (min)
48.76	2.716	0.019	0.620	0	0.068	2.748	0
46.83	2.542	0.019	1.585	10	0.068	2.668	10
43.45	2.195	0.019	3.275	20	0.068	2.293	20
39.89	1.861	0.019	5.055	30	0.068	1.714	30
36.67	1.512	0.019	6.665	40	0.068	1.467	40
32.38	1.324	0.019	8.810	50	0.068	1.315	50
29.46	1.124	0.019	10.270	60	0.068	1.154	60

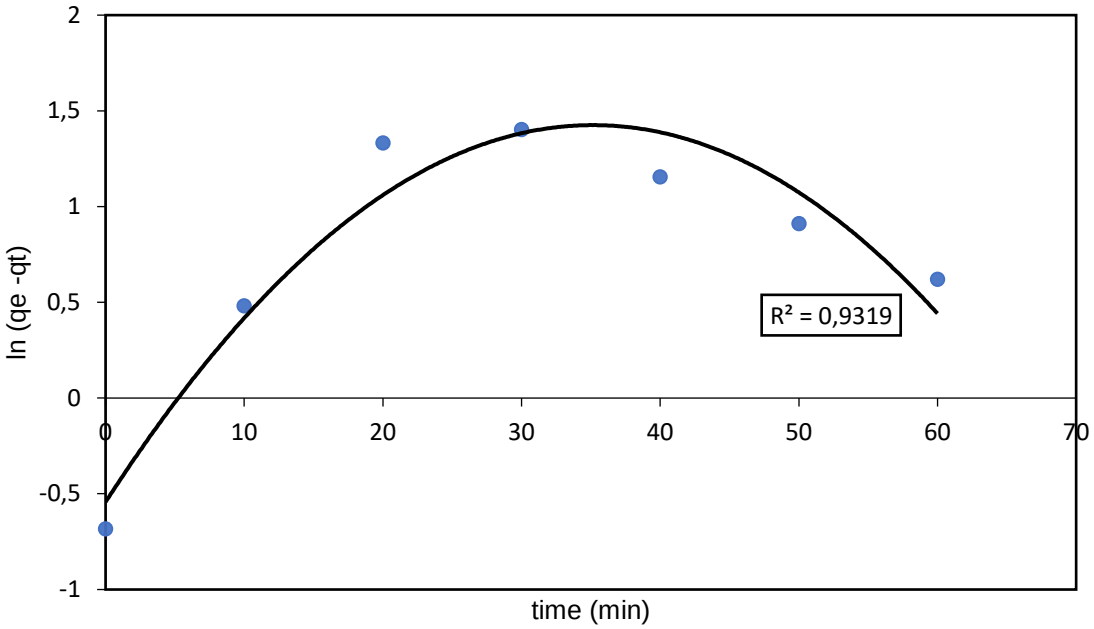

Figure 4.1.a: Pseudo First-order Kinetic for Adsorption of Sulphur Using 20 wt. % PAC.

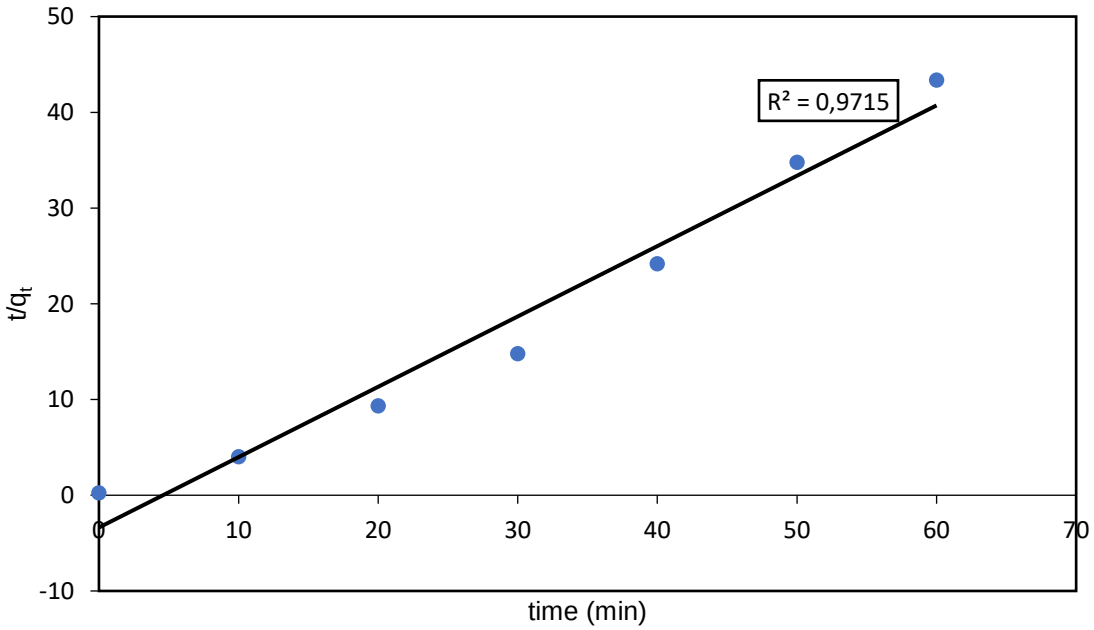

Figure 4.1.b: Pseudo Second-order Kinetic for Adsorption of Sulphur Using 20 wt. % PAC.

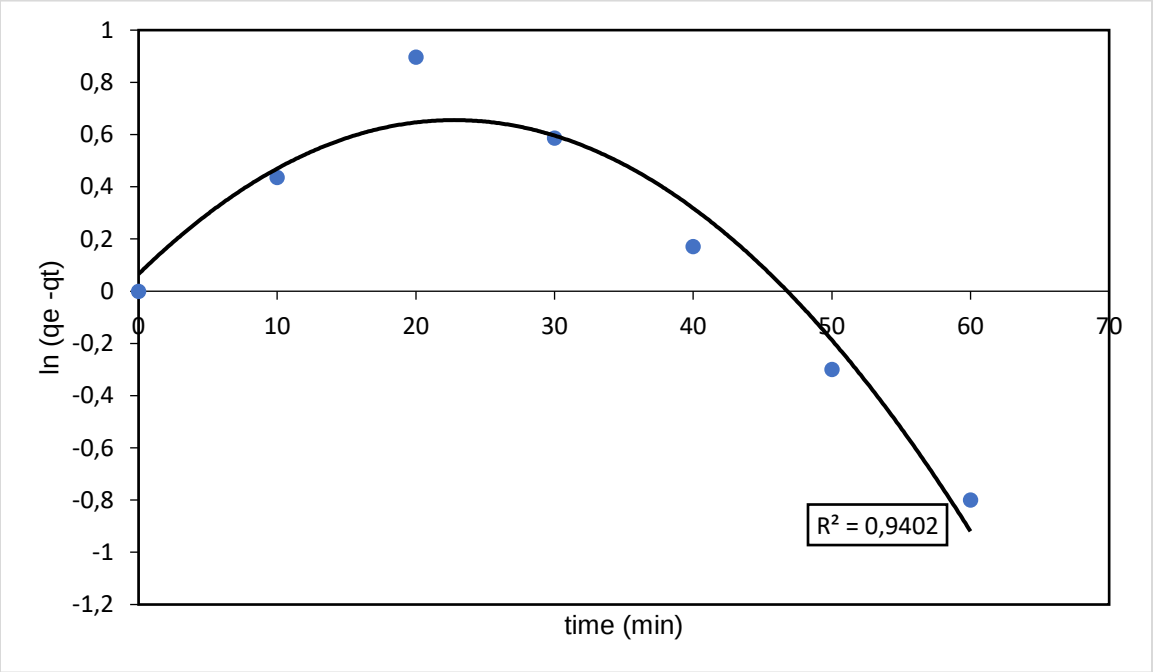

Figure 4.2.a: Pseudo First-order Kinetic for Adsorption of Sulphur Using 20 wt. % AC.

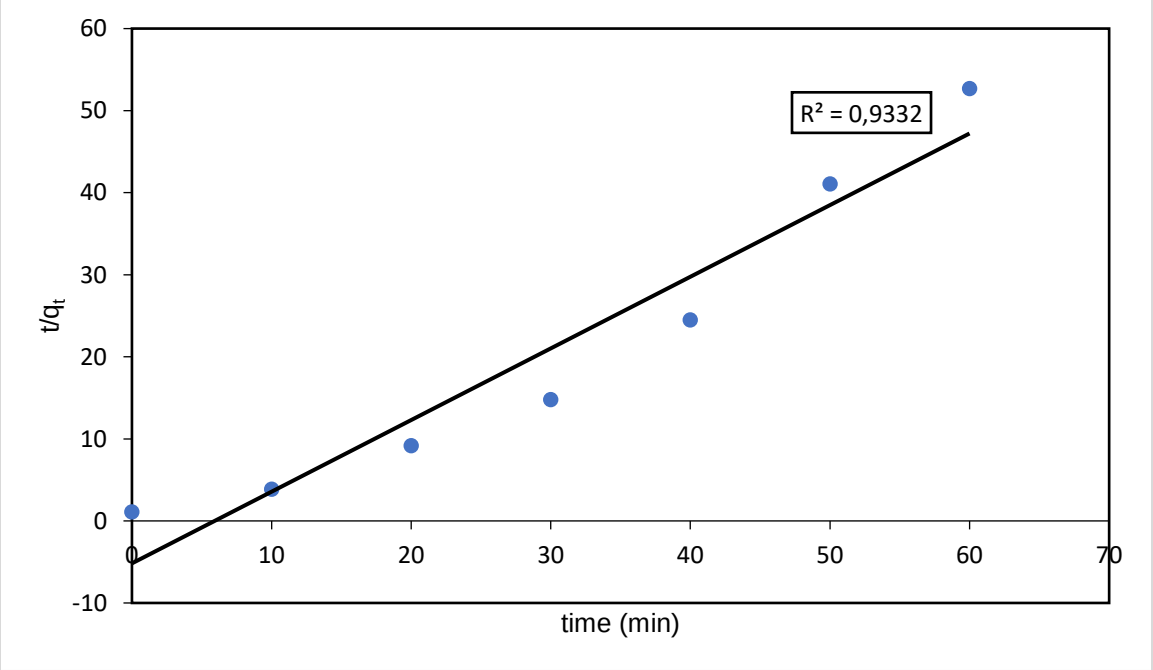

Figure 4.2.b: Pseudo Second-order Kinetic for Adsorption of Sulphur Using 20 wt. % AC.

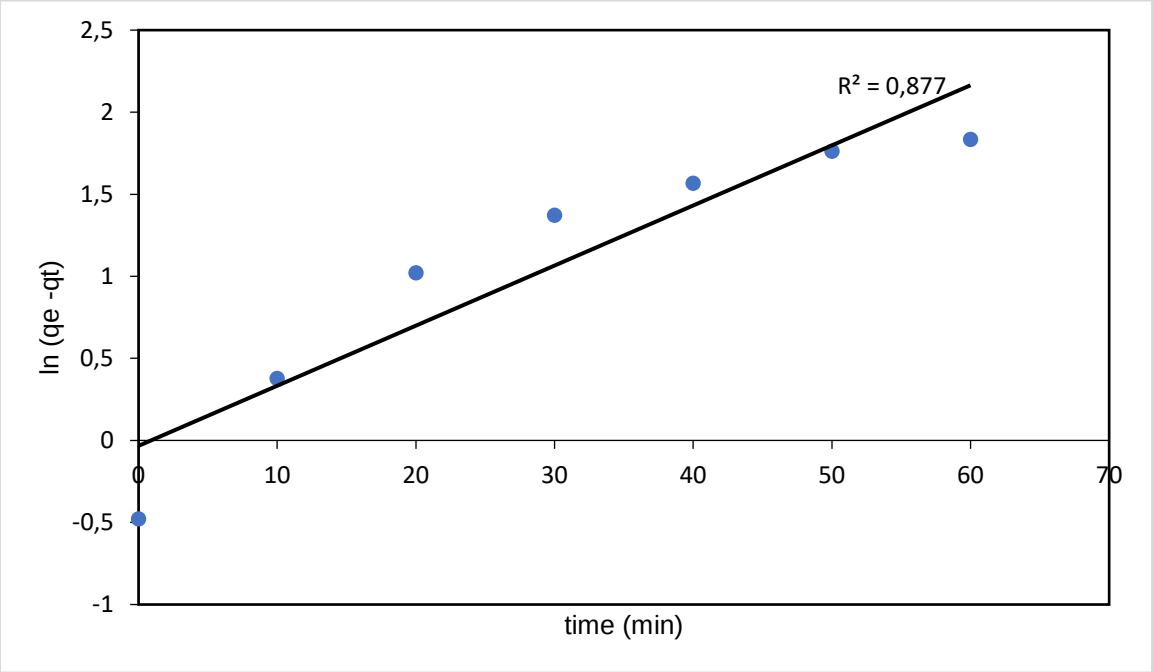

Figure 4.3.a: Pseudo First-order Kinetics for Adsorption of Sulphur Using 20 wt. % GAC.

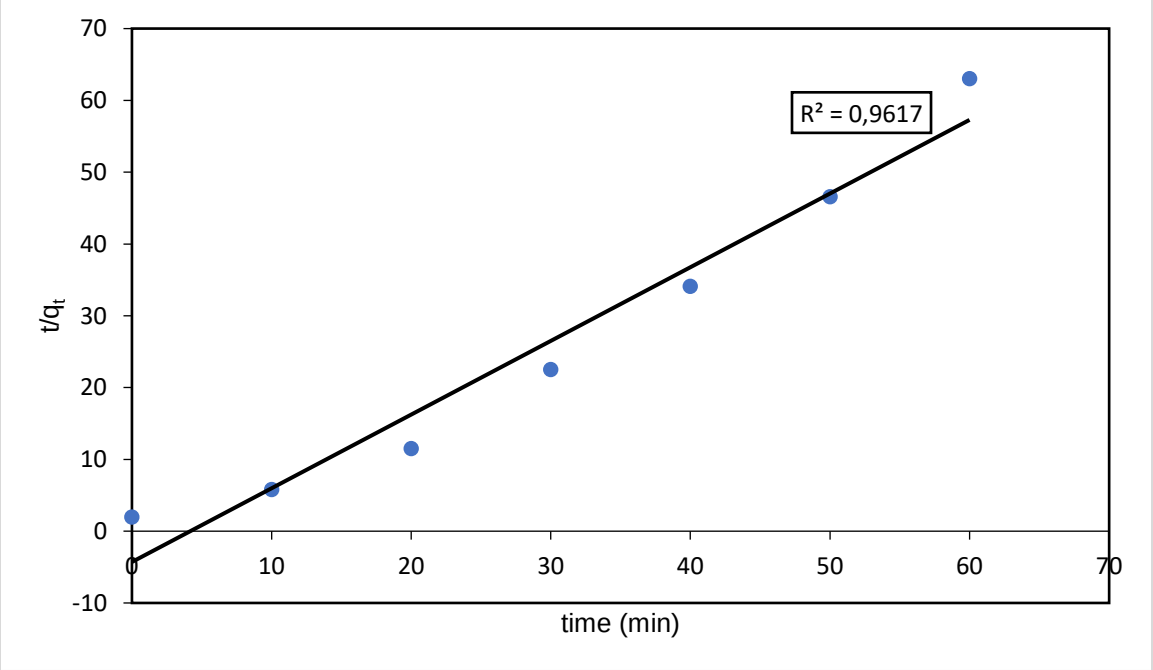

Figure 4.3.b: Pseudo Second order Kinetics for Adsorption of Sulphur Using 20 wt. % GAC.

4.1.2. ISOTHERM MODELS

4.1.2.1. FREUNDLICH ISOTHERM

The Freundlich adsorption isotherms for GO and GAC were generated at 30^{o}C and 80^{o}C and room temperature. (Figures 4.6 to 4.8). The Freundlich isotherm constants were determined by non-linear regression and are shown in Table 4.3, respectively.

4.1.2.2. LANGMUIR ISOTHERM

The Langmuir adsorption isotherms for GO and GAC were studied at room temperature and 30^{o}C (Figures 4.4 and 4.5). The Langmuir isotherm constants were determined by non-linear regression and are shown in Table 4.2.

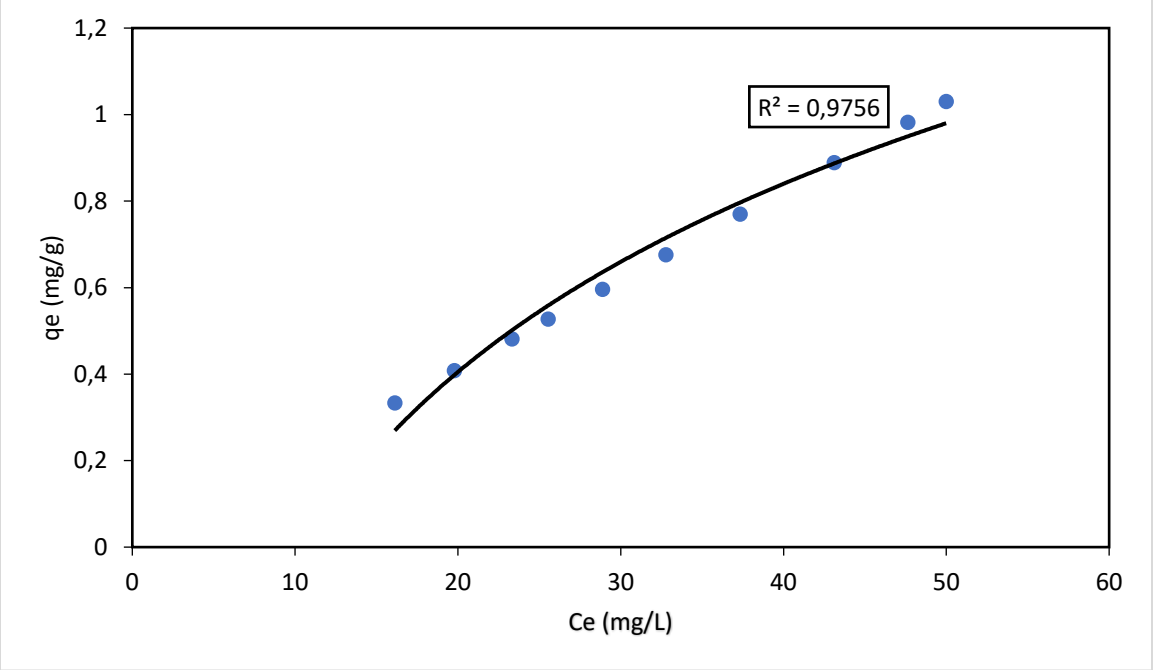

Figure 4.4.a: Fitting of Langmuir Adsorption Isotherms on GO and Room Temperature.

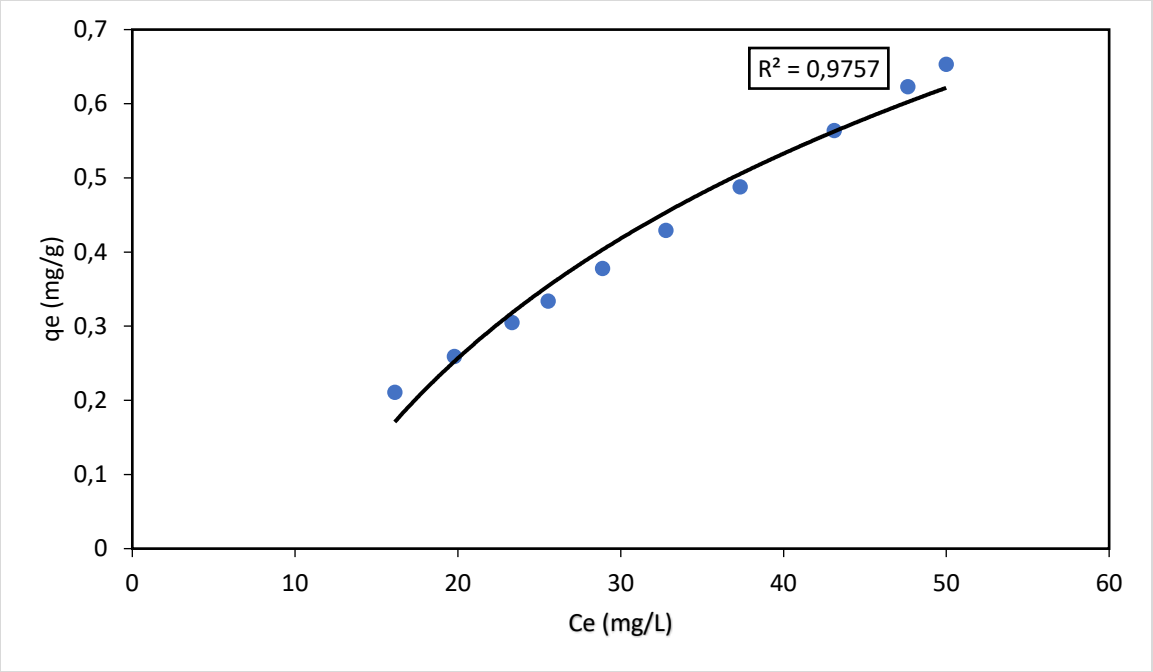

Figure 4.4.b: Fitting of Langmuir Adsorption Isotherms on GAC at Room Temperature.

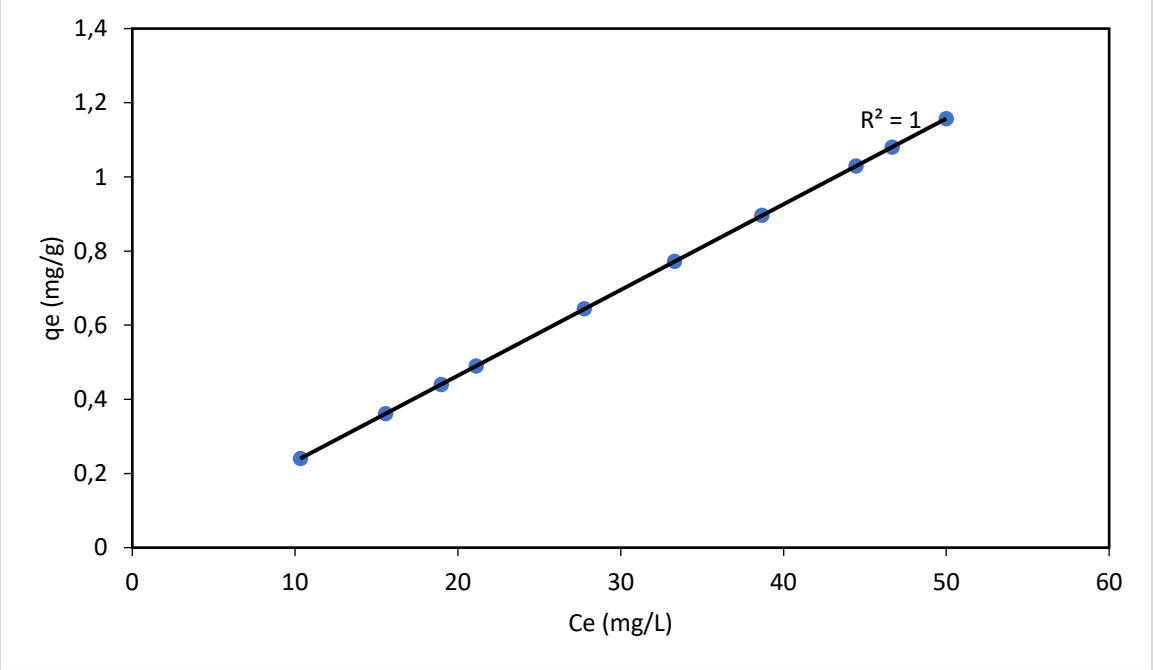

Figure 4.5.a: Fitting of Langmuir Adsorption Isotherms on GO at 30 ºC.

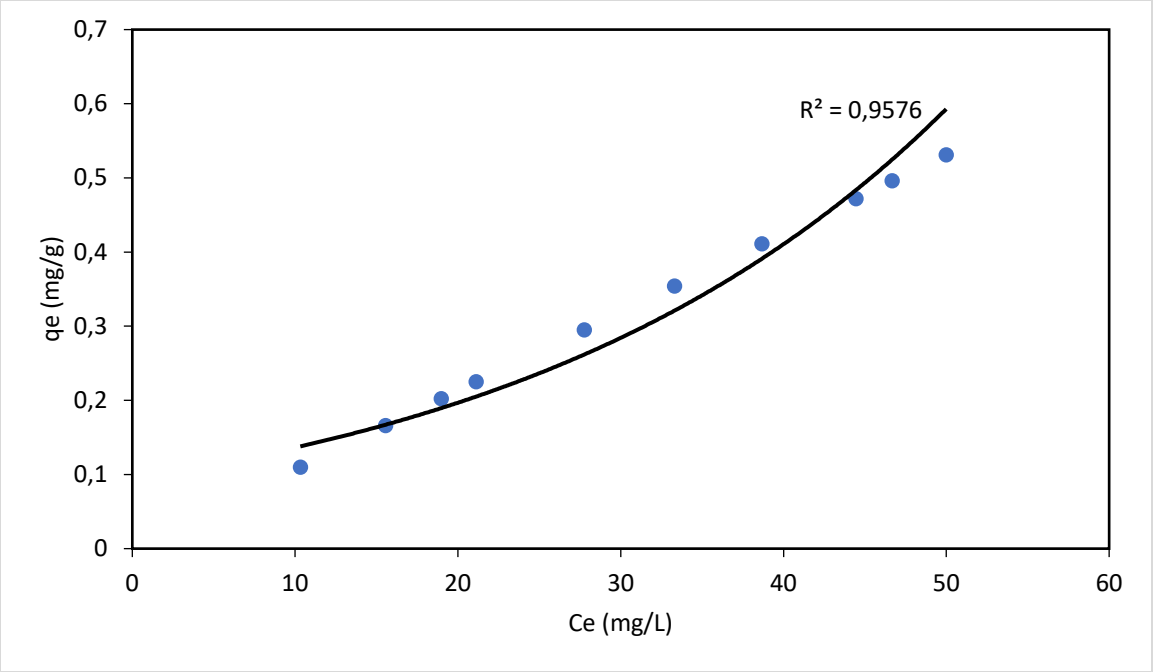

Figure 4.5.b: Fitting of Langmuir Adsorption Isotherms on GAC at 30 ºC.

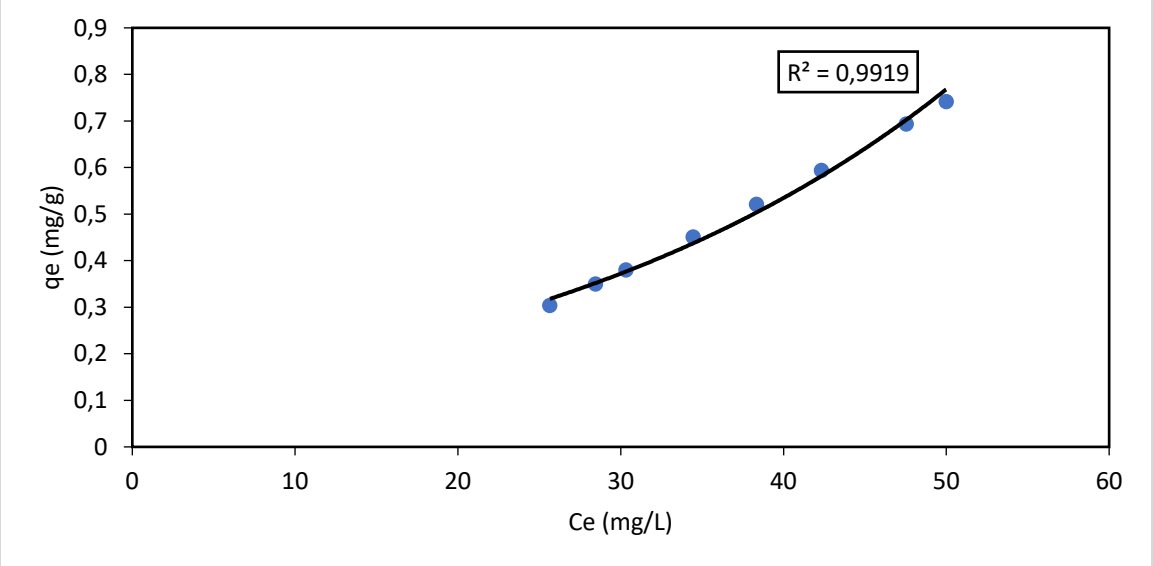

Figure 4.6.a: Fitting of Freundlich Adsorption Isotherms on GO at Room Temperature.

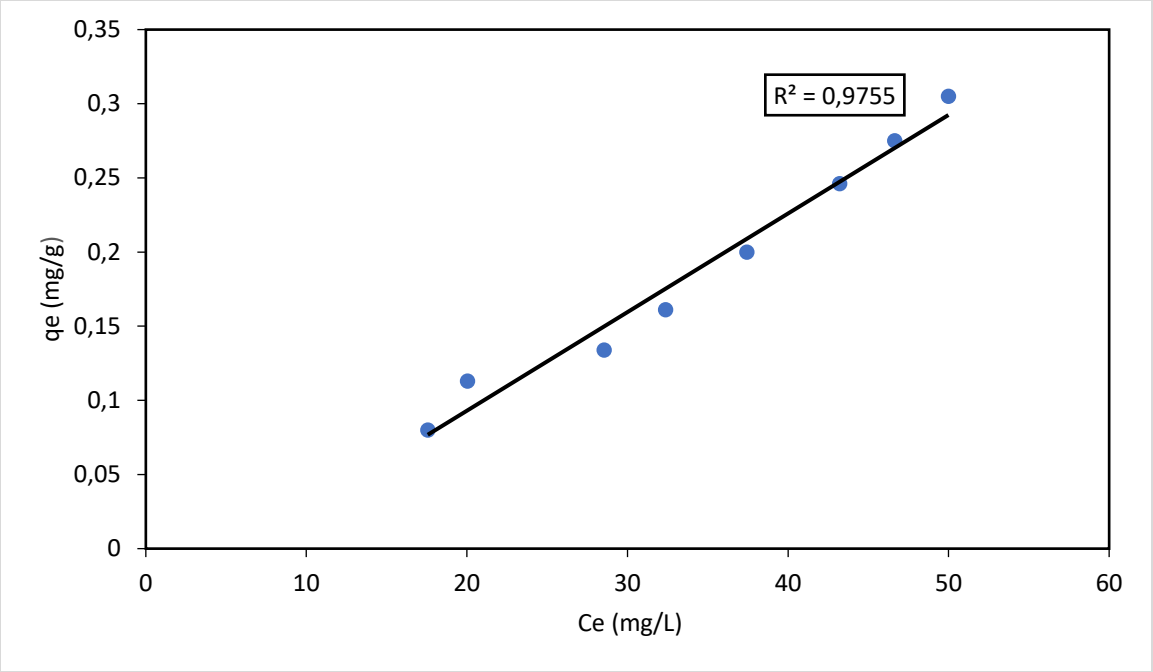

Figure 4.6.b: Fitting of Freundlich Adsorption Isotherms on GAC at Room Temperature.

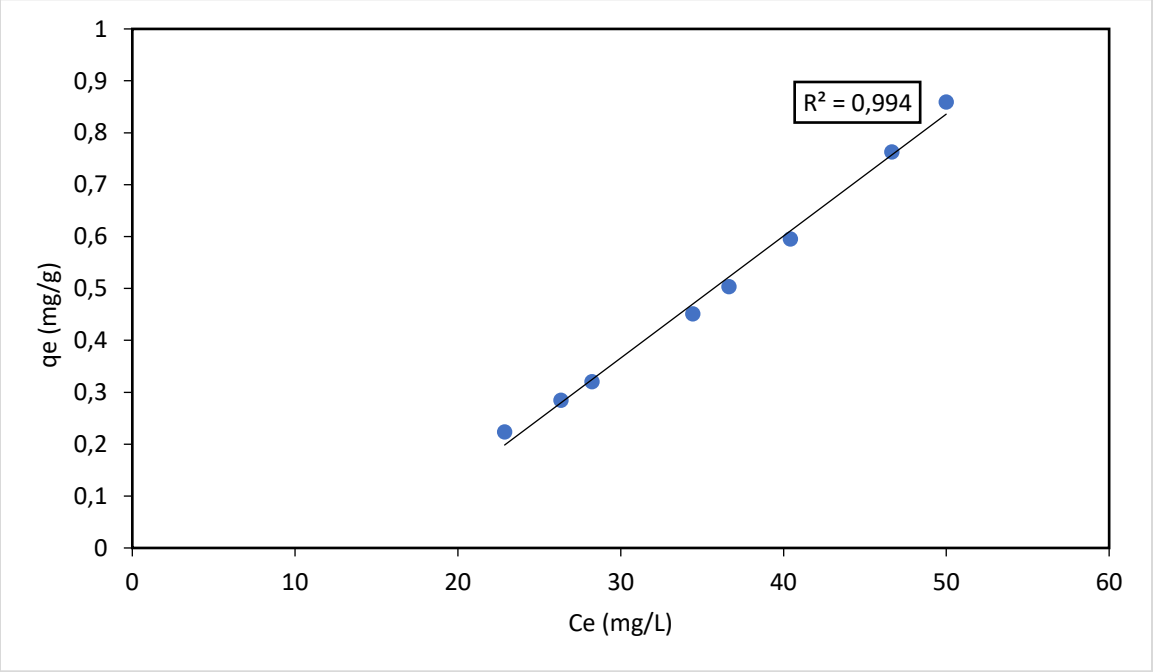

Figure 4.7.a: Fitting of Freundlich Adsorption Isotherms on GO at 30 ºC.

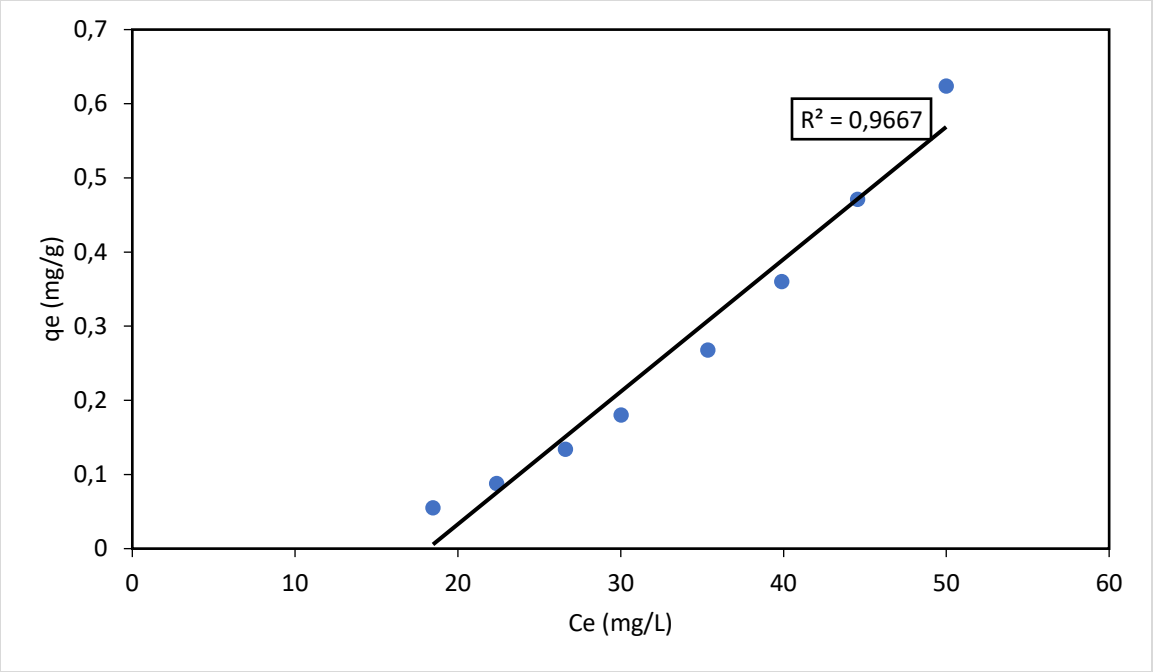

Figure 4.7.b: Fitting of Freundlich Adsorption Isotherms on GAC at 30 ºC.

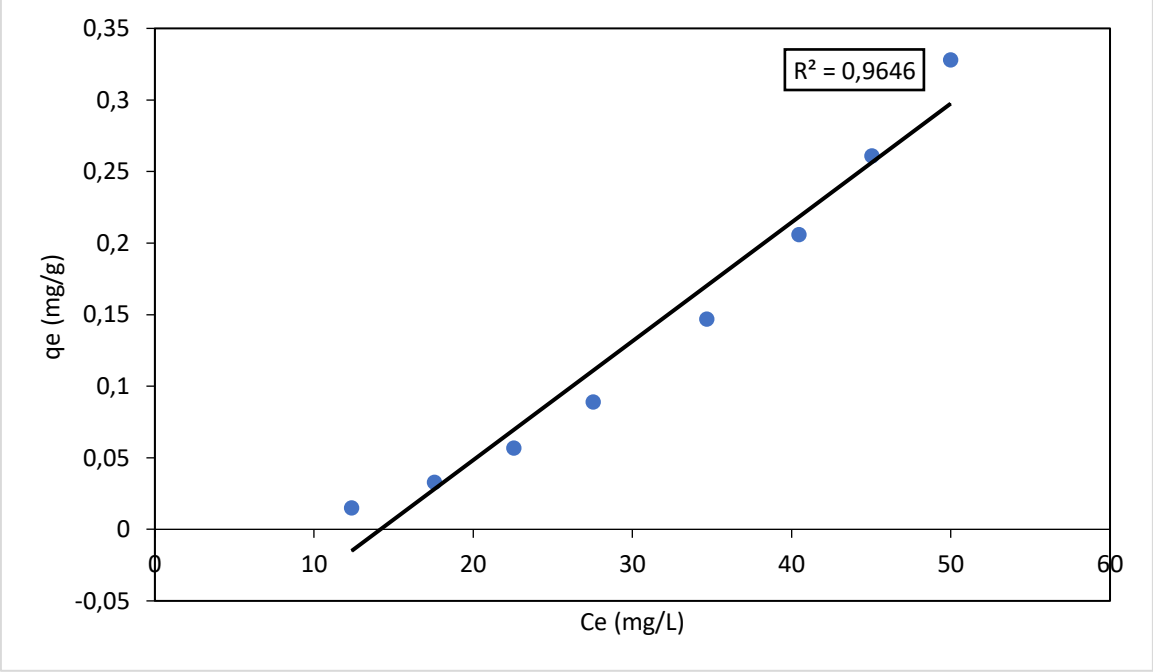

Figure 4.8.a: Fitting of Freundlich Adsorption Isotherms on GO at 80 ºC.

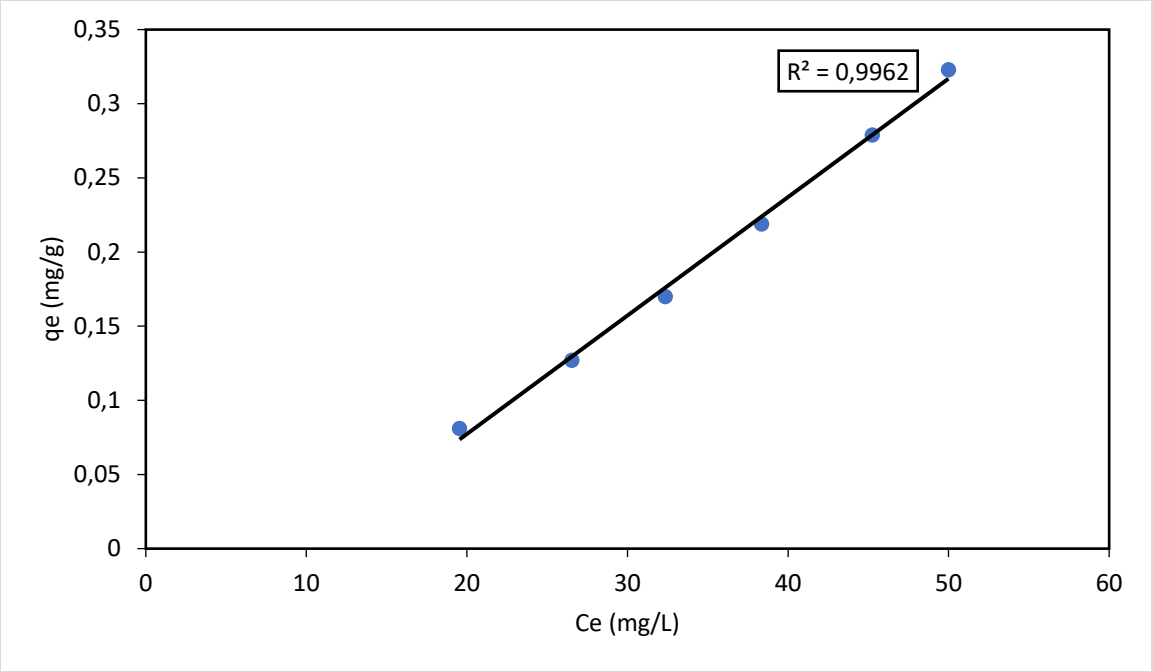

Figure 4.8.b: Fitting of Freundlich Adsorption Isotherms on GAC at 80 ºC.

Table 4.2: Langmuir Adsorption Parameters.

Sorbent	**GO**			**GAC**		
Parameter	q_m	k_{eq}	R^2	q_m	k_{eq}	R^2
Room Temperature	381.6	5.413×10^{-5}	0.9756	434	3.015×10^{-5}	0.9757
30ºC	278.8	8.334×10^{-5}	1	244.8	4.348×10^{-5}	0.9576
Ce at room temp	49.99	47.64	43.12	37.34	32.78	28.88
	25.55	23.32	19.79	16.12		
Ce at 30ºC	49.99	46.67	44.46	38.68	33.31	27.12
	21.12	18.97	15.56	10.32		

Table 4.3: Freundlich Adsorption Parameters.

Sorbent	**GO**				**GAC**			
Parameter	K_f	n	R^2		K_f	n	R^2	
Room Temperature	0.004	0.749	0.9919		0.001	0.684	0.9755	
30ºC	0.001	0.579	0.994		4.480×10^{-5}	0.410	0.9667	
80ºC	6.17×10^{-5}	0.456	0.9646		0.001	0.677	0.9962	
Ce at room temp (GO)	49.99	47.54	42.32	38.34	34.45	30.31	28.45	25.65
Ce at 30ºC (GO)	49.99	46.65	40.42	36.65	34.42	28.23	26.32	22.87
Ce at 80ºC (GO)	49.99	45.04	40.46	34.68	27.53	22.56	17.56	12.36
Ce at room temp (GAC)	49.99	46.64	43.21	37.44	32.38	28.54	25.33	20.03
Ce at 30ºC (GAC)	49.99	44.54	39.89	35.36	30.03	26.60	22.38	18.47
Ce at 80ºC (GAC)	49.99	45.24	38.36	32.36	26.54	19.54	14.35	10.12

In the same way, the studies of samples from the prepared commercial diesel were done using XRD, BET and TGA analysis for their surface porosity to mass characteristics. The equilibrium of sulphur removal percentages was done using a 20wt% of the adsorbents (MeO, AC, GAC and PAC) while using a temperature range from room temperature to 80ºC respectively. The equilibrium and kinetics of sulphur adsorption on the different used adsorbents were examined using two kinetic models (pseudo first order and second order, see Figures 4.1 to 4.3) and tested in determining the adsorption kinetics while using Langmuir and Freundlich isotherm equations.

4.1.3. DBT TEST

In order to develop re-generable adsorbents for diesel fuel desulphurization with DBT adsorption tests, a wide variety of new adsorbents based on graphite oxides, mixed metal oxides, activated carbon and supported metal compounds have been tested using a diesel fuel model containing 50 ppmw. Sulphur content such as 4.6-DMDBT in a mixture of toluene/methanol solvents. The breakthrough curves for adsorption removal of 4.6 DMDBT from model diesel fuel at 80°C on transition metal oxides supported on mesoporous material and activated carbon are shown in Figure 4.9. It is interesting to note that in both cases the 4,6-DMDBT was completely removed. The transition metal oxide adsorbent has a breaking capacity of 5 mg of sulphur per g of adsorbent, while the transition metal supported on activated carbon has a very high breaking capacity of 16 mg/g of adsorbent.

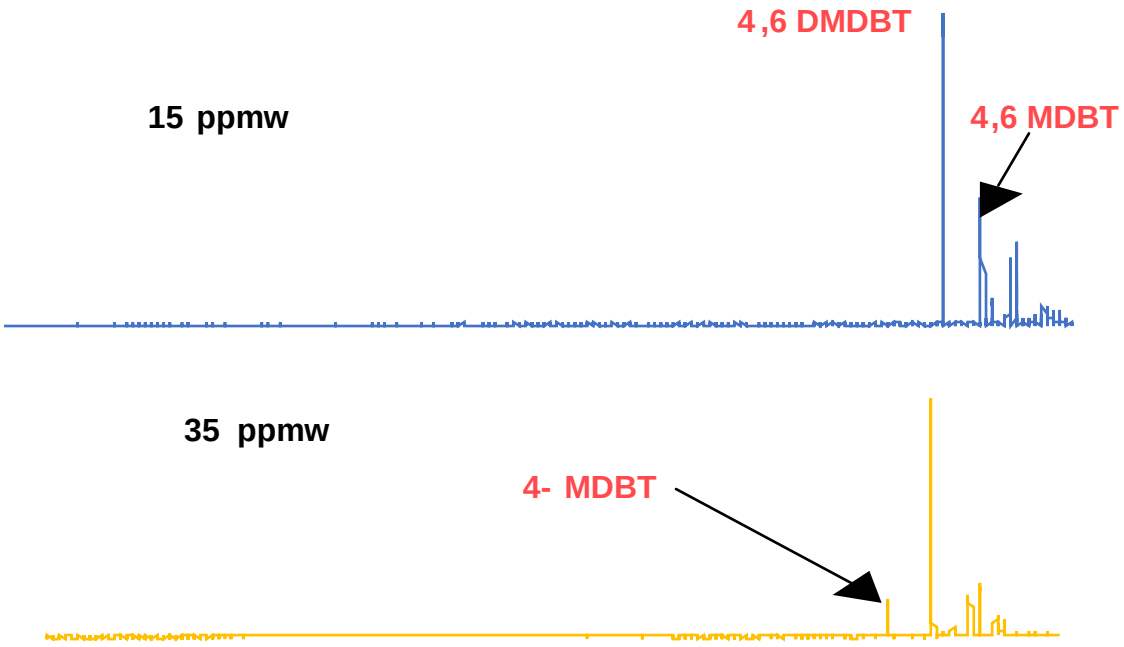

Figure 4.9: Sulphur selective GC PFPD Chromatogram of low sulphur diesel fuels containing 15 ppmw and 35 ppmw sulphur.

An attempt was made to regenerate these adsorbents by rinsing with a 1:1 ratio mixture of methanol and toluene at 80°C. In order to estimate the amount of solvent needed to completely recover 4,6-DMDBT and to regenerate the adsorbent for further use, the solvent fractions were collected and analysed using the total sulphur analyser. The results

indicate that most of the sulphur compounds could be recovered using at least 13 cc of solvent per g of adsorbent. However, more than 90 cc of the solvent is required under the present experimental conditions for the complete removal of all sulphur compounds adsorbed on this particular adsorbent.

This indicates that the sulphur compounds on these adsorbents are removed by surface reactions rather than weak interactions. Experiments using model fuels have revealed that sulphur compounds are destroyed and converted to the corresponding organic fraction although no hydrogen gas was used during adsorption. The results indicate that the adsorbent is able to detect sulphur compounds from this very dilute feed (feed containing 50 ppmw sulphur) and remove them completely (below 1 ppmw) by the surface reaction. The adsorbent was regenerated by treatment with H_2 gas at 450°C for 1 to 2h, then reused for the next cycle. After the solvent wash, the regenerated adsorbent was flushed with N_2 gas (45 mL/min) for about 1.5h at 300°C to remove all adsorbed solvent molecules.

4.1.4. METAL-OXIDE CHARACTERIZATIONS ON GRAPHITE OXIDE

Based on the results analysis, the functional groups on rGO did play a critical role to anchor the ions on the GO surface. This method was performed before by Liu et al., (2012) and the aggregation of the nano-sized ZnO particles was avoided since the remaining functional group on the metal graphite oxide sheets acted active for the ions deposit. From the SEM analysis (see Figure 4.10), the ZnO particles dispersed and have a smaller particle in the Zn ions to be deposited on rGO sheets.

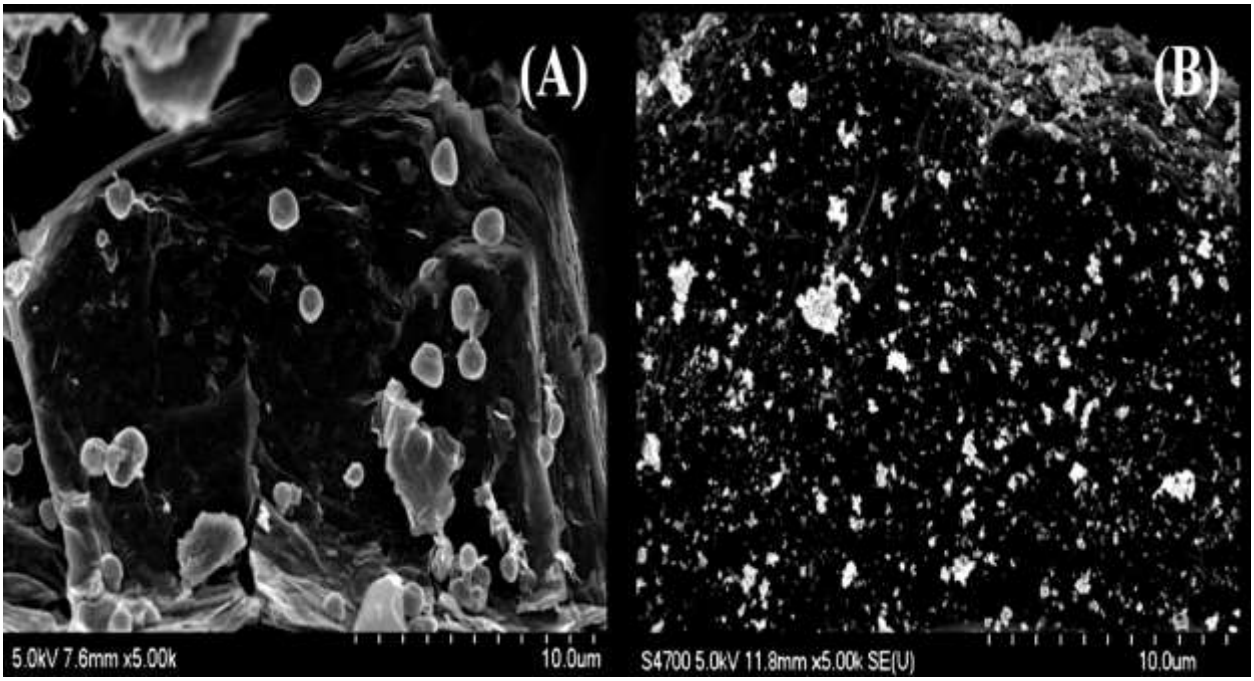

Figure 4.10: SEM images of (A) ZnO/rGO – R and (B) ZnO/rGO – N.

Thus, critical roles of rGO for H_2S adsorption is not only ZnO dispersion but also to adjust Zn oxidation states to a more preferable state. In addition, it shows that Zn particles at the oxygen sites play important roles for the H_2S adsorption. Another metal oxide, copper oxide, which has been known as active metal oxide was added to the ZnO/rGO composite to increase the adsorption capacity beyond H_2S. Based on the copper content, the H_2S adsorption capacity has been increased 18 times for $Cu_{15}Zn_{85}$/rGO compared to pure ZnO. As increasing the Cu mol% to ZnO, the H_2S adsorption capacity increased to 15 mol% Cu showed a higher H_2S adsorption capacity. With more than 15 mol% Cu, the H_2S adsorption capacity had been reduced. Various tests were performed to determine the H_2S breakthrough on ZnO and ZnO/rGO and are shown in Table 4.4

Table 4.4: trial of H_2S adsorption on ZnO and ZnO/rGO

Material	Condition	Trial 1	Trial 2	Trial 3	Trial 4	Average
ZnO	H_2S	19.20	19.47	19.31	19.34	19.26
	SO_2	16.56	16.94	16.04	15.97	16.25
ZnO/rGO	H_2S	77.84	77.42	75.28	78.42	77.28
	SO_2	67.05	66.12	67.63	66.88	66.90

The rGO substrate which contains abundant oxygen functional groups promoted the metal oxide dispersion and increased the H_2S adsorption efficiency. In addition, it was found that the optimum content of copper was 15% in order to maximize the adsorption. The percentage of copper corresponded to the highest portion of zinc ions located in the ZnO lattice. The Cu^{+} and Cu^{2+} ions co-existed with ZnO due to the oxygen containing functional groups from rGO, the majority of the oxygen ions were located at the oxygen deficient region and on the surface of the oxide. After exposure to H_2S, not only zinc sulphide and copper sulphide were produced, but also sulphate because of the loosely bonded oxygen ions from the rGO surface.

4.2. DESULPHURIZATION PROCESS

As shown in Table 4.5, some of the physical properties of diesel fuel after the adsorption process were evaluated and compared with those for the untreated diesel fuel samples. The equilibrium sulphur removal percentages using 20 wt. % of the three adsorbents were determined, where the optimum contact time required to reach equilibrium was found to be one hour. When 20 wt. % of PAC, AC and GO/GAC was mixed with diesel fuel at 30^{o}C temperature, the sulphur content in diesel fuel was reduced respectively. For the un-Desulphurized diesel fuel sample, the calculated diesel indices, and accordingly the cetane numbers showed good ignition quality that can be improved further by the adsorption process. Moreover, results show an improvement in the properties of diesel

oil caused by removing heavy metals and some aromatic compounds from diesel fuel samples. The results for the sulphur removal percentages and the calculated diesel indices after the adsorption process using the three adsorbents at different conditions are given in Table A.6 in Appendix.

Table 4.5: Physical Properties of Untreated and Desulphurized Diesel fuel

Property	ASTM Number	Diesel fuel	Desulphurized diesel fuel		
			(PAC)	(AC)	(GAC)
Aniline point, ^{o}C	D 611	9.403	9.905	9.529	6.654
Ash content, wt.%	D482	0.012	0.11	0.001	0.008
Calorific value, J/g	D 240	5766.579	5766.445	5767.223	5765.489
Cetane index	D613	7.484	8.036	7.760	7.485
Copper strip corrosion rating 3h at 50^{o}C	D130	-	-	-	-
Diesel index	D611	8.662	9.427	9.039	8.938
Flash point, CCPM, ^{o}C	D 93	10.154	10.154	10.154	10.154
Kinematic viscosity at 40^{o}C, cSt	D445	1.320	1.098	1.118	1.118
Lubricity, 60^{o}C	D6079	312	310	312	312
Specific gravity at 15^{o}C	D98	0.103	0.102	0.102	0.102
Sulphur content, ppm	D5453	49.931	16.924	21.061	39.489
Water and sediment vol. %	D1796	-	-	-	-
Water content, vol. %	D96	-	-	-	-

4.3. SURFACE CHARACTERIZATION ON SORBENT

The difference in the amount of trace metals on the surface of the sorbent material provides an indication of the amount of metals leached into diesel fuel from the sorbent materials, which is most likely due to the process used to prepare the commercial sorbent materials. The results showed a decrease in the amount of metals such as aluminium, chromium, iron and nickel on the surface of all adsorbents. In addition, the amount of trace metals in the sorbents before and after the adsorption process was determined during the analysis, and the results are shown in Table 4.6. However, PAC showed an increase in the amount of cobalt and lead; while AC and GAC showed a slight decrease in the amount of these metals. A scanning electron microscopy (SEM) instrument was used to study the surface structure of sorbent materials before and after the adsorption process. The results showed that fresh activated carbon and granular carbon sorbent materials have a smooth surface with a compact structure. After adsorption, the results showed that sulphur is adsorbed homogeneously on the surfaces of sorbent materials, proving the validity of using both activated carbon and granular carbon for the adsorption of sulphur from diesel fuel.

Table 4.6: Heavy Metals in ppm for the Different Sorbents

Sorbent Material	Aluminium	Cobalt	Chromium	Copper	Iron	Nickel	Lead
PAC (fresh)	262	0.00	16.3	6.70	135	11.3	4.55
PAC (after adsorption)	142	1.67	6.26	12.3	64.3	8.46	5.15
AC (fresh)	91	1.22	3.47	13.1	108	4.13	5.48
AC (after adsorption)	82.1	1.25	1.39	7.80	40.3	4.02	5.33
GAC (fresh)	110.4	0.45	142	14.9	895	568	7.98
GAC (after adsorption)	20.4	0.36	1.37	4.48	13.1	5.69	0.44

4.4. MASS FLOW CONTROLLER CALIBRATION

The calibration of all the mass flowrates were done on each set and trial as indicate with table 4.7 to 4.10 during the course of the experiment.

Table 4.7: Nitrogen

N_2 (10 mL)					
SET	Trial 1	Trial 2	Average	mL/sec	mL/min
100	40	40	40.0	2.5	150.0
120	39	40	39.5	3.0	180.0
140	38	39	38.5	2.6	156.0
160	36	36	36.0	2.7	162.0
180	34	35	34.5	2.8	168.0
200	33	32	32.5	3.1	186.0
220	30	30	30.0	3.3	198.0

Table 4.8: Carbon dioxide

CO_2 (10 mL)					
SET	Trial 1	Trial 2	Average	mL/sec	mL/min
14	22.21	21.28	21.75	0.043	2.58
16	18.42	18.02	18.22	0.055	3.30
18	16.38	16.33	16.36	0.066	3.96
20	14.63	14.54	15.48	0.074	4.44
22	12.94	12.78	12.86	0.078	4.68

Table 4.9: Sulphur dioxide

SO_2 (10 mL)							
	Trial 1	Trial 2	Trial 3	Trial 4	Average	mL/sec	mL/min
15	16.53	15.30	15.60	16.20	15.91	0.061	3.7
17	14.59	13.93	14.58	14.18	14.32	0.071	4.3
19	12.40	12.38	12.76	12.68	12.48	0.079	4.7
21	11.24	11.75	11.43	11.07	11.45	0.088	5.3
23	10.98	10.93	10.54	10.25	10.77	0.096	5.7

Table 4.10: Hydrogen sulphide

H_2S (10 mL)							
SET	Trial 1	Trial 2	Trial 3	Trial 4	Average	mL/sec	mL/min
5	10.66	10.85	10.71	10.71	10.73	0.11	6.6
7	7.84	7.08	7.59	7.07	7.58	0.14	8.4
9	5.09	6.01	6.04	6.13	5.82	0.17	10.2
10	5.51	5.06	5.63	5.59	5.45	0.19	11.4

4.5 RAW DATA

Table 4.11 DBT adsorption data

Component	Trial 1	Trial 2	Trial 3	Trial 4	Average
Graphite	0.22	0.13	0.14	0.21	0.18
GO	0.15	0.14	0.17	0.18	0.16
rGO	0.21	0.15	0.26	0.21	0.21
GAC	5.48	5.68	6.39	4.87	5.61
ZnO	10.59	9.87	11.15	10.53	10.54

Unit: mg.S adsorbed/g of adsorbent

The DBT trial test (table 4.11) on for adsorption on graphite, GO, rGO, GAC and ZnO absorbent in all four trials in regard to the sulphur adsorption s, ZnO showed a greater desulphurization (11.15 mg.S adsorbed/g of adsorbent) than others followed by GAC (5.61 mg.S adsorbed/g of adsorbent) while the graphite (0.13 mg.S adsorbed/g of adsorbent) had the lowest desulphurization absorption capacity (figure 4.11).

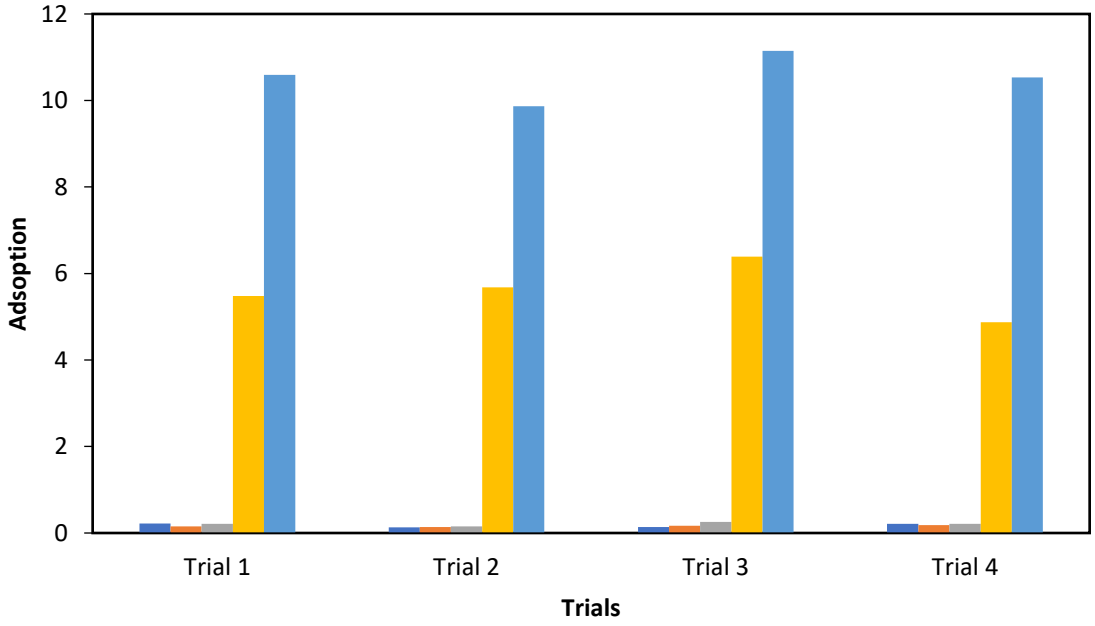

Figure 4.11: DBT test against trial

Each trial on absorbents used, both zinc oxide (ZnO) and granular activated charcoal (GAC) showed a significant sulphur removal as a dominant sorbent than others. With the abundant oxygen functional group in ZnO turned it to have a great sulphur absorption efficiency while the dispersion of metal oxide in the solution. Coming to GAC in regards of sulphur removal, this in turn showed the capacity to compete with a metal oxide due to homogeneous absorption of sulphur capacity than the remain sorbent materials form the diesel fuel.

Table 4.12: H_2S and SO_2 adsorption on ZnO in H_2S/N_2 environment at 300°C

Sample weight: 3.55 g				
Trial	Time (min)	min/g of adsorbent	H_2S (ppm)	SO_2 (ppm)
1	5	2.8	0.00	5.6
	10	31.0	0.00	8.5
	15	33.8	0.00	11.3
	20	5.6	1.20	12.1
	25	14.1	1.25	14.1
	30	19.7	1.33	16.2
	35	36.6	1.61	16.8
	40	42.5	1.80	19.4
	45	50.7	2.00	19.7
	50	62.0	2.21	22.1
	55	67.6	2.62	22.5
	60	76.1	5.68	23.2

Trial	Time (min)	min/g of adsorbent	H_2S (ppm)	SO_2 (ppm)
2	5	2.9	0.00	8.6
	10	8.6	0.00	14.4
	15	11.5	0.00	17.4
	20	17.2	0.00	20.1
	25	23.1	1.56	23.6
	30	31.6	1.89	34.5
	35	35.4	2.22	36.7
	40	37.4	2.85	40.2
	45	46.0	3.80	43.1
	50	51.7	4.60	48.6
	55	63.2	5.46	48.6
	60	66.1	7.92	48.6
Sample weight: 3.62 g				
3	5	3.8	2.62	0.00
	10	19.3	2.91	0.23
	15	30.4	3.40	0.56
	20	35.9	4.10	1.62
	25	44.2	4.72	1.68
	30	49.7	5.10	2.31
	35	60.8	5.75	2.55
	40	66.3	7.01	2.89
	45	71.8	7.82	3.22
	50	80.1	8.30	3.66
	55	89.7	9.54	4.10
	60	93.9	11.00	4.67

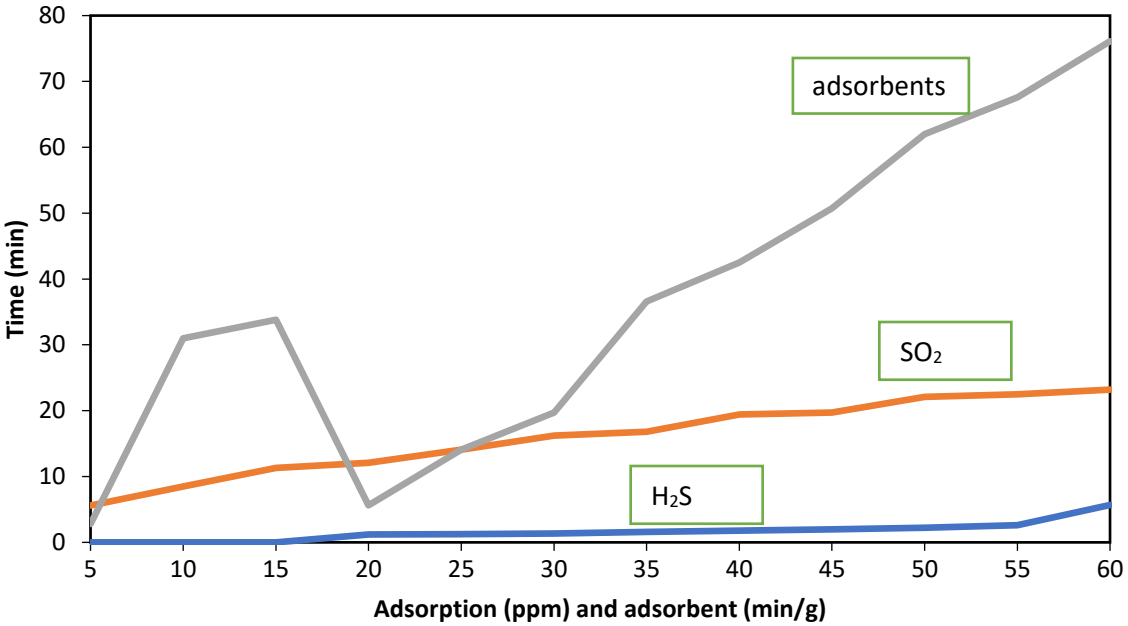

Figure 4.12: Adsorbent, H_2S and SO_2 adsorption against time.

The adsorbent showed a greater removal of SO_2 than H_2S respectively with five minutes interval on sample collections for an hour (figure 4.12 on trial 1 from table 4.12). As discussed earlier from Figure 4.11, the sorbent has a high capacity of desulphurisation due to its metal oxide bonds. The higher the sorbent introduced in the system, the higher the sulphur compound removed at a given time.

Table 4.13: Sulphur content (ppm) experimental data for PAC

Temperature ($_oC$)	Amount of PAC (wt. %)							
	2	4	6	8	10	16	18	20
Room Temperature	49.9	43.6	37.4	39.4	34.7	31.1	32.5	28.6
30	41.3	38.7	35.3	34.5	30.7	25.2	27.3	24.4
80	41.7	28.7	26.2	26.2	23.4	23.4	21.7	18.6

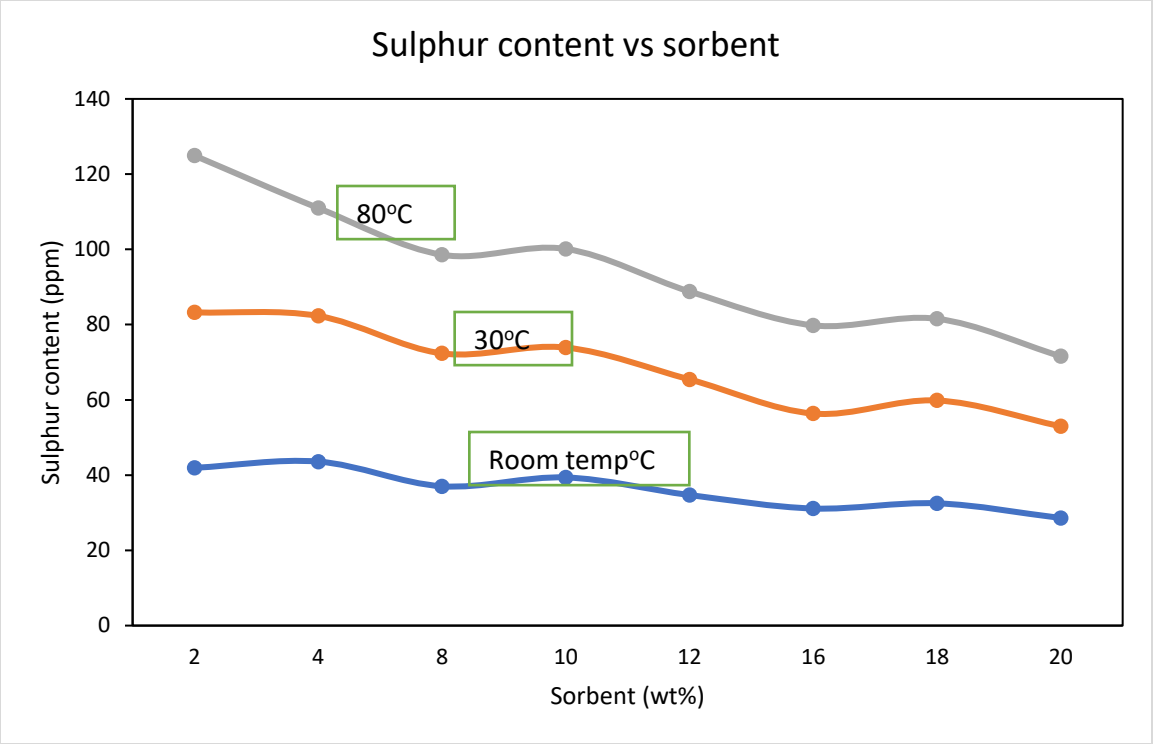

Figure 4.13: sulphur content (ppm) against temperature.

Figure 4.13 showing the sulphur removal at each temperature (room temperature, 30°C and 80°C) on each amount of PAC (from 2 wt. % to 20 wt. % sorbent). The observation on the behaviour of each wt. % of sorbent on the sulphur removal from the sample is indicated from the graph. The higher the sorbent used on each temperature, the higher the sulphur content was removed. On each three chosen temperatures, 80°C showed highest removal of sulphur content to 18.6 ppm with 20 wt. %. Also, at each temperature, 20 wt. % had a great removal capacity. This means, the higher the percentage of sorbent for the sulphur removal together with the high temperature, will result in the great sulphur removal from the diesel samples when using PAC sorbent.

The experimental date for AC shown in table 4.14 for the sulphur content per amount of sorbent used indicate that at each temperature had high removal of sulphur content at 20 wt. %. The 30°C temperature had the most removal of 16.6 ppm sulphur content in the diesel fuel.

Table 4.14: Sulphur content (ppm) experimental data for AC.

Temperature (°C)	Amount of AC (wt. %)							
	4	6	8	10	12	16	18	20
Room Temperature	40.3	36.3	35.9	33.4	32.5	29.9	31.3	24.5
30	29.1	28.3	27.5	27.4	26.4	25.3	24.5	16.6
80	32.9	30.4	29.3	26.8	25.4	24.1	23.7	19.8

4.6 XRD TEST

The effect of metals oxides and rGO composite with regard to the adsorption capacity of hydrogen sulphide were studied on the oxidation changes. Specially, on metals species such as copper, zinc oxides, etc. by using crystallite analysis (XRD) (figure 4.14). To identify the lattice of those atoms with the use of x-ray beam diffracted by atoms as it has a regular lattice waves since the crystals had regular and repeated arrays of atoms. For the desulphurization process by adsorption considered, the two powdered activated carbon (PAC and AC) showed a better affinity for removal of sulphur compared to the granular activated carbon (GAC). Therefore, positively charged metal Zn^{2+} ions in zinc salt solution are able to be adsorbed on the surface of GO from negatively charged oxygen functional groups and form ZnO masses which may act as nuclei for the particle growth in subsequent thermal heat treatment. After reduction by reflux and microwave, the characteristic peak of GO disappeared by removing the oxygen functional groups which link the GO layers indicating that the structure of GO disappeared. The experimental data for PAC and AC are well suited to Freundlich isotherm and pseudo second-order kinetic models.

In addition, the defects of ZnO which implied oxygen vacancy sites in ZnO lattice increased the portion of heterogeneity of ZnO, and the oxygen vacancy was able to obstruct the electron-hole recombination which could increase the reactivity of H_2S adsorption. Therefore, over the cycles, the Zn-O lattice structure was destroyed to produce ZnS structure, but there was no ZnO regeneration due to the lack of oxygen source. The crystallite size of ZnO increased and its lattice structure was maintained over several cycles.

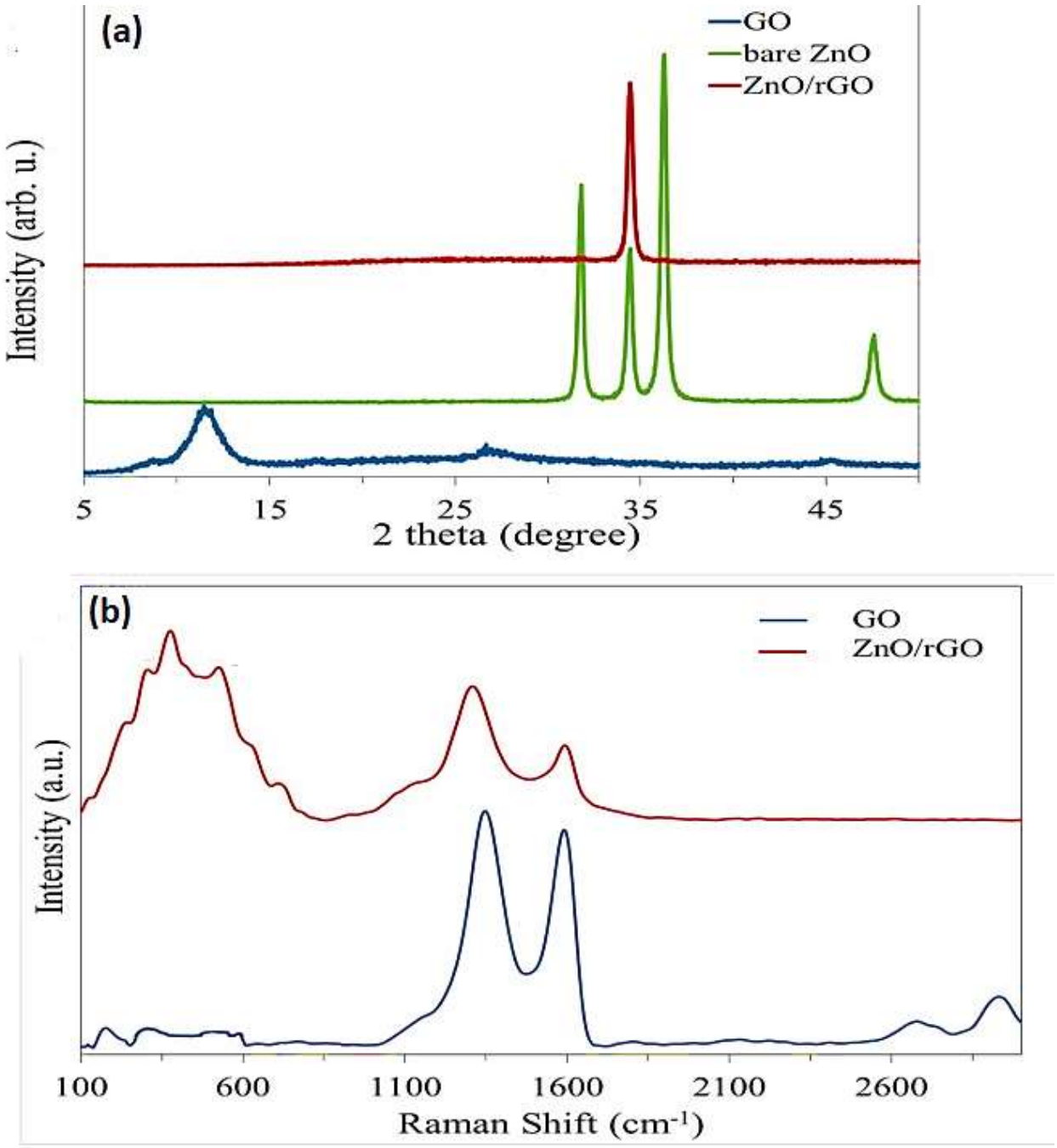

Figure 4.14: XRD analysis for (a) GO, ZnO and ZnO/rGO and (b) GO and Zn/rGO.

The crystallite size of ZnO/rGO remained constant while the sizes of ZnO were smaller than of ZnO/rGO. Beside he morphology changes, the chemical state of Zn and O in the ZnO matrix was also modified during the H_2S sulphidation-regeneration cycles; and it caused a decrease in adsorption capacity over multiple cycles.

The main characteristic peaks of GO (Raman Shift (b)), D-band at 1300 and 2682 cm^{-1} corresponded to disordered sp^2 carbon atoms and G-band at 1600 and 2938 cm^{-1} to the E_2 vibrational mode of sp^2 bonded carbon atoms was found. The ratio of intensities of the bands of rGO increased from 1.08 to 1.58 compared to GO Raman pattern in the mean crystallite size. The three Raman shifts located at 312, 390 and 530 cm^{-1} of ZnO crystal. The stronger band was the one of 390 cm^{-1} and smaller peaks at 312 cm^{-1} and 530 cm^{-1} are assigned to the second order arising from zone boundary.

4.7 FTIR AND TGA TEST

The use of FTIR (figure 4.15) in the identification of the functional group present on the surface of the MeO/GO and MeO/GAC sorbents and studied before and after each sulphidation regeneration cycle. The FTIR helped also on identifying the vibration on the structure formed during the contact of the metal oxides onto the prepared diesel samples. As the identification of the functional groups on the metal oxides by FTIR, the Thermogravimetric analysis (TGA) was also performed on the sample to give a clear understanding about the mass characterization after and before desulphurization at a given time and temperature during the whole process.

For the FTIR spectra of GO, rGO and ZnO/rGO composite, the composites from the microwave method (rGO-M and ZnO/rGO-M) possess stronger peaks of hydroxyl groups than that those obtained from the reflux method (rGO-R and ZnO/rGO-R). It implies that the 3 min irradiation with 30 sec interval of microwave reduction provides a milder reduction environment, even though the microwave provides rapid heating of the solution. The vibrational peaks are contributed by the three different components that make up of oxide groups. The broad band at the interval from 3250 to 3400 cm^{-1} that was assigned to the -OH group stretching increases in intensity and shifted slightly to lower wavenumbers. This can be attributed to the presence of inter- and intramolecular hydrogen bonded hydroxyl groups having form association between the three different sorbent components used in the experiment.

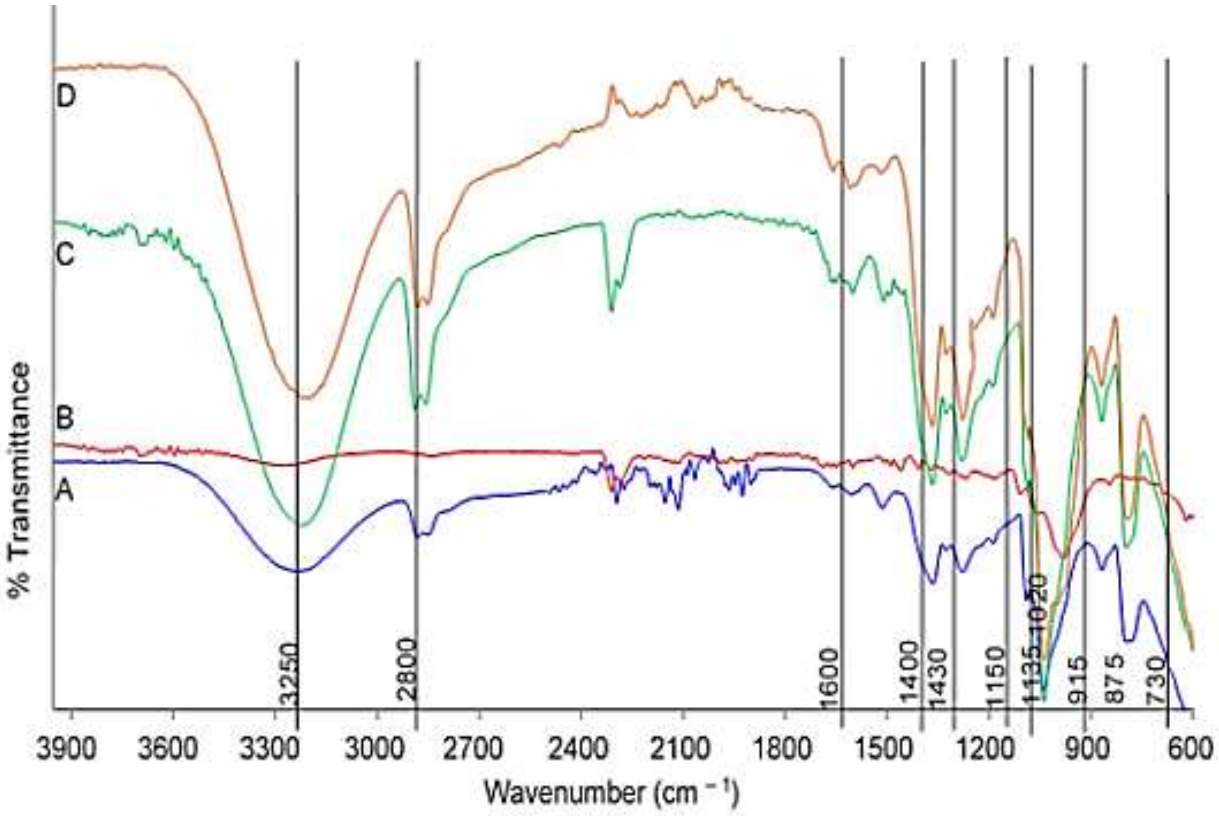

Figure 4.15. FTIR spectrum of pure ZnO (A), treated rGO (B), ZnO/rGO (C) and GO (D) at the frequency range of 650-3900 cm^{-1}

However, after the H_2S adsorption test, the amount of the hydroxyl groups decreased. It indicates that the hydroxyl groups, which are attached on the ZnO surface, play a critical role for the H_2S adsorption. The amount of hydroxyl group on ZnO surface after the moisturizing process increased compared to that of the fresh sample. It implies that the moist air provides –OH groups to the ZnO/rGO surface. In addition, the intensity of Zn-O bond also decreased after the adsorption test. It also confirms that a portion of Zn-O bond reacted with H_2S and changed to ZnS.

TGA analysis is an ideal method of proving the particle size of ZnO deposited on the rGO surface and thus it is observed that nano-size ZnO particles were deposited on the surface of rGO. Those ZnO particles are well dispersed and separated from each other on the rGO surface which displays a good combination between rGO sheet and ZnO nanoparticles. One possible reason is that the rapid and short heating process by microwave decreases the particle size of ZnO. Therefore, the surface area of ZnO for the

H_2S adsorption has increased. The sulphur content and TGA weight loss obtained from the impregnated carbons at different reaction temperatures. The weight losses in all the samples caused by heating in TGA apparatus are in agreement with the amount of sulphur measured by the apparatus with the temperature range from room temperature to 400^oC. For higher H_2S concentrations in the feed stream, it was seen that room temperature is sufficient to achieve high sulphur loading. Therefore, nearly no sulphur loss from these adsorbents would occur in full-scale applications even if they were produced through low temperature impregnation processes. However, more than 100°C temperatures are not desirable since they will cause other pollutants, such as SO_x and SO_2, to form and will reduce sulphur loading on the carbon surface. Actual catalyst bed temperature increases during the reaction and the degree of increase varies with different H_2S concentrations in the influent gases.

4.8 BET TEST

The surface area and pore size distribution on the metal oxide sorbents species where characterised and analysed by the BET analyser (table 4.15) as a quantitative analysis (yield percent of carbon and carbon functionality). This was conducted with N_2 adsorption isotherm to find out the pore size distribution and surface area on each used sorbent, and the analysis showed a heterogenous surface and several sizes while the surface roughness indicated the high surface area for adhering adsorbate molecules from the prepared feed diesel adsorption. The studied internal surface area from the analysis was confined to the pore structure of the adsorbent materials (AC of 125.56, GAC of 128.40, PAC of 122.55, GO of 118.30 and rGO of 120.68 in pore diameter) while keeping in mind that the pore structure as a major factor which could affect the adsorption process. Also, if the diameter of the adsorbate molecules is higher, the lower the adsorption would take place due to the steric barrier (interference) at low pressure in the N_2 adsorption. The sulphur content removal favoured in the increase in adsorption time, temperature and concentration on all the technics and sorbents used to sulphurise the diesel fuel feed stream.

Table 4.15: Surface area, pore volume and pore diameter of the adsorbents with 5 wt. % impregnation.

Adsorbent	Surface area (m^2/g)	Pore volume (m^3/g)	Pore diameter (Å)
AC	118	0.45	125.56
GAC	184	0.39	128.40
PAC	217	1.55	122.55
GO	799	0.06	118.30
rGO	825	0.41	120.68

4.9 FINDINGS

In this chapter, the effects of copper with zinc oxide (ZnO) and reduced graphite oxide (rGO) composite on the adsorption capacity of hydrogen sulphide (H_2S) were investigated. It was found that depending on the copper load, the adsorption capacity of H_2S was increased up to 18 times compared to pure ZnO. In order to study the oxidation changes on copper and zinc oxides, crystallite analysis by XRD and chemical state analysis by XPS were performed. The rGO substrate, containing abundant oxygen functional groups, was confirmed to promote the dispersion of metal oxide and increase the adsorption efficiency of H_2S by providing oxygen ions weakly bound to sulphur molecules.

For the desulphurization process by adsorption considered, the two powdered activated carbon (PAC and AC) showed a better affinity for the removal of sulphur compared to granular activated carbon (GAC). The adsorption isotherms for PAC and AC were determined using the isothermal models of Langmuir and Freundlich. The results showed that for PAC and AC, the adsorption behaviour was better described by the isothermal model of Freundlich at all the temperatures considered. The kinetic data of the three adsorbents follow a pseudo-second order model. The results indicated that the adsorption of sulphur in the kinetic study proved the applicability of the pseudo-second order model.

From H_2S breakthrough tests, ZnO/rGO composite was confirmed to have almost 4 times higher ZnO utilization efficiency than pure ZnO particle at 200°C. In addition, it also showed that the presence of H_2 in the H_2S/N_2 environment, the H_2S breakthrough time had been increased since the hydrogen molecules provided the reducing environment for the Zn – S product. The presence of H_2 led to the decomposition of Zn – S and provided Zn^{2+} active for the sulphur molecules. In contrast, the presence of CO_2 inhibited the adsorption of H_2S. This is explained by the competitive adsorption between H_2S and CO_2. In addition, the optimum copper content was 15% bound to ZnO to maximize the adsorption of H_2S. The 15% copper with ZnO/rGO led to most of the zinc ions located in the Zn-O network; and the coexistence of Cu^{+} and Cu^{2+} ions with ZnO.

For the removal of hydrogen sulphide (H_2S) in the gas phase, the critical role of reduced graphite oxide (rGO) for active dispersion of ZnO nano-particles was investigated. XPS and FT-IR analysis confirmed that the microwave-assisted the reduction process provided a gentle reduction environment to GO. As a result, the oxygen functional groups remained attached on the rGO surface. These oxygen functional groups anchored the metal oxide, thus aiding the dispersion of the active ZnO particles on the surface. From calcination experiments, ZnO/rGO was shown to prevent the aggregation effect on ZnO at 300°C which could allow for larger specific surface area of the active ZnO to H_2S gas.

For the removal of the dibenzothiophene (DBT) compound in liquid phase, the characteristics of graphite oxide and graphene were changed depending on the preparation method used. The interlayer *d*-spacing for graphite oxide was especially controlled by the synthesis method. The synthesis of graphite oxide led to a higher degree of oxidation than synthesizing it by the Hummers' method and it also led to a larger crystallite size and thinner graphene than that from Hummers' method. DBT adsorption tests were performed for a commercial diesel. However, graphene materials, which have a sp^2 configuration, were able to adsorb DBT compounds *via* π-π interactions. Graphene which has a higher surface area and thinner thickness showed a higher DBT adsorption capacity.

The reduced DBT adsorption selectivity in the presence of aromatic compounds was confirmed by performing DBT adsorption tests in the presence of different concentrations

of toluene. Desulphurization by adsorption of diesel fuel using activated charcoals has shown good performance for sulphur removal and has significantly improved the ignition quality of fuel. Comparing the ignition quality measure (diesel index) before and after the adsorption process showed a direct increase between the calculated diesel indices and the amounts of sorbent material used. This result was achieved at the three temperatures considered and as the temperature increases, the calculated diesel index decreases.

The temperature conditions for the experiment were found to be room temperature, 30^{o}C, 80^{o}C and 100^{o}C, while the sorbents materials used the volume levels as 1wt% to 20wt%. The contact times for the sorbents to the influents were from 1 hour to 3 hours. The production of GO using incipient wetness impregnation method with metals species on GAC was performed at temperature range from 120^{o}C to 500^{o}C with 2 hours to 24 hours intermediate while mixing different mass numbers of sorbents, keeping in mind that GO and different adsorbents have been prepared using different practices such as chemical exfoliation, microwave-assisted chemical reduction and incipient impregnation methods using different masses, chemicals and temperatures conditions as explained in Chapter 3.

In order to estimate the amount of solvent needed to regenerate the adsorbent for further use, the fractions of the solvent were collected and analysed using total sulphur analyser. The results indicate that the sulphur compounds can be recovered using at least 15 cc of the solvent per each gram of adsorbent under the present experimental condition on a particular adsorbent. This indicates that the sulphur compounds on these adsorbents are removed by surface reactions rather than weak interactions. The results indicate that the adsorbent is able to detect the sulphur compounds from this very dilute feed (feed containing 50 ppmw of sulphur) and remove them completely (below 1 ppmw) by the surface reaction. The adsorbent was regenerated by treatment with H_2 gas at 450˚C for 1 to 2 hours and then reused for the subsequent run. After washing off the solvent, the regenerated adsorbent was rinsed with N_2 gas (45 ml/min) for about 1 hour and half at 300˚C to remove all solvent molecules adsorbed in the solution.

The deposit of heavy metals on GO materials was achieved in the experiment thanks to exceptional adsorbents while the applications of graphene oxide (GO), reduce graphene

oxide (rGO), and graphene-based nanocomposites for the removal of various metals were analyzed. The adsorption of heavy metals including arsenic, lead, cadmium, nickel, mercury, chromium and copper using graphene-based materials is reviewed and analyzed using different techniques as stated in the point 3.2 of this thesis. The adsorption isotherms, kinetics, capacity, and removal efficiency for each metal on different graphene materials, as well as the effects of the synthesis method and the conditions of the adsorption process on the recyclability of the graphene materials, were discussed.

CHAPTER 5: CONCLUSIONS AND RECOMMENDATIONS

5.1. CONCLUSIONS

Based on the results obtained in this work for commercial diesel fuel in how to reduce its sulphur content with a metal-based nanocomposite. The experiment on the adsorption capacity of carbon-based adsorbents for the removal of sulphur compounds from diesel fuel was carried out. This provided essential data to model the physical adsorption process. Develop an appropriate regeneration method for the spent sorbent materials for the study. Considering the loss of adsorption capacity of spent sorbent materials after several tests on adsorption regeneration cycles, the study helped to understand the overall sulphur removal process when different adsorbents are used to verify which one is effective and convenient to remove a high percentage of sulphur in a short period of time and other conditions. PAC and AC showed a better sulphur removal affinity compared to GAC. The adsorption behaviour is best described by the Freundlich isothermal model. The results indicate that the sulphur adsorption kinetics study proves the applicability of the pseudo-second order model.

Organic sulphur compounds can be recovered by separating them from the solvent and concentrated sulphur compounds can be treated in small HDS reactors to remove sulphur and the remaining organic fraction can be mixed with the fuel. Solvent regeneration aimed to avoid SO_x emissions generated by oxidative regeneration or H_2S generated during reductive regeneration. The study shows that the sorbents used can effectively remove sulphur compounds.

The synthesis of hydrated zirconia / graphene composites resulting in chemical synergy, new pores and new surface chemistry are formed, which leads to improved sulphur dioxide removal capacity in dry and wet conditions. The addition of a graphene component makes the surface less competitive for water adsorption. SO_2 is retained on the surface by physical adsorption in small pores and via reactions with terminal -OH groups of hydrated zirconia. This latter reaction leads to the formation of sulphides. There is an indication that small amounts of sulphates are also formed due to the oxidation of SO_2 by oxygen activated by the specific chemistry of the graphene layers.

A new modification of GO and rGO via the development of nanocomposites with metal oxides and organic molecules improves their sorption characteristics. Heat treatment at different temperature ranges, vacuum promoted exfoliation, physical incorporation of additives, and surface modifications using oxidative agents were among the few techniques used in the synthesis processes.

5.2. RECOMMENDATIONS

In this study, several recommended works are proposed below for future studies.

- In order to maximize the H_2S adsorption capacity, well dispersed metal oxide on the rGO surface is necessary.
- In general, deep understanding of metal oxide/graphene interaction is required to produce an appropriate adsorbent. Essentially, the graphite oxide (GO) possessing a larger interlayer spacing is required to provide easier exfoliation which can produce a thinner layered rGO.
- The exfoliation of GO to rGO can be controlled depending on the reduction methods. It can be expected that a thinner layered rGO sheet increases the larger surface area for metal oxide deposition.
- An optimum period of reduction using reducing agent (i.e. hydrazine) needs to be determined while the metal oxide/GO solution is reduced by microwave irradiation.
- It can be proposed that the rGO possessing an abundant amount of oxygen functional groups resisted the destruction of the ZnO lattice matrix over cycles.

REFERENCES

Aguila P., Gracia G., Araya F. and Baeza P., 2008. "Desulfurization by adsorption with copper supported on zirconia," *Catalysis Communications*, vol. 9, pp. 751 – 755.

Aida T. and Funakoshi I., 1998. "Process for recovering organic sulphur compounds from fuel oil," U.S. Patent 5753102 A.

Al-Malki, 2004. "Desulfurization of Gasoline and Diesel Fuels, Using Non-Hydrogen Consuming Techniques," M.S. thesis, King Fahd University of Petroleum & Minerals.

Bagheri, S., Muhd, N. & Green, I.Á., 2016. Effect of hybridization on the value-added activated carbon materials. *International Journal of Industrial Chemistry*, 7(3), pp.249 – 264.

Bamufleh, H.S., 2009. Applied Catalysis A: General single and binary sulphur removal components from model diesel fuel using granular activated carbon from dates' stones activated by $ZnCl_2$. 365, pp.153 – 158.

Behl, M., 2014. *Desulfurization by reactive adsorption on oxide/metal composites*. University of Illinois at Urbana-Champaign.

Bharvani R. R. and Henderson R. S., 2014 "Revamp your hydrotreater for deep desulfurization".Internet:http://www.hydrocarbonprocessing.com/Article/2600166/Revamp-yourhydrotreater-for-deep-desulfurization.html. Accessed March 2019.

Campos-Matin, J.M. et al., 2010. Oxidative processes of desulfurization of liquid fuels. Instituto de catalysisy petro leoquimica, CSIC, Marie Currie 2, Cantoblanco.

Chandra V. and Kumar S. R., 2012. "Studies on Adsorptive Desulfurization by Activated Carbon," *Clean-Soil Air Water*, vol. 40, pp.545 – 550.

Chevron, 2007. Diesel fuels technical review report. *Journal of Global Marketing.*

Choi K H., Korai Y., Mochida I. and Sano Y., 2004. "Selection, further activation of activated carbons for removal of nitrogen species in gas oil as a pre-treatment for its deep hydrodesulfurization," *Energy Fuels*, vol. 18, p. 644.

Darwish, N.N., 2015. *Adsorption study of desulfurization of diesel oil using activated charcoal*. Sharjah, United Arab Emirates.

Dastgheib S. A., Elham R. K., and Moosavi S.,2012. "Adsorption of Thiophenic Compounds from Model Diesel Fuel Using Copper and Nickel Impregnated Activated Carbons," *Energies*, vol. 5, pp. 4233 – 4250.

De Klerk., 2007. Environmentally friendly refining: Fisher-Tropsch versus crude oil. *Green Chem*. 9, pp 560 – 565.

Djega-Mariadassou M., Pessayre G., Geantet S., Vrinat C., Perot M., Lemaire G., and Breysse M., 2003. "Deep desulfurization: reactions, catalysts and technological challenges," *Catalysis Today*, vol. 84, pp. 129 – 138.

Dubey, S.P. et al., 2015. Synthesis and characterization of metal-doped reduced graphene oxide composites, and their application in removal of Escherichia coli, arsenic and 4-nitrophenol. *Journal of Industrial and Engineering Chemistry*, 29, pp.282 – 288.

Fallah, R.N. et al., 2012. Selective desulfurization of model diesel fuel by carbon nanoparticles as adsorbent*. Ind. Eng. Chem. Res.*, *51* (44), pp 14419 – 14427

Fronczak M., Pyrzyńska K., Bhattarai A., Pietrowski and P. Bystrzejewski M., 2019. Improved adsorption performance of activated carbon covalently functionalised with sulphur-containing ligands in the removal of cadmium from aqueous solutions. *International Journal of Environmental Science and Technology.* 16, pp.7921 – 7932.

Gatan, R., 2004. Oxidative desulfurization: A new technology for Ulsd. Prepr. Pap. -Am. Chem. Soc., Div. Fuel Chem. 49(2), pp.577 – 579.

Hae-Kyung Jeong, Yun Pyo Lee, Rob J. W. E. Lahaye, Min-Ho Park, Kay Hyeok An, Ick Jun Kim, Cheol-Woong Yang, Chong Yun Park, Rodney Ruoff S. and Young Hee Lee, 2008. Evidence of Graphitic AB Stacking Order of Graphite Oxides. *JACS articles*.

Hernandez-Maldonaldo A.J.; Yang R.T.,2004. Desulfurization of Transportation Fuels by Adsorption. *Catalysis Reviews*, *46*(2), pp111 – 150.

Karayilan, D., 2004. *Removal of hydrogen sulfide by regenerable metal oxide sorbents*. Middle East Technical University.

Katzer, J. R., Ramage, M. P., and Sapre, A. V., 2000. Petroleum refining: poised for profound changes. *Chem. Eng. Prog.*, vol. 6, pp. 41 – 51.

Kim J. H., Ma X., Zhou A. and Song C., 2006. "Ultra-deep desulfurization and denitrogenation of diesel fuel by selective adsorption over three different adsorbents: a study on adsorptive selectivity and mechanism," *Catalysis Today*, vol. 111, pp. 74 – 83.

Lam,V., Li, G., Song, C., Chen, J., Fairbridge, C., Hui, R. and Zhang, J., 2012. A review of electrochemical desulfurization technologies for fossil fuels. *Fuel Process. Technol.*, vol. 98, pp. 30 – 38.

Lee, M. J., Prince, M. K., Garrett, R. C., George, K. K., Pickering, G. N., and Grossman I. J., 1999. "Microbial desulfurization of a crude oil middle-distillate fraction: Analysis of the extent of sulphur removal and the effect of removal on remaining sulphur," *Applied and Environmental Microbiology,* vol. 65, pp. 181 – 188.

Leliveld R. G. and Eijsbouts S. E., 2008. How a 70-year-old catalytic refinery process is still ever dependent on innovation. *Catalysis Today*, 130, pp. 183 – 189.

Li D., Li W., Peng J., Xia H., Zhang L., Guo S., Chen G. and Wang X., 2013. "Optimization of Mesoporous Activated Carbon from Coconut Shells by Chemical Activation with Phosphoric Acid," *BioResources*, vol. 8, pp. 6184 – 6195.

Li, H., 2008. *Selective catalytic oxidation of hydrogen sulfide from syngas*. University of Pittsburgh.

Lison, J., 2010. Selective adsorption of dibenzothiophenes on activated carbons with metal species deposited on their surfaces. *City College of New York* (CUNY).

Liu Y., Hu Y., Zhou M., Qian H. and Hu X., 2012. Microwave-assisted non-aqueous route to deposit well-dispersed ZnO nanocrystals on reduced graphene oxide sheets with improved photoactivity for the decolorization of dyes under visible light. *Journal of Appl. Catal. B Environ.*, vol. 125, pp. 425 – 431.

Lonkar, S.P. et al., 2016. Facile in situ fabrication of nanostructured graphene – cuo hybrid with hydrogen sulfide removal capacity. *Nano-Micro Letters*, 8(4), pp.312–319.

Ma, X. L., Song, C. and Zhou, A. N., 2006. "Liquid-phase adsorption of multi-ring thiophenic sulphur compounds on carbon materials with different surface properties," *Physical Chemistry*, vol. 110, pp. 4699 – 4707.

Ma, X., Song, C. and Velu, S., 2003. "Selective adsorption for removing sulphur from jet fuel over zeolite-based adsorbents," *Industrial and Engineering Chemistry Research*, vol. 42, pp. 5293 – 5304.

Ma, X., Turaga, U.T., Watanabe, S., Velu, S. and Song, C., 2014 "Deep Desulfurization of Diesel Fuels by a Novel Integrated Approach". Internet: https://www.netl.doe.gov/publications/proceedings/03/ucr-hbcu/posters/Song-Ma_p.pdf. Accessed May 2018

Mabayoje, O., Seredych, M. & Bandosz, T.J., 2012. *Enhanced reactive adsorption of hydrogen sulfide on the composites of graphene/graphite oxide with copper (hydr)oxychlorides.*

Mey, S., Pérot, D., Bouchy, G., Diehl, C., and Brunet. F., 2005. "On the hydrodesulfurization of FCC gasoline: A review," *Applied Catalysis A*, vol. 278, pp. 143 – 172.

Mykola, S. and Teresa, J.B., 2010. Effects of surface features on adsorption of SO_2 on the graphite oxide/$Zr(OH)_4$ composites*. Department of Chemistry, The City College Of New York.*

Nazal, M.K. et al., 2015. The nature and kinetics of the adsorption of dibenzothiophene in model diesel fuel on carbonaceous materials loaded with aluminium oxide particles. *Arabian Journal of Chemistry*.

Randal, M. C. A. 2012. Ecotoxicity and environmental fate of diesel and diesel blends produced by Sasol's Fischer-Tropsch processes using natural gas and coal as feedstock as well as biodiesel and biodiesel blends.

Rang, H.; Kann, J.; Oja, V., 2006. Advances in Desulfurization Research of Liquid Fuels. *Oil Shale, 23*(2), pp. 164 – 176

Reed, N. J., 2008. A comparative study of adsorption desulfurization of liquid transportation fuels over different sorbents for fuel cell applications, M.S thesis, College of Earth and Mineral Sciences, The Pennsylvania State University.

Reinoso, F. R. and Marsh, H., 2006. *Activated Carbon*. Amsterdam: Elsevier Science & Technology Books. Rodríguez-Reinoso, F.,1998. "The role of carbon materials in heterogeneous catalysis," *Carbon,* vol. 36, pp. 159 – 175.

Samira, Bagheri, Nurhidayatullaili Muhd Julkapli, 2016. Effect of hybridization on the value-added activated carbon materials. *Int J Ind Chem.* 7, pp.249 – 264.

Shairanada S., 2013. The effects of sulphur on the atmosphere. Available at: https://steemit.com/science/@shairanada/the-effects-of-air-pollution-to-the-environment-human-health-as-well-as-other-land-and-marine-life. Accessed May 2018

Shi, L. et al., 2015. Characterization and mechanisms of H2S and SO2 adsorption by activated carbon. College of Chemical Engineering, Nanjing Tech University, Nanjing, Jiangsu 210009, P. R. China. *Energy Fuels*, *29* (10), pp 6678 – 6685.

Song and Ma, 2003. An overview of new approaches to deep desulfurization for ultraclean gasoline, diesel fuel and jet fuel. *Journal of Catalysis Today* 86 (1), pp. 211 – 263.

Song, C.,2002. Fuel Processing for Low-Temperature and High-Temperature Fuel Cells: Challenges, and Opportunities for Sustainable Development in the 21st Century. *Catal. Today*, *77*(1–2), pp.17 – 49.

Song, H.S., 2014. *Desulfurization by metal oxide / graphene composite*s. *UWSpace,* Waterloo, Ontario, Canada.

Srinivas, Gadipelli and Zheng, Xiao Guo, 2015. Graphene-based materials: Synthesis and gas sorption, storage and separation. *Progress in materials science.* 69, pp.1 – 60.

Srivastava, V. C., and Srivastav, A., 2009. "Adsorptive desulfurization by activated alumina," *Journal of Hazardous Materials*, vol. 170, pp. 1133 – 1140.

Stanislaus, A, Marafi, A and Rana, M.S.,2010. Recent advances in the science and technology of ultra-low sulphur diesel (ULSD) production. *Catalysis Today*, vol. 153, pp.1 – 68.

Thomas J.K., 2008. "A Flow Calorimetric Study of Adsorption of Dibenzothiophene, Naphthalene and Quinoline on Zeolites," M.S. thesis, Department of Chemical Engineering, University of Waterloo, Ontario, Canada.

Topalova P., and Toteva, L., 2007. "extractive dearomatization and desulphurization of a distillate gasoil cut with dimethylformamide," *Univ. Chem. Technol. Metall.*, vol. 42, pp. 17 – 20.

Van Veen, J. A. and Ito, E., 2006. "On novel processes for removing sulphur from refinery streams," *Catalysis today*, vol. 16, pp. 446 – 460.

Velu, S., Kim, J. H., Song, C., and Ma, X., 2005. "Deep desulfurization of gasoline by selective adsorption over solid adsorbents and impact of analytical methods on ppm level sulphur quantification for fuel cell applications," *Applied. Catalysis B: Environment*, vol. 56, pp. 137 – 147.

Velu, S. et al., 2003. Regenerable adsorbents for the adsorptive desulfurization of transportation fuels for fuel cell applications. *AIChE Letter* 48(2), pp.526 – 528.

Wang, QH, Bellisario, DO, Drahushuk, LW, Jain, RM, Kruss, S, Landry, MP, Mahajan SG, Shimizu SFE, Ulissi ZW, Strano MS, 2014. Low dimensional carbon materials for applications in mass and energy transport. Chem Mater 26(1), pp.172 – 183.

Wang, L. & Yang, R.T., 2013. Graphene and other carbon sorbents for selective adsorption of thiophene from liquid fuel. AIChE Journal 59(1), pp.29 –32.

Wu, J., Bai, S., Shen, X. and Jiang L., 2010. Preparation and characterization of graphene/Cds nanocomposites. *Appl. Surf. Sci. vol 257, no. 3, pp. 747 – 751.*

Yang, R. T., and Hernández-Maldonado, A. J., 2004. “Desulfurization of Diesel Fuels via π-Complexation with Nickel (II)-Exchanged X- and Y-Zeolites,” *American Chemical Society*, pp. 1081 – 1089.

Yang, R. T., Hernández-Maldonado A. J. and Yang. F. H., 2003. "Desulfurization of Transportation Fuels with Zeolites Under Ambient Conditions, "*Science Magazine*, pp. 79 – 81.

You, X., 2002. *Sulfur impregnation of activated carbon through hydrogen sulfide oxidation*. University of Pittsburgh.

Zaheer, K. & Syed, A., 2010. Oxidative desulphurization followed by catalytic adsorption method. *South African Journal of Chemical Engineering* 18, (2), pp.14–28.

Zhou, Ma X. and Song, C., 2009. "Effects of oxidative modification of carbon surface on the adsorption of sulphur compounds in diesel fuel," *Applied Catalysis: B Environment*, vol. 87, pp. 190 –199.

Zhou, Song, C., and Ma X.,2007. "A novel method for oxidative desulfurization of liquid hydrocarbon fuels based on catalytic oxidation using molecular oxygen coupled with selective adsorption," *Catalysis Today,* vol. 123, pp. 276–284.

Zubaidy, Al, Bin Tarsh, F., Darwish, N. N., Sweidan, B., Abdul Majeed, S., Al Sharafi, A. and Abu Chacra, L.,2013. "Adsorption Process of Sulfur Removal from Diesel Oil Using Sorbent Materials," *Journal of Clean Energy Technologies*, vol. 1, pp. 66 – 68.

APPENDIX

Table A.1: H_2S and SO_2 adsorption on MeO in H_2S/N_2 environment at 300°C.

Sample weight: 4.56 g				
TRIAL	TIME (min)	min/g of adsorbent	H_2S (ppm)	SO_2 (ppm)
1	5	30.9	0.00	2.6
	10	33.7	0.00	5.6
	15	39.3	0.00	8.3
	20	42.2	1.35	11.1
	25	44.7	1.53	14.1
	30	47.3	1.43	16.9
	35	50.2	1.64	16.8
	40	54.3	1.98	19.4
	45	61.5	2.10	19.4
	50	63.4	2.26	22.1
	55	65.7	2.26	22.6
	60	70.2	5.68	23.5
Sample weight: 4.48 g				
2	5	42.1	0.00	0.0
	10	44.9	0.00	2.8
	15	47.8	0.00	5.6
	20	50.6	0.00	8.4
	25	53.4	0.00	11.2
	30	61.8	0.00	14.0
	35	64.6	0.00	16.9
	40	67.4	0.00	19.7
	45	70.2	0.00	22.5
	50	73.0	0.00	30.9
	55	75.8	5.45	33.7
	60	78.7	7.77	36.5

Sample weight: 5.62 g				
TRIAL	TIME (min)	min/g of adsorbent	H_2S (ppm)	SO_2 (ppm)
3	5	3.8	0.00	0.0
	10	19.3	2.81	0.0
	15	30.4	5.62	0.5
	20	35.9	8.46	1.5
	25	44.2	11.26	1.8
	30	49.7	14.08	2.1
	35	60.8	16.92	2.5
	40	66.3	19.75	2.9
	45	71.8	22.59	3.6
	50	80.1	30.92	4.1
	55	89.7	33.77	4.7
	60	93.9	44.85	8.4

Table A.2: H_2S and SO_2 adsorption on ZnO in $H_2S/N_2/H_2$ environment at 300°C.

Sample weight: 3.45 g				
TRIAL	TIME (min)	min/g of adsorbent	H_2S (ppm)	SO_2 (ppm)
1	5	31.6	0.00	2.9
	10	34.5	0.00	5.7
	15	37.4	0.00	8.9
	20	40.2	0.00	11.6
	25	43.1	0.00	13.4
	30	46.0	0.00	14.6
	35	48.9	0.00	17.3
	40	51.7	0.00	18.5
	45	54.6	0.00	19.7
	50	63.2	2.35	22.1
	55	66.1	2.65	22.5
	60	69.0	8.68	23.2

Sample weight: 3.48 g				
2	5	43.1	0.28	2.9
	10	46.0	1.11	5.7
	15	48.9	1.23	8.6
	20	51.7	1.25	11.5
	25	54.6	1.33	14.4
	30	63.2	1.61	17.2
	35	66.1	1.80	20.1
	40	69.0	2.00	23.0
	45	71.8	2.21	31.6
	50	74.7	2.62	34.5
	55	77.6	5.68	37.4
	60	80.5	11.23	40.2

Sample weight: 3.51 g				
TRIAL	TIME (min)	min/g of adsorbent	H_2S (ppm)	SO_2 (ppm)
3	5	3.8	0.00	0.0
	10	19.3	0.00	0.1
	15	30.4	0.00	0.2
	20	35.9	0.00	0.5
	25	44.2	0.00	1.6
	30	49.7	0.00	1.6
	35	60.8	0.00	2.3
	40	66.3	0.00	2.5
	45	71.8	0.00	2.8
	50	80.1	8.30	3.2
	55	89.7	9.54	3.6
	60	93.9	11.00	4.1

Table A.3: H_2S and SO_2 adsorption on ZnO in H_2S/N_2 environment at 300°C.

Sample weight: 3.77 g				
TRIAL	TIME (min)	min/g of adsorbent	H_2S (ppm)	SO_2 (ppm)
1	5	31.3	0.00	0.0
	10	34.2	0.00	2.8
	15	37.0	0.00	5.7
	20	39.9	0.00	8.4
	25	42.7	0.00	11.4
	30	45.6	0.00	16.2
	35	48.4	1.20	16.8
	40	51.3	1.25	19.4
	45	54.1	1.33	19.7
	50	62.7	2.25	22.8
	55	67.6	2.62	22.5
	60	76.1	5.88	23.2
Sample weight: 6.58 g				
2	5	30.9	0.00	0.0
	10	33.7	0.00	2.4
	15	36.5	0.00	3.5
	20	39.3	0.00	5.6
	25	42.1	0.00	8.6
	30	44.9	0.00	14.4
	35	47.8	0.00	16.9
	40	50.6	2.85	17.4
	45	53.4	3.80	18.5
	50	61.8	1.56	19.4
	55	64.6	1.89	19.7
	60	67.4	2.22	22.5

Sample weight: 3.62 g				
TRIAL	TIME (min)	min/g of adsorbent	H_2S (ppm)	SO_2 (ppm)
3	5	61.8	0.00	0.0
	10	64.6	0.00	0.2
	15	67.4	0.00	0.5
	20	70.2	0.00	1.6
	25	73.0	4.72	1.6
	30	75.8	5.10	2.3
	35	78.7	5.75	2.5
	40	81.5	7.44	2.8
	45	84.3	7.89	3.2
	50	92.7	8.37	3.6
	55	95.5	9.56	4.1
	60	98.3	11.10	4.6

Table A.4: H_2S and SO_2 adsorption on ZnO/rGO in H_2S/N_2 environment at 300°C

Sample weight: 3.55 g				
TRIAL	TIME (min)	min/g of adsorbent	H_2S (ppm)	SO_2 (ppm)
1	5	94.0	0.00	3.6
	10	96.9	0.00	6.5
	15	99.7	0.00	8.3
	20	102.6	0.00	11.1
	25	105.4	0.00	13.1
	30	108.3	1.02	16.2
	35	111.1	1.45	16.8
	40	114.0	2.74	17.4
	45	116.8	8.12	18.7
	50	125.4	2.71	20.1
	55	128.3	2.62	21.5
	60	133.7	5.68	21.7

Sample weight:7.48 g				
2	5	354.8	0.00	2.9
	10	361.3	0.00	8.6
	15	367.7	0.00	11.5
	20	374.2	0.00	17.2
	25	380.6	1.56	23.1
	30	387.1	1.89	31.6
	35	393.5	2.22	35.4
	40	400.0	2.85	37.4
	45	406.5	3.80	46.0
	50	412.9	4.60	51.7
	55	419.4	5.46	63.2
	60	425.8	7.92	66.1
Sample weight: 4.66 g				
3	5	71.0	0.00	2.6
	10	77.4	0.00	2.1
	15	83.9	0.26	3.4
	20	90.3	1.32	4.0
	25	96.8	1.58	4.2
	30	103.2	2.19	5.1
	35	109.7	2.45	5.5
	40	116.1	2.75	7.1
	45	122.6	3.20	7.2
	50	129.0	3.64	8.0
	55	135.5	3.70	9.4
	60	141.9	4.40	10.2

Table A.5: H_2S and SO_2 adsorption on ZnO/rGO in $H_2S/N_2/H_2/CO_2$ environment at 300°C

Sample weight: 3.55 g				
TRIAL	TIME (min)	min/g of adsorbent	H_2S (ppm)	SO_2 (ppm)
1	5	71.0	0.00	5.6
	10	77.4	0.00	8.5
	15	83.9	0.00	11.3
	20	90.3	1.20	12.1
	25	96.8	1.25	14.1
	30	103.2	1.33	16.2
	35	109.7	1.61	16.8
	40	116.1	1.80	19.4
	45	122.6	2.00	19.7
	50	129.0	2.21	22.1
	55	135.5	2.62	22.5
	60	141.9	5.68	23.2
Sample weight: 3.88 g				
77+2	5	94.0	0.00	0.2
	10	100.7	0.00	0.6
	15	107.4	0.00	1.5
	20	114.1	0.00	1.2
	25	120.8	1.56	2.1
	30	127.5	1.79	3.6
	35	134.2	2.12	3.4
	40	140.9	2.85	3.4
	45	147.7	3.70	5.0
	50	154.4	4.60	5.7
	55	161.1	5.36	6.2
	60	167.8	7.82	6.6

Sample weight: 3.62 g				
TRIAL	TIME (min)	min/g of adsorbent	H_2S (ppm)	SO_2 (ppm)
3	5	221.5	0.00	2.6
	10	228.2	0.00	2.9
	15	234.9	0.4	3.4
	20	241.6	3.9	4.1
	25	248.3	4.2	4.7
	30	255.0	4.7	5.1
	35	261.7	6.8	5.7
	40	268.5	6.3	7.1
	45	275.2	7.8	7.2
	50	281.9	8.1	8.0
	55	288.6	8.7	9.4
	60	302.0	9.9	9.7

Table A.6: Results of the Adsorption Adsorptive Desulphurization Process

Trial	Sorbent Material	Amount of Sorbent Material (wt. %)	Temperature ^{o}C	Contact Time (hr)	Sulphur Concentration (ppm)	% Sulphur Removal	Diesel Indices
PAC							
1	PAC	1	30	1	27.03	45,94	69.28
2	PAC	2	30	1	30.63	38,74	68.57
3	PAC	4	30	1	26.03	47,95	70.25
4	PAC	6	30	1.5	27.66	44,67	69.45
5	PAC	8	50	1	24.34	51,32	-70.38
6	PAC	10	50	1.5	22.84	54,33	76.64
7	PAC	12	50	1	21.87	56,27	78.54
8	PAC	14	50	1	20.09	59,82	73.83
9	PAC	16	80	1.5	35.73	28,54	71.03
10	PAC	18	80	1	28.28	43,45	70.44
11	PAC	20	80	1	21.46	57,07	71.39
12	PAC	3	30	2	33.91	32,18	70.74
13	PAC	6	30	2	24.18	51,65	69.86
14	PAC	9	50	2	19.48	61,04	74.04
15	PAC	12	50	2	37.90	24,19	69.33
16	PAC	15	80	2	26.98	46,64	69.86
17	PAC	18	80	2	25.32	49,35	71.52
18	PAC	20	80	2	35.59	28,81	64.63
19	PAC	5	30	2.5	29.84	40,32	69.72
20	PAC	10	30	2.5	20.97	58,06	73.21
21	PAC	15	80	2	28.80	42,41	70.84
22	PAC	20	50	1	28.93	42,14	69.10

AC							
1	AC	3	30	1	32,71	34,57	68.49
2	AC	4	30	1	40,99	18,02	68.49
3	AC	5	30	1	30,05	39,90	69.23
4	AC	6	30	1	34,10	31,79	71.56
5	AC	7	50	1	33,22	33,55	71.44
6	AC	8	50	1	31,87	36,27	73.22
7	AC	9	50	1	30,45	39,10	74.56
8	AC	15	50	1.5	24,97	50,07	71.88
9	AC	3	80	1.5	41,90	16,20	70.87
10	AC	5	80	1	30,71	38,59	69.07
11	AC	20	80	1	26,62	46,76	70.49
12	AC	3	30	2	42,90	14,21	69.74
13	AC	5	30	2	31,78	36,44	68.45
14	AC	10	50	2	24,92	50,16	70.51
15	AC	3	50	2	43,51	12,98	70.50
16	AC	5	80	2	31,51	36,98	70.62
17	AC	15	80	2	29,92	40,17	70.42
18	AC	13	80	1	43,57	12,86	64.08
19	AC	5	30	1	37,03	25,95	69.60
20	AC	10	30	1	24,68	50,64	70.57
21	AC	5	80	1.5	33,84	32,33	70.89
22	AC	15	50	1.5	36,22	27,56	68.48
23	AC	10	30	2.5	26,95	46,10	70.91
24	AC	20	30	2.5	26,34	47,33	68.96
GAC							
1	GAC	3	30	1	42,03	15,95	70.56
2	GAC	4	30	2.5	40,65	18,71	69.60
3	GAC	5	30	1	40,07	19,85	70.57
4	GAC	6	30	2	39,16	21,69	70.89
5	GAC	7	50	2	37,09	25,82	68.48
6	GAC	8	50	2	36,97	26,05	70.91
7	GAC	9	50	1	36,16	27,68	68.96

8	GAC	15	50	1	36,17	27,66	71.24
9	PAC	20	80	2	15,65	68,70	71.35
10	PAC	20	80	2.5	16,89	66,22	69.73